

Imperial College of Science, Technology and Medicine
Department of Electrical and Electronic Engineering
Control and Power Research Group

**MULTI-LEVEL OPTIMISATION MODELS FOR
TRANSMISSION EXPANSION PLANNING
UNDER UNCERTAINTY**

ALEXANDRE MOREIRA DA SILVA

Submitted in partial fulfillment of the requirements for the degree of
Doctor of Philosophy and for the Diploma of Imperial College, 11th March 2019

Abstract

The significant integration of renewable energy sources to electricity grids poses unprecedented challenges to power systems planning. Each of these challenges is implied by a particular circumstance faced by the system planner when devising the expansion plan, which should be tailored to address the needs and objectives of the system under consideration. Within this context, this thesis is dedicated to propose methodologies to address three timely situations that may arise when planning the expansion of the grid.

In the first situation, we consider the case in which the system planner must meet established renewable penetration targets while complying with multiple deterministic security criteria. Renewable targets have been largely adopted as an important mechanism to foster the decarbonization of power systems. Hence, we propose a methodology that simultaneously identifies the optimal subset of candidate assets as well as renewable sites to be developed, while introducing the concept of compound GT $n - K$ security criteria.

In the second situation, we aim to minimize the regret of the system planner under generation expansion uncertainty. In many cases, e.g. the United Kingdom, the decision on the transmission expansion plan is taken by a market player that does not determine the future generation expansion. Within this context, we propose a 5-level MILP formulation to represent the minimization of the regret of the system planner in light of a set of credible scenarios of generation expansion while enforcing $n - 1$ security criterion.

Finally, in the third situation, the objective is to inform the optimal transmission expansion plan under ambiguity in the probability distribution of RES generation output. To do so, we present a methodology capable of determining the transmission plan under deterministic security criterion while accommodating a set of different probability distributions for RES output in order to integrate ambiguity aversion.

Statement of originality and copyright declaration

I hereby declare that this work is the result of my own endeavour, and that any ideas or quotations from the work of other people, published or otherwise, are appropriately referenced.

The copyright of this thesis rests with the author. Unless otherwise indicated, its contents are licensed under a Creative Commons Attribution-Non Commercial-No Derivatives 4.0 International Licence (CC BY-NC-ND).

Under this licence, you may copy and redistribute the material in any medium or format on the condition that; you credit the author, do not use it for commercial purposes and do not distribute modified versions of the work.

When reusing or sharing this work, ensure you make the licence terms clear to others by naming the licence and linking to the licence text.

Please seek permission from the copyright holder for uses of this work that are not included in this licence or permitted under UK Copyright Law.

ALEXANDRE MOREIRA DA SILVA

Department of Electrical and Electronic Engineering

Imperial College London, London, U.K.

11th March 2019

Acknowledgements

All honor and glory to God forever and ever. I would like to express my deepest gratitude to God for the opportunity to live and serve and for all that I could learn in the good and in the bad moments of my life so far.

Repeating the words once said by Abraham Lincoln, I have no doubts that “*all that I am or ever hope to be, I owe to my angel mother*”. I am extremely grateful to my mother, Maria José Moreira da Silva, for all her unconditional pure love and dedication. *Eu te amo, Mãe!*

I am extremely grateful to my father, Francisco Moreira da Silva, whose presence in my heart will be always constant.

To my supervisor, Professor Goran Strbac, my enormous gratitude for all his support and brilliant guidance that were essential to improve the value of my research.

I am grateful to my examiners, Professor Richard Vinter and Professor Derek Bunn, for their positive and constructive comments about my thesis as well as for their suggestions to enhance the quality of my work.

I would like to thank my aunt, Maria José da Silva Araújo, whose love has a very special place in my heart.

I wish to thank my uncle, Manoel Moreira da Silva, for his life example on how to be a great human being.

I wish to thank my sisters, Alessandra Moreira, Andressa Moreira and Ana Carla Moreira, for all the immense support they have always offered me since my childhood. Thank you very much for helping to shape my character.

I wish to thank my cousin Willian Araújo and my uncle João Araújo for all the great support and motivation dedicated to me.

I am very grateful for all the help and motivation that came from my Brazilian friends. I wish to specially thank Alexandre Street for opening the doors of research

for me and for his great and enlightening friendship. I am also very grateful to my great friend Bruno Fanzeres, whose friendship has always motivated me to go further. My sincere gratitude to all the friends I have made at LAMPS at PUC-Rio. Particularly, Ana Luiza Lopes, Aderson Passos, Arthur Brigatto, Henrique Helfer, Joaquim Garcia, Lucas Freire, Mario Souto, Raphael Saavedra, and Sebastian Maier.

I would like to thank David Pozo and Enzo Sauma for their extremely valuable collaboration in part of my research.

To be part of the CAP group is one of the most enriching experiences of my life. It is a great privilege to have friends from many countries, whose cultural backgrounds have definitely improved my way of understanding the world. I would like to thank Rodrigo Moreno for his support throughout my PhD. I am also thankful to Ioannis Konstantelos for his great willingness to help. I am extremely pleased that I could share my time at Imperial with many incredible friends, especially Adam Jones, Alberto Padoan, Alberto Mellone, Alex Gallo, Anastasis Georgiou, Ankur Majumdar, Arghavan Nazemi, Caspar Collins, Claudia Spallarossa, David Kurka, Diptargha Chakravorty, Firdous Nazir, Francesca Boem, Georgios Anagnostou, Himadri Das, Husni Ali, Joan Marc Rodriguez, Jinrui Guo, Jochen Cremer, José Calvo, Julio Perez, Luis Badesa, Martina Zambelli, Michael Evans, Nathalie Beaufond, Nicolas Cifuentes, Paolo Forni, Pedro Ramirez, Peng Li, Roberto Moreira, Tiago Rodrigues, Thiago Mendonça, Vinicius Schettino, and Yousef Pipelzadeh.

During my PhD, I also had the privilege to meet fantastic people in London. Special thanks to everyone who participates in the Spiritist Psychological Society. I also would like to thank Carlos Matamala (also known as “*Carlitos La Leyenda*”), Lucrezia Bilgeri who kindly introduced me to the amazing Italian bresaola, Laia Gisbert who can cook the best Catalan paella in London, and last but not least Paula Maldonado who is the best “*furró*” dancer I have ever met.

I am extremely grateful to Brazil and CNPq for the financial support via the *Science without Borders* scholarship program under grant 203274/2014-8, which made this dream possible.

“Hearing that Jesus had silenced the Sadducees, the Pharisees got together. One of them, an expert in the law, tested Him with this question: Teacher, which is the greatest commandment in the Law?" Jesus replied: 'Love the Lord your God with all your heart and with all your soul and with all your mind.' This is the first and greatest commandment. And the second is like it: 'Love your neighbor as yourself'. All the Law and the Prophets hang on these two commandments.”

Mathew, 22:34-40.

Contents

| | |
|--|----------|
| Abstract | i |
| Statement of originality and copyright declaration | i |
| Acknowledgements | v |
| 1 Introduction | 1 |
| 1.1 Contributions | 4 |
| 1.2 List of publications | 6 |
| 1.3 Structure of the thesis | 7 |
| 2 Reliable Renewable Generation and Transmission Expansion Planning: Co-Optimizing System's Resources for Meeting Renewable Targets | 8 |
| 2.1 Nomenclature | 12 |
| 2.2 Mathematical Formulation | 16 |

| | | |
|----------|--|-----------|
| 2.2.1 | The TEP mathematical framework | 18 |
| 2.2.2 | The $n - K$ -contingency-constrained TEP | 20 |
| 2.2.3 | Modeling correlated RES generation and demand uncertainty | 23 |
| 2.2.4 | The reliable TEP model for large renewable energy penetration | 24 |
| 2.3 | Solution approach | 26 |
| 2.4 | Case Studies | 28 |
| 2.4.1 | (3e+2c)-Bus System Case Study | 28 |
| 2.4.2 | Main Chilean Power System Case Study | 31 |
| 2.4.3 | (118e+4c)-Bus System Case Study | 36 |
| 3 | A Five-Level MILP Model for Flexible Transmission Network Planning under Uncertainty: A Min-Max Regret Approach | 38 |
| 3.1 | Nomenclature | 43 |
| 3.2 | 5-level framework | 48 |
| 3.3 | Mathematical Formulation | 50 |
| 3.4 | Solution Methodology | 57 |
| 3.4.1 | Obtaining Operation Costs | 57 |
| 3.4.2 | Obtaining Transmission Expansion Plan | 60 |
| 3.5 | Case Studies | 64 |
| 3.5.1 | 6-Bus System | 64 |
| 3.5.2 | Solutions under perfect information and MMR solution | 67 |
| 3.5.3 | Role played by the phase shifter under perfect information of generation expansion | 70 |

| | | |
|----------|--|------------|
| 3.5.4 | Role played by the phase shifter under uncertainty of generation expansion | 73 |
| 3.5.5 | Comparison with industry practice | 74 |
| 3.5.6 | IEEE 118-Bus System | 76 |
| 4 | An Ambiguity Averse Approach for Transmission Expansion Planning | 81 |
| 4.1 | Nomenclature | 85 |
| 4.2 | Mathematical Formulation | 87 |
| 4.2.1 | RES Output and Equipment Availability Uncertainties | 88 |
| 4.2.2 | Transmission Expansion Planning Model | 89 |
| 4.3 | Solution Methodology | 92 |
| 4.4 | Case Studies | 95 |
| 4.4.1 | 5-Bus System: Illustrative Example | 96 |
| 4.4.2 | 128-Bus System: Case Study | 99 |
| 5 | Conclusions | 106 |
| 5.1 | Summary | 106 |
| 5.2 | Future Work | 109 |
| A | Detailed formulation of the model presented in Chapter 2 | 125 |
| A.1 | First-level problem: minimization of investment and operative costs | 125 |
| A.2 | Middle-level: worst-case demand, RES supply and contingency scenario | 129 |
| A.3 | Lower-level: system corrective actions | 131 |

| | | |
|----------|---|------------|
| B | Detailed solution methodology for the problem of Chapter 2 | 133 |
| B.1 | Master Problem | 134 |
| B.2 | Subproblem | 135 |
| B.3 | Solution Algorithm | 138 |
| C | Oracle formulation for methodology presented in Chapter 3 | 140 |

List of Tables

| | | |
|-----|---|----|
| 2.1 | Total Reserve Cost (\$/hour) | 30 |
| 2.2 | Total Investment in Lines (\$/hour) | 30 |
| 2.3 | Results for the Chilean Power System | 32 |
| 2.4 | Out-of-sample Monte Carlo Simulation Test for the Chilean Power System | 35 |
| 2.5 | Results for the (118e+4c)-Bus System | 37 |
| 3.1 | 6-Bus System – Costs of alternative expansion plans under perfect information and under uncertainty (MMR solution) and regrets of the MMR solution under each scenario. | 68 |
| 3.2 | 6-Bus System – New infrastructure of alternative expansion plans. Decisions under perfect information (S1,S2,S3,S4) and under uncertainty (MMR). | 69 |
| 3.3 | Scheduling with and without PS1 under realization of S1 | 71 |

| | | |
|------|--|----|
| 3.4 | Redispatch (in MW) under the considered outages of G1, G2, and L1 with and without PS1 | 71 |
| 3.5 | 6-Bus System – Overall costs and regrets per scenario (in MM\$/year) of implementing the min-max regret solution (i) with its two proposed phase shifters, (ii) with only one of its proposed phase shifters, and (iii) without any of its proposed phase shifters. Costs and regrets are indicated without and within brackets, respectively. | 74 |
| 3.6 | 6-Bus System – Overall costs and regrets per scenario (in MM\$/year) of implementing decisions under perfect information (S1, S2, S3 and S4) and under uncertainty (MMR). Costs and regrets are indicated without and within brackets, respectively. | 75 |
| 3.7 | 118-Bus System – New infrastructure of alternative expansion plans (no security) and the associated computing time. Decisions under perfect information (S1, S2,...,S7) and under uncertainty (MMR). . . | 76 |
| 3.8 | 118-Bus System – Costs of alternative expansion plans under perfect information and under uncertainty (MMR solution) and regrets of the MMR solution under each scenario. | 77 |
| 3.9 | 118-Bus System – New infrastructure of alternative expansion plans (with $n - 1$ security) and the associated computing time. Decisions under perfect information (S1, S2,...,S7) and under uncertainty (MMR). 78 | |
| 3.10 | Results of the contingency analysis for the MMR transmission plan without security criterion. | 79 |
| 3.11 | Results of the contingency analysis for the MMR transmission plan with $n - 1$ security criterion. | 79 |
| 4.1 | 5-bus system – Data of conventional generators. | 96 |
| 4.2 | 5-bus system – data of transmission lines. | 97 |

| | | |
|-----|---|-----|
| 4.3 | 5-bus system – expansion plan and resulting investment and operation costs. | 99 |
| 4.4 | 5-bus system – operation costs considering different probability distributions (MM\$/year). | 99 |
| 4.5 | 128-bus system – expansion profiles for both Nominal and Ambiguity Cases. | 101 |
| 4.6 | 128-bus system – operational and expansion costs [MM\$/year] from each Nominal and Ambiguity Cases, along with the computational time [s] and number of iterations required to solve each instance. . . . | 102 |
| 4.7 | Out-of-sample probability distribution of load shedding cost. | 105 |
| 4.8 | Out-of-sample probability distribution of wind spillage cost. | 105 |

List of Figures

| | | |
|-----|---|----|
| 2.1 | Three-level robust TEP framework | 17 |
| 2.2 | 3(existing)+2(candidate)-nodes power system | 29 |
| 2.3 | Empirical CDF of renewable curtailment from Monte Carlo simulation | 36 |
| 3.1 | Framework diagram. | 49 |
| 3.2 | Procedure to obtain operation cost for each snapshot. | 59 |
| 3.3 | Solution algorithm to determine the optimal transmission plan. | 62 |
| 3.4 | Generation, network, and demand data of 6-Bus system, where continuous lines refer to existing infrastructure and dashed lines refer to candidate infrastructure. Normal brackets refer to generation and network capacities and peak demand conditions, while square brackets refer to reactances. | 65 |
| 3.5 | Solution under perfect information for scenario 1 with and without $n - 1$ security criterion. | 66 |

| | | |
|------|--|-----|
| 3.6 | Solution under perfect information for scenario 2 with and without $n - 1$ security criterion. | 66 |
| 3.7 | Solution under perfect information for scenario 3 with and without $n - 1$ security criterion. | 66 |
| 3.8 | Solution under perfect information for scenario 4 with and without $n - 1$ security criterion. | 67 |
| 3.9 | Min-max regret solution under generation expansion uncertainty with and without $n - 1$ security criterion. | 67 |
| 3.10 | Power flow with and without PS1 under the realization of S1 considering $n - 1$ security criterion. | 71 |
| 3.11 | Power flow with and without PS1 under the realization of S1 considering a failure in G1. | 72 |
| 3.12 | Power flow with and without PS1 under the realization of S1 considering a failure in G2. | 72 |
| 3.13 | Power flow with and without PS1 under the realization of S1 considering a failure in L1. | 72 |
| 4.1 | Model scheme. | 87 |
| 4.2 | 5-bus illustrative system. | 97 |
| 4.3 | Out-of-sample inverse cumulative distributions of the system imbalance under the realization of the lower limit distribution. | 103 |
| 4.4 | Out-of-sample inverse cumulative distributions of the system imbalance under the realization of the point estimative distribution. | 103 |
| 4.5 | Out-of-sample inverse cumulative distributions of the system imbalance under the realization of the upper limit distribution. | 104 |

CHAPTER 1

Introduction

In both centralized and competitive frameworks, decisions on investments in energy transmission infrastructure play a crucial role in power systems planning. Such decisions are, for instance, one of the keys to achieve the integration of the volumes of renewable energy sources (RES) required to satisfactorily decrease the current levels of greenhouse gases emissions [1]. This expansion planning problem consists in the selection of the most appropriate assets in order to meet the objectives of interest for the power system planner. In this work, three methodologies are proposed to address the transmission expansion planning (TEP) problem under different conditions. The first one co-optimizes generation and transmission expansion in order to meet renewable targets while imposing multiple security criteria. The second one minimizes the regret of the transmission expansion planner under uncertainty in generation capacity expansion while securing operation. Finally, the third one

determines the transmission expansion plan to better accommodate RES generation under uncertainty in the underlying process that governs the realization of the RES output. In order to withstand the computational burden associated with the aforementioned objectives, the models proposed in this work are formulated within the framework of multi-level optimization.

Multi-level optimization [2] is a powerful framework to mathematically model hierarchical decision-making processes. This framework has been successfully used to develop new methodologies in several different fields, such as for example supply-chain [3–5], transportation [6–8], government decisions on taxes [9], safety [10–12], and unit commitment in power systems [13–18].

Within the context of the TEP problem, several multi-level optimization models have been also proposed. Works [19–21] are some of the relevant examples of bi-level approaches for TEP. In [19], a bilevel approach was proposed to minimize costs associated with the transmission expansion plan while facilitating trades in the electricity market. In [20], the framework presented in [19] was extended by the inclusion of security constraints. In [21], the authors used a bilevel framework to model the efficiency benefit (benefit of accessing lower cost distant generation) and the competition benefit (benefit of improving competition among generators) associated with additional transmission capacity. In addition, trilevel models such as [22–24] were also presented to tackle the TEP problem. In [22], a trilevel model was developed to determine the transmission expansion plan while considering the equilibria associated with generation expansion and pool-based market clearing. In [23], a trilevel formulation was proposed to address the TEP problem under uncertainty in demand and in available generation capacity of existing generating units. In [24], the TEP problem was tackled under uncertainty in future generation investments without considering security standards.

The first methodology proposed in this work is a two-stage min-max-min model for co-optimizing the expansion of the transmission system and renewable generation capacity to meet renewable targets under high security standards and renewable uncertainty. In order to account for realistic reserve needs and its interaction with the expansion plan, correlations between renewables injection as well as generation and transmission (GT) outages are accounted for in a worst-case fashion. In order to ensure security within a flexible framework, the concept of compound GT $n - K$ security criteria is presented. Three case studies are proposed to illustrate the applicability of the proposed model. A case study with realistic data from the Chilean system is presented and solutions obtained with different levels of security are tested against a set of 10,000 simulated scenarios of renewable injections and system component outages.

The second methodology presented in this work aims to solve the transmission expansion planning (TEP) problem under generation expansion uncertainty in a min-max regret fashion, when considering flexible network options and $n - 1$ security criterion. To do so, we propose a five-level mixed integer linear programming (MILP) based model that comprises: (i) the optimal network investment plan (including phase shifters), (ii) the realization of generation expansion, (iii) the co-optimization of energy and reserves given transmission and generation expansions, (iv) the realization of system outages, and (v) the decision on optimal post-contingency corrective control. In order to solve the five-level model, we present a cutting plane algorithm that ultimately identifies the optimal min-max regret flexible transmission plan in a finite number of steps. The numerical studies carried out demonstrate: (a) the significant benefits associated with flexible network investment options to hedge transmission expansion plans against generation expansion uncertainty and system outages, (b) the fact that strategic planning-under-uncertainty uncovers the full benefit of flexible options which may remain undetected under deterministic, perfect

information, methods that only consider a few of the candidate feasible solutions and (c) the computational scalability of the proposed approach.

Finally, the third methodology aims to deliver a methodology to devise an optimal transmission expansion planning under ambiguity in renewable probability distribution while addressing industry's security criterion for failures of equipments. On the one hand, the uncertainty in renewable production is accounted for by an user-defined set of "credible" probability distributions (usually referred to as an *ambiguity set*), described by exogenously simulated scenarios, as customary in stochastic programming. On the other hand, the outages of generators and/or transmission lines are addressed via adjustable robust optimization.

1.1 Contributions

In this work, three novel methodologies to address the TEP problem are presented. The main contributions of the first methodology are the following.

- (i) Formulating a novel two-stage min-max-min static RG-TEP model for co-optimizing transmission and renewable generation capacity expansion to meet renewable targets under correlated uncertainty for renewable injections and equipment failures.
- (ii) Accounting for reserve deliverability through the expanded network by explicitly modeling the cost of the optimal siting and deployment under the presence of different security criteria and correlated renewable generation. It is worth emphasizing that under such new features, the trade-off between building more lines to ensure cheaper reserve deliverability and to reduce renewable curtailment or relying in existing reserve resources is implicitly embedded in the optimal plan.

- (iii) Expanding the notion of uncertainty sets in the framework of robust optimization for power systems planning by considering two sets of uncertainties, not simultaneously covered in the state of the art literature: (a) lines and generating units outages and (b) correlated renewable generation (and loads) through the Cholesky decomposition of the covariance matrix. It is worth mentioning that the solutions obtained are tested against out-of-sample simulated scenarios to corroborate the effectiveness of the worst-case modeling choice.
- (iv) Introducing the concept of compound (combined) GT $n - K$ security criteria in transmission expansion planning in which the level of imbalance under line and generation contingency events (independent or not) can be controlled in the planning stage for different user-defined levels of severity.

With respect to the second methodology, the main contributions are as follows.

- (i) A novel 5-level MILP formulation that represents the min-max regret TEP problem under generation expansion uncertainty while imposing $n - 1$ security criterion. It is worth mentioning that the proposed model is sufficiently general to consider $n - K$ security, however, in this work, we focus on $n - 1$ security. The solution for the proposed model determines optimal portfolios of conventional and flexible network investments (e.g. phase shifters) while optimizing pre- and post-fault operational measures (from both generation and phase shifters) to efficiently and securely deal with long-term uncertainties (volume and location of future generation deployment) and system failures. It should be emphasized that in the literature all the aforementioned features have not been addressed yet in the same model.
- (ii) A solution method that effectively determines the global optimal solution of the proposed 5-level model in a finite number of iterations. This solution

method is based on Benders decomposition to obtain the optimal transmission expansion plan and on column and constraint generation to impose a deterministic security criterion.

Finally, the third proposed methodology has the following main contributions.

- (i) To formulate a novel three-level system of optimization problems to determine the transmission expansion plan under uncertainty in RES output while considering the possibility of outages of system elements. Renewable variability is addressed in a scenario-based framework, whereas equipment failure is considered by modeling deterministic security criterion in adjustable robust optimization framework.
- (ii) To derive a tailored outer-approximation/column-and-constraint generation algorithm to solve the proposed multi-level problem to optimality in a finite number of steps. This solution algorithm effectively approximates the CVaR_α of the system power imbalance.
- (iii) To introduce a practical method to consider ambiguity on renewable production probability distribution in the TEP problem.

1.2 List of publications

- A. Moreira, B. Fanzeres, and G. Strbac, “An Ambiguity Averse Approach for Transmission Expansion Planning,” *IEEE PES PowerTech Milano 2019*.
- A. Moreira, B. Fanzeres, and G. Strbac, “Energy and Reserve Scheduling under Ambiguity on Renewable Probability Distribution,” *Electric Power Systems Research*, vol. 160, pp. 205–218, Jul. 2018.

- A. Moreira, G. Strbac, R. Moreno, A. Street, and I. Konstantelos, “A Five-Level MILP Model for Flexible Transmission Network Planning Under Uncertainty: A Min–Max Regret Approach,” *IEEE Trans. Power Syst.*, vol. 33, no. 1, pp. 486–501, Jan. 2018.
- A. Moreira, D. Pozo, A. Street, and E. Sauma, “Reliable Renewable Generation and Transmission Expansion Planning: Co-Optimizing System’s Resources for Meeting Renewable Targets,” *IEEE Trans. Power Syst.*, vol. 32, no. 4, pp. 3246–3257, Jul. 2017.

1.3 Structure of the thesis

The content of this thesis comprises three methodologies to address different circumstances of the TEP problem. Each methodology is fully presented and described within a chapter.

In chapter 2, we present a methodology to determine generation and transmission expansion to achieve RES penetration targets under multiple deterministic security criteria.

In chapter 3, we propose a methodology to minimize the regret of the system planner while expanding the transmission grid under uncertainty in future generation expansion.

In chapter 4, we introduce a methodology to devise the transmission expansion plan under ambiguity in the probability distribution associated with RES generation.

Finally, in chapter 5, we pose the main conclusions and comment potential future avenues of research.

CHAPTER 2

Reliable Renewable Generation and Transmission Expansion Planning: Co-Optimizing System's Resources for Meeting Renewable Targets

Aiming to reduce greenhouse gases emissions, power systems worldwide are increasing the utilization of renewable energy sources (RES). In order to do so, the establishment of renewable targets is one of the mechanisms largely adopted to guide this RES integration process. Within this context, many countries have set policy targets related to renewable energy. The European Union (EU), for example, established a target to meet 20% of its energy consumption by means of renewable sources by

2020 [25]. Some EU member countries have even more strict targets, e.g., Germany with 30% by 2020 and 60% by 2050.

In order to accommodate the variability of renewable sources under tight security criteria, the system might require additional levels of quick-response reserves. Within this framework, the transmission system plays a key role, since it allows the system operator to use the cheapest resources to ensure system reliability. However, transmission systems were not originally designed to cope with such levels of renewable penetration. Therefore, a renewable-driven expansion of the generation demands a reorientation of current electricity networks. In this vein, several technical reports and scientific articles have highlighted the importance of transmission investments to achieve renewable energy targets [26–28].

Transmission expansion planning (TEP) has typically been addressed by a reactive approach, where the transmission planner reacts by building transmission lines to interconnect committed generation expansion projects. However, a proactive approach for TEP has recently captured the attention of researchers and Regulatory Authorities as an alternative to the reactive approach. In the proactive approach, the transmission planner anticipates the best generation investment decisions. In this manner, the transmission planner is able to induce generation expansions with higher social welfare. Several works have shown the benefits of using a proactive TEP instead of a reactive TEP (see [29–31]).

Proactive transmission planning is a type of co-optimization that is particularly relevant for large transmission investments intended to connect load centers to remote areas with high renewable generation potential. The recognition of co-optimization for transmission and generation capacity expansion has been reported in several works and technical reports [26–29,32]. In the specific case of renewables, candidate areas are, in general, known in advance. Therefore, aggressive incentive (subsidies)

policies can be largely used to drive new investments. Hence, the co-optimization of the transmission system and the new capacity of renewable generation is a powerful tool for planners, policy makers, and regulators. Within this framework, it is possible to efficiently achieve high renewable penetration targets [27] while accounting for the complex interaction between the selection of new renewable sites and candidate transmission lines.

In addition to that, the proper determination of reserve levels and siting for a reliable operation of power systems under the presence of large amounts of renewable energy sources is a timely topic. Several works [33–36] have suggested that reserve needs and costs increase when renewable penetration rises. Clearly, the expansion of renewable projects changes the manner of operating power systems, and therefore, significantly impacts the optimal transmission plan and the optimal reserve siting. Furthermore, renewable energy resources are usually located in remote areas, distant from load-demand centers and conventional generation (reserves). Such characteristics of renewable sources generally impact the capability of the system to guarantee *reserve deliverability*, whose importance has been highlighted in [37] and [38]. On the other side, investments in intermittent renewable projects, such as wind farms, can be financially jeopardized by renewable curtailment. Nevertheless, the side effect of curtailing renewable resources could be mitigated by means of the joint optimization of system’s resources in the planning level.

Two-stage robust optimization [39], also known as adjustable robust optimization (ARO), has been extensively utilized for operation problems with large renewable penetration [40–42]. This approach is also emerging in transmission expansion planning applications with renewable energy generation [43]. Within power systems operation framework, robust models have been proposed in the literature considering reserve deliverability. For instance, [42] explicitly considers deliverability while determining reserve levels by means of joint energy and reserve scheduling. Within

the context of transmission planning, some of the relevant two-stage robust optimization models proposed in the literature are presented in [23] and [44]. On the one hand, in [23], renewable variability and generation contingencies are considered by means of demand and generation capacity uncertainty sets while neglecting failures of transmission lines. On the other hand, in [44], outages of transmission and generating assets are taken into account while disregarding the effect of renewable variability.

Within this context, the objective of the work developed in this chapter is to propose a two-stage renewable generation and transmission expansion planning (RG-TEP) model in order to jointly identify the best subset (within a set of candidates) of new transmission assets and renewable sites to be developed. The main goal of this co-optimization planning model is to address renewable targets. While addressing these targets, the model takes into account the least-cost reserve scheduling to ensure reserve deliverability under renewable variability and outages of generation and/or transmission assets.

To achieve the aforementioned objective and goal, the model proposed in this chapter also considers the cost of optimal reserve levels allocated throughout the expanded network. This consideration enables the possibility of simultaneously balancing two types of cost. On the one hand, the cost of expensive reserve resources, which may possibly lead to significant amounts of penalties due to renewable curtailment. On the other hand, the cost of building new lines to ensure least-cost reserve deliverability and minimal loss of available renewable generation. In order to model realistic reserve requirements and their interaction with the expansion plan, the proposed formulation comprises outages of generation and transmission assets and nodal injection correlation in a worst-case fashion. It is worth mentioning that the worst-case metric is used to identify the events which must be comprised such that the planner will be guarded against any scenario within a defined uncertainty set.

With the objective of ensuring security within a flexible framework, we present in this chapter the concept of compound GT (generation and transmission) $n - K$ security criteria. Within the proposed security criteria, we can set different user-defined thresholds for the maximum allowed system power imbalance. More specifically, we can plan the expansion of the system in order to simultaneously guarantee 0% of system power imbalance for $n - 0$ and $n - 1$ security criteria, while permitting, e.g., a maximum of 1% and 2.5% of system power imbalance for $n - 2$ and $n - 3$ security criteria, respectively. Such modeling feature extends previous works ([23,36,44,45]) while providing more flexibility and constitutes a highly practical feature for system planners.

As a consequence of the aforementioned features included in the modelling, the proposed framework provides planners with an effective computational methodology capable of assessing the trade-off between additional security criteria in a very flexible fashion based on industry standards ($n - K$ criteria) and the cost of operating and expanding the system under different levels of renewable penetration and correlation patterns.

The remainder of the chapter is organized as follows. Section 2.1 specifies the nomenclature associated with this chapter. Section 2.2 describes the mathematical model for the TEP problem. Section 2.3 presents the solution methodology developed to solve the problem. Finally, Section 2.4, illustrates the performance of the proposed methodology with case studies.

2.1 Nomenclature

The mathematical symbols used throughout this chapter and its corresponding appendices are classified below as follows.

Sets

I Set of generator indexes.

I_b Set of indexes of generators connected to bus b .

\mathcal{L}^C Set of indexes of candidate transmission lines.

\mathcal{L}^E Set of indexes of existing transmission lines.

\mathcal{L} Set of indexes of all transmission lines, equal to $(\mathcal{L}^E \cup \mathcal{L}^C)$.

N^E Set of indexes of existing buses.

N^{RE} Set of indexes of candidate buses with potential renewable energy.

N Set of indexes of buses, equal to $(N^E \cup N^{RE})$.

Parameters

Γ^D Conservativeness parameter.

Γ^W Conservativeness parameter.

Σ^D Estimated nodal demand covariance matrix.

Σ^W Estimated nodal renewable generation covariance matrix.

$\overline{\Delta D}_{K,\Sigma}$ Maximum level of system power imbalance for an $n - K$ security criterion.

C_l^{Cap} Cost per MW of candidate lines.

C^{RE} Construction cost of new node with potential renewable energy.

C_K^I Cost of imbalance under the worst-case contingency having K contingencies.

C_l Construction cost of candidate line l .

C_i^p Production cost of generator i .

C_i^d Reserve-down cost of generator i .

C_i^u Reserve-up cost of generator i .

\hat{D}_b Nominal demand at bus b .

\bar{F}_l^{Min} Minimum power flow capacity of candidate line l .

\bar{F}_l^{Max} Maximum power flow capacity of candidate line l .

\bar{F}_l Power flow capacity of existing line l .

$fr(l)$ Sending or origin bus of line l .

K Number of unavailable system components.

L^D Lower triangular matrix that satisfies the equality $\Sigma^D = L^D L^{DT}$.

L^W Lower triangular matrix that satisfies the equality $\Sigma^W = L^W L^{WT}$.

n Number of system components.

\bar{P}_i Capacity of generator i .

R_i^D Reserve-down limit of generator i .

R_i^U Reserve-up limit of generator i .

$to(l)$ Receiving or destination bus of line l .

Target Target of renewable generation as percentage of the total demand.

\hat{W}_b Expected renewable generation at bus b .

x_l Reactance of line l .

Decision Variables

ΔD_b^{+wc} Power surplus equivalent to the energy spillage at bus b under the worst-case contingency.

ΔD_b^{-wc} Power deficit equivalent to the energy insufficiency at bus b under the worst-case contingency.

$\Delta D_{K,\Sigma}$ Worst-case system power imbalance, given K and first-level decisions.

θ_b Phase angle at bus b in the pre-contingency state.

θ_b^{wc} Phase angle at bus b under the worst-case contingency.

a_i^G Binary variable that is equal to 0 if generator i is unavailable under the worst-case contingency, being 1 otherwise.

a_l^L Binary variable that is equal to 0 if line l is unavailable under the worst-case contingency, being 1 otherwise.

D_b Demand at bus b .

\mathbf{e}^d Error on the demand.

\mathbf{e}^w Error on the renewable generation.

\bar{F}_l^C Power flow capacity of line l .

f_l Power flow of line l in the pre-contingency state.

f_l^{wc} Power flow of line l under the worst-case contingency.

p_i Power output of generator i in the pre-contingency state.

p_i^{wc} Power output of generator i under the worst-case contingency.

v_l Binary variable that is equal to 1 if candidate line l is built, being 0 otherwise.

W_b Renewable generation at bus b .

y_b Binary variable that is equal to 1 if candidate bus b is built, being 0 otherwise.

2.2 Mathematical Formulation

The proposed RG-TEP model aims at determining the optimal renewable generation and transmission expansion plan considering correlated nodal injection uncertainty as well as multiple security criteria while ensuring reserve deliverability. A conventional method to address this problem would be a single-level formulation that exhaustively and explicitly enumerates all possible cases of contingencies for all the comprised multiple security criteria combined with several possible scenarios of renewable generation realization. This approach would, in fact, lead to a highly combinatorial problem that can easily become intractable. In [44], for comparison purposes, a conventional single-level formulation to address a TEP problem considering individual security criteria was implemented. Due to computational limitations, when the imposed security criterion was tighter than $n - 1$, such model could not be solved to optimality for the 118-bus system with 311 elements (number of generators plus the number of existing and candidate transmission lines). For $n - 3$, it was not even possible to load the matrix of the problem into the computer memory.

In this chapter, we not only consider individual security criteria, but also multiple security criteria simultaneously along with nodal injection uncertainty. In this case, it is necessary to decompose the problem in different levels. In this context, we propose an adaptive robust optimization model to address the aforementioned objectives. The proposed model is a trilevel formulation, where the two lowermost optimization problems represent an oracle that finds the worst-case scenario, i.e., a single scenario that causes the most severe imbalance in the system. This oracle

replaces the very large set of constraints added to the RG-TEP problem mimicking all future operations for each scenario.

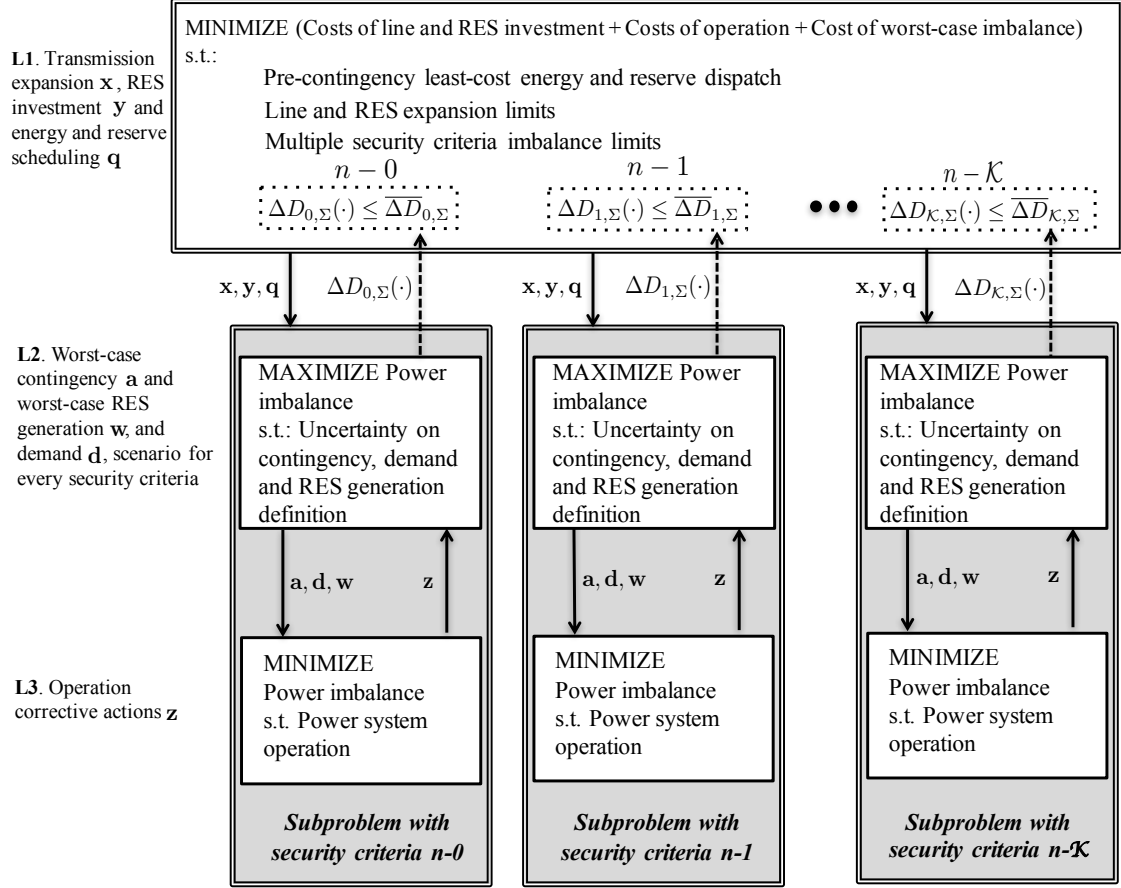


Figure 2.1: Three-level robust TEP framework

Each level, as illustrated in Figure 2.1, has its role described below.

- (i) *First Level*: This level determines the investment plan, i.e., it decides which candidate buses with potential renewable generation, \mathbf{y} , should be built and which candidate lines should be installed and how much should be their capacities, \mathbf{x} . In addition, pre-contingency energy and reserve system dispatch, \mathbf{q} , is also determined by the first level while meeting constraints associated with power balance, power flow, and generation limits.
- (ii) *Second Level*: Given the first-level decisions on investments and operation, the second level seeks to identify the contingency as well as the renewable nodal

injection and load demand realization that would together lead to the worst-case system power imbalance. If the imposed security criterion is $n - 1$, the contingency state identified in the second level will comprise the worst-case failure of one of the system elements. If it is $n - 2$ instead, the contingency identified will comprise the worst case combination of failures of two system elements. The same rationale applies for any $n - K$ security criterion. Hence, the second level finds simultaneously the values for the uncertainty parameters of renewable generation \mathbf{w} , load demand \mathbf{d} , and element failures \mathbf{a} that generate the worst imbalance in the system.

- (iii) *Third Level:* Once first and second level decisions are taken, the third level determines the post-contingency corrective actions, \mathbf{z} , to circumvent the worst-case realization of renewable generation and outages of system elements imposed in the second level. These corrective actions are performed by making use of the resources provided by the first level decision, e.g., newly built lines and scheduled reserves.

Note that, as we comprise multiple security criteria simultaneously in our formulation, second and third levels are replicated for each considered security criterion (see Figure 2.1). For example, for the compound security criterion $K(0 \rightarrow 1)$, we have replicated second and third level problems for each individual security level, namely $n - 0$ (where only renewable uncertainty is considered) and $n - 1$ (where both renewable and $n - 1$ security criterion are considered).

2.2.1 The TEP mathematical framework

In its compact mathematical programming form, the TEP problem involves the minimization of the total network investment cost and future operational costs to find

an optimal transmission expansion plan that enables the system to meet the future demand growth. In addition, in order to achieve national and/or regional renewable energy targets, a reinforced transmission infrastructure is also needed to deliver new renewable energy and reliably operate the power system while accommodating the variability of RES.

Under a deterministic framework, the load and supply (including RES generation) parameters are assumed to be known and given in advance. The compact form of a traditional TEP problem with RES co-optimization is depicted in (2.1).

$$\begin{aligned}
\min_{\mathbf{x}, \mathbf{y}, \mathbf{q}} \quad & \mathbf{c}_{lin}^\top \mathbf{x} + \mathbf{c}_{res}^\top \mathbf{y} + \mathbf{c}_{ope}^\top \mathbf{q} \\
\text{s.t.} \quad & (\mathbf{x}, \mathbf{y}) \in \mathcal{I} \\
& \mathbf{q} \in \mathcal{Q}(\mathbf{x}, \mathbf{y})
\end{aligned} \tag{2.1}$$

Variable \mathbf{x} is related to the investment in new transmission lines and their optimal capacity, \mathbf{y} is associated with the investment in renewable energy sources, and \mathbf{q} refers to the system operation variables (line flows, energy generated and nodal voltage angles). Within this context, model (2.1) does not consider investments in conventional units. Nevertheless, this model could be adapted to do so without interfering in the mathematical properties of the formulation. In addition, model (2.1) belongs to the class of static transmission planning, which determines the subset of candidate assets that should be built and where they should be located. Unlike dynamic planning however, the static framework does not consider the timing of the investments. Despite this limitation, static models allow for a better description of the system requirements, such as the security criteria imposed in this work. It is worth mentioning that static and dynamic approaches are likely to lead to different

results and a comparison between both frameworks to understand which one is more suitable is case-dependent. This comparison is out of the scope of this work. Here, we have chosen to formulate a static model in order to focus the investigation on the benefits provided by a reliability oriented expansion planning.

The objective function in (2.1) seeks to minimize the total investment costs related to the expansion/reinforcement of the network, the construction of new nodes for absorbing new renewable potential (or expanding existing capacities), and the system operation costs. Note that, in the presence of a deregulated competitive market for generation, RES investment are done by private entities (as in most of the countries). In this setting, \mathbf{c}_{res} is the cost of generation expansion. Notwithstanding, this cost could reflect centralized planning decisions by also including investment costs in RES. Feasible decisions on transmission investment and on development of new RES nodes belong to set \mathcal{I} , which represents: (i) candidate lines for expansion, (ii) candidate buses with RES potential, (iii) logic constraints that do not allow the construction of lines connecting the system to any candidate RES node where there is not investment in RES generation, and (iv) minimum renewable energy generation target. Finally, the system operation is modified by the network configuration and RES investments. The system operation is described by set $\mathcal{Q}(\mathbf{x}, \mathbf{y})$. Without loss of generality, we simplify the set of constraints for this basic TEP model with the symbol \mathcal{H} , i.e., $(\mathbf{x}, \mathbf{y}, \mathbf{q}) \in \mathcal{H} \iff \{(\mathbf{x}, \mathbf{y}, \mathbf{q}) | (\mathbf{x}, \mathbf{y}) \in \mathcal{I}, \mathbf{q} \in \mathcal{Q}(\mathbf{x}, \mathbf{y})\}$.

2.2.2 The $n - K$ -contingency-constrained TEP

The network planner should expand the system with adequate resources in order to ensure the reliability required in the operational level. Under the $n - K$ security criterion approach, the system should withstand the loss of up to K elements (see [14, 16, 17] and references therein). To achieve this objective, the scheduling of

reserves is necessary to meet demand under any possible post-contingency operation, i.e., after the loss of any combination K system elements. To deal with this problem, conventional contingency-constrained (CC) approaches are based on contingency-dependent models, which characterize the availability of the elements (generators or lines) under a given post-contingency state of the system by means of binary parameters. Within this context, a_i^G is defined to represent the availability of the generation unit i , i.e., a_i^G is equal to 1 if generator i is available, being 0 otherwise. Similarly, a_l^L is related to the availability of transmission line l . A post-contingency state κ represents a state of the system where a given set of its elements is out of service. Under this framework, any post-contingency state κ can be represented by a binary vector $\mathbf{a}(\kappa) = [\mathbf{a}^{G^\top}(\kappa), \mathbf{a}^{L^\top}(\kappa)]^\top$.

Under an $n - 1$ criterion, there must exist a feasible operating point after the outage of any individual element. Therefore, in contingency-dependent models, n sets of operation constraints, one for each possible post-contingency state κ , should be explicitly incorporated in the optimization problem. If the adopted security criterion is $n - 2$, then we have $\binom{n}{2}$ possible cases of post-contingency states to account for in the model and each one requires a set of operation constraints to be embedded into the problem. Clearly, the size of the problem easily reaches intractability as the security criterion considers higher order criteria. To cope with this problem, [44] proposes to consider the elements of the availability, or contingency, vector \mathbf{a} as binary decision variables of a second-level mixed integer optimization problem. This optimization level searches for the worst-case post-contingency state by maximizing, in the space of the availability vectors \mathbf{a} , the imbalance of the system given the first-level operational schedule. In this way, all contingencies are implicitly modeled in the formulation by the lower-level optimization problem (we refer to [17] for a simple example of this rationale). Thus, following the findings in [44], the $n - K$ -contingency-constrained TEP problem with RES co-optimization is formulated in

(2.2)–(2.4), where a cost penalty and a constraint are both considered for the worst-case imbalance, (2.4).

$$\min_{(\mathbf{x}, \mathbf{y}, \mathbf{q}) \in \mathcal{H}} \quad \mathbf{c}_{lin}^\top \mathbf{x} + \mathbf{c}_{res}^\top \mathbf{y} + \mathbf{c}_{ope}^\top \mathbf{q} + C^I \Delta D_K(\mathbf{x}, \mathbf{y}, \mathbf{q}) \quad (2.2)$$

$$\text{s.t.} \quad \Delta D_K(\mathbf{x}, \mathbf{y}, \mathbf{q}) \leq \overline{\Delta D}_K \quad (2.3)$$

$$\Delta D_K(\mathbf{x}, \mathbf{y}, \mathbf{q}) = \max_{\mathbf{a} \in \mathcal{U}_K^a} \left(\min_{\mathbf{z} \in \mathcal{Z}(\mathbf{x}, \mathbf{y}, \mathbf{q}, \mathbf{a})} \mathbf{c}_{cor}^\top \mathbf{z} \right) \quad (2.4)$$

The objective function (2.2) comprises the extra cost of the worst-case system power imbalance, $C^I \Delta D_K(\mathbf{x}, \mathbf{y}, \mathbf{q})$, which is the cost related to the worst realization of up to K simultaneous outages. The outer optimization problem in (2.4) is devoted to identify the availability binary vector \mathbf{a} with the worst combination of K outages (zeros) for a given solution of the TEP problem (line expansion, RES investments, and nominal operational plan that defines the scheduling of energy and reserves). The inner problem in (2.4) minimizes the system damage (imbalance) by means of corrective actions (up- and down-reserve deployment within the limits scheduled in the upper-level and taking into account the decision on network expansion) after a contingency occurs. The lower-level vector of variables \mathbf{z} is associated with the set of feasible corrective actions that can be taken by the system operator to redispatch the system after the occurrence of a given contingency. Such variables belong to set $\mathcal{Z}(\mathbf{x}, \mathbf{y}, \mathbf{q}, \mathbf{a})$, which depends on the remaining network configuration given by the availability vector \mathbf{a} , on the investment decisions, and on the scheduling of energy and reserves. Finally, in (2.3), an upper bound on the worst-case imbalance is imposed to express the reliability level required by the planner for the adopted criterion.

In order to comply with the aforementioned requirement for the imbalance function $\Delta D_K(\mathbf{x}, \mathbf{y}, \mathbf{q})$, the availability uncertainty set, \mathcal{U}_K^a , is defined as follows.

$$\mathcal{U}_K^a = \left\{ \mathbf{a} \in \{0, 1\}^n \mid \sum_i a_i^G + \sum_l a_l^L \geq n - K \right\}, \quad (2.5)$$

where n is the total number of elements in the system (generators and transmission lines). Note that the maximum number of simultaneous outages is K , regardless if they are lines or generators. This practice is referred to as a joint GT $n - K$ security criterion [17].

2.2.3 Modeling correlated RES generation and demand uncertainty

The expansion planning of a transmission infrastructure is a long-term problem. Some of the relevant issues that should be considered while determining such expansion are demand growth and future RES generation, which are not easy to forecast. Furthermore, RES generation variability requires higher levels of spinning reserves (generally from conventional generators) to ensure a secure operation. Hence, the transmission network plays a key role in making reserve sources accessible and in connecting RES injection to nodes with net demand. Within this context, in this chapter, we address the TEP problem while taking into account reserves needs, RES generation and demand uncertainty and their spatial correlation to guarantee deliverability of reserves. Spatial correlation between nodal demands and between nodal renewable injections are characterized by their nodal covariance matrices $(\boldsymbol{\Sigma}^d, \boldsymbol{\Sigma}^w)$, which are factorized via Cholesky decomposition [46], i.e, $\boldsymbol{\Sigma}^d = \mathbf{L}^d(\mathbf{L}^d)^\top$ for demand and $\boldsymbol{\Sigma}^w = \mathbf{L}^w(\mathbf{L}^w)^\top$ for RES generation. Within this context, RES generation and demand polyhedral uncertainty set is defined as:

$$\mathcal{U}_{\boldsymbol{\Sigma}}^{\mathbf{d}, \mathbf{w}} = \left\{ (\mathbf{d}, \mathbf{w}) \in \mathbb{R}^{n^d \times n^w} \mid \begin{aligned} \mathbf{d} &= \hat{\mathbf{d}} + s^d \mathbf{L}^d \mathbf{e}^d, \quad \|\mathbf{e}^d\|_1 \leq \Gamma^d, \quad \mathbf{e}^d \in [-1, 1]^{n^d} \\ \mathbf{w} &= \hat{\mathbf{w}} + s^w \mathbf{L}^w \mathbf{e}^w, \quad \|\mathbf{e}^w\|_1 \leq \Gamma^w, \quad \mathbf{e}^w \in [-1, 1]^{n^w} \end{aligned} \right\}, \quad (2.6)$$

where \mathbf{e}^d and \mathbf{e}^w are normalized error vectors whose components assume values between -1 and 1 for all n^d -demand-variable nodes and n^w -RES nodes; $\hat{\mathbf{d}}$ and $\hat{\mathbf{w}}$ are the vectors of nominal values of demand and RES generation, respectively. The uncertainty budget represented by Γ^d and Γ^w for demand and RES generation, respectively, controls the number of uncertain parameters that can deviate from their nominal value by means of norm-1 constraints imposed on the error vectors. Additionally, the amplitude of such deviations is controlled by s^d and s^w , respectively. Therefore, the level of conservativeness or stress associated with the uncertainty set is controlled by those four parameters. It is worth mentioning that such uncertainty set does not depend on the binary variable \mathbf{y} , which represents the decision to build or not a candidate bus. Finally, it is relevant to say that although possible cross-correlation between loads and renewable injections could be accounted for in the proposed framework, for the sake of simplicity, we do not consider this option in this work.

2.2.4 The reliable TEP model for large renewable energy penetration

The Cartesian product between the previously described uncertainty sets associated with the security criteria, demand and RES generation uncertainty results in $\mathcal{U}_{\Sigma, K}^{\mathbf{a}, \mathbf{d}, \mathbf{w}} = \mathcal{U}_K^{\mathbf{a}} \times \mathcal{U}_{\Sigma}^{\mathbf{d}, \mathbf{w}}$. By considering such combined uncertainty set, the transmission planning is intended to withstand, under a controlled level of imbalance, the loss of up to K elements of the system for all demand and RES generation scenarios comprised in $\mathcal{U}_{\Sigma}^{\mathbf{d}, \mathbf{w}}$.

In order to provide a wider control of the system reliability, we propose the utilization of multiple (simultaneous) GT $n - K$ security criteria. Although imbalance is not allowed in the pre-contingency state, the planner has the flexibility to control the

maximum imbalance under each $n - K$ security criterion comprised in the set of criteria \mathcal{K} , for all demand and renewable generation scenarios in $\mathcal{U}_{\Sigma}^{\mathbf{d},\mathbf{w}}$. The model is sketched in Fig. 2.1 and its compact mathematical formulation is the following:

$$\min_{(\mathbf{x},\mathbf{y},\mathbf{q}) \in \mathcal{H}} \mathbf{c}_{lin}^{\top} \mathbf{x} + \mathbf{c}_{res}^{\top} \mathbf{y} + \mathbf{c}_{ope}^{\top} \mathbf{q} + f\left(\{\Delta D_{K,\Sigma}(\mathbf{x},\mathbf{y},\mathbf{q})\}_{K \in \mathcal{K}}\right) \quad (2.7)$$

$$\text{s.t.} \quad \Delta D_{K,\Sigma}(\mathbf{x},\mathbf{y},\mathbf{q}) \leq \overline{\Delta D}_{K,\Sigma}, \quad \forall K \in \mathcal{K} \quad (2.8)$$

$$\Delta D_{K,\Sigma}(\mathbf{x},\mathbf{y},\mathbf{q}) = \max_{(\mathbf{a},\mathbf{d},\mathbf{w}) \in \mathcal{U}_{\Sigma,K}^{\mathbf{a},\mathbf{d},\mathbf{w}}} \left(\min_{\mathbf{z} \in \mathcal{Z}(\mathbf{x},\mathbf{y},\mathbf{q},\mathbf{a},\mathbf{d},\mathbf{w})} \mathbf{c}_{cor}^{\top} \mathbf{z} \right), \quad \forall K \in \mathcal{K}. \quad (2.9)$$

The rationale behind (2.7)–(2.9) comprises the minimization of costs associated with investment in lines, investment in new renewable generation, operation (reserve and generation scheduling) and system imbalance. The system imbalance is represented by the linear penalty function $f(\cdot)$, which returns the cost associated with the worst-case imbalance incurred under each security criteria. Additionally, the imbalance associated with the solution of (2.9) is limited by a user-defined threshold in (2.8). Problem (2.9) and imbalance limits (2.8) are parameterized by the security criterion level $K \in \mathcal{K}$. Under this framework, it is possible to set different admissible levels of system power imbalance depending on the security parameter K . For instance, we can impose no system power imbalance for conventional criteria, e.g. $n - 1$, while admitting an acceptable maximum amount of system power imbalance for higher-order security criteria.

The simultaneous consideration of multiple security criteria facilitates the control of the system reliability under customary and severe contingency conditions in the planning stage. Such framework can be used to assess the trade-off between the reliability provided by higher order security criteria and the cost to implement such criteria, which is incurred by network reinforcement and more conservative operation of the system. In a combined $(n - 0)(n - 1)(n - 2)(n - 3)$ security criterion, for example, the user may set a higher penalty cost and/or impose a stricter limit in

the right hand side of constraints (2.8) for imbalances caused by outages of one component, which have a larger probability to occur. On the other hand, a smaller penalty cost would be set for imbalances caused by contingencies comprising three components, which are less likely to materialize. It is worth mentioning that when considering a single $n - 3$ security criterion and allowing an acceptable amount of system power imbalance, it is not possible to guarantee that the decision will impose a null imbalance for lower order security criteria such as $n - 2$, $n - 1$, or even $n - 0$ security criteria.

Finally, the set of corrective actions of the third-level, $\mathcal{Z}(\mathbf{x}, \mathbf{y}, \mathbf{q}, \mathbf{a}, \mathbf{d}, \mathbf{w})$, considers the redispatch of the system after the occurrence of a given contingency, \mathbf{a} , and realization (scenario) of demand and renewable generation, (\mathbf{d}, \mathbf{w}) . It is worth mentioning that \mathcal{Z} is a polyhedral set of the form $\mathbf{A}\mathbf{z} \leq \mathbf{b}(\mathbf{x}, \mathbf{y}, \mathbf{q}, \mathbf{a}, \mathbf{d}, \mathbf{w})$. Thus, the first and second-level variables only affect the third-level problem through its right-hand-side. In appendix A, the detailed mathematical formulation for the three-level model (2.7)–(2.9) is provided.

2.3 Solution approach

The proposed TEP formulation, (2.7)–(2.9), is a three-level optimization model (see Fig. 2.1), which can be conveniently reformulated as an equivalent bilevel program. To carry out this transformation, we first notice that the third level minimization problem is a linear program, therefore its primal and dual versions have the same optimal solution. In addition, the dual of the third level is a maximization problem aligned with the objective of the middle level problem. Then, the original middle level maximization problem, (2.9), which aims to find vectors $(\mathbf{a}, \mathbf{d}, \mathbf{w})$ that maximize the optimal value of the third-level problem, is thus rewritten to maximize the lower-level dual-objective function, $\mathbf{b}(\mathbf{x}, \mathbf{y}, \mathbf{q}, \mathbf{a}, \mathbf{d}, \mathbf{w})^\top \boldsymbol{\mu}$. In such new problem, the

original lower-level dual decision vector, $\boldsymbol{\mu}$, is considered as an additional optimization variable. Moreover, due to strong duality, by taking into account the lower-level dual feasibility, $\boldsymbol{\mu} \in \mathcal{Z}^D$, the optimal value of the new second-level problem meets the third-level one. As a result, levels 2 and 3 are recast as an equivalent single-level mixed integer nonlinear problem parameterized on the upper-level decisions. After this transformation, the following equivalent-bilivel optimization problem, (2.10)–(2.12), is obtained:

$$\min_{(\mathbf{x}, \mathbf{y}, \mathbf{q}) \in \mathcal{H}} \quad \mathbf{c}_{lin}^\top \mathbf{x} + \mathbf{c}_{res}^\top \mathbf{y} + \mathbf{c}_{ope}^\top \mathbf{q} + f\left(\{\Delta D_{K,\Sigma}(\mathbf{x}, \mathbf{y}, \mathbf{q})\}_{K \in \mathcal{K}}\right) \quad (2.10)$$

$$\text{s.t.} \quad \Delta D_{K,\Sigma}(\mathbf{x}, \mathbf{y}, \mathbf{q}) \leq \overline{\Delta D}_{K,\Sigma}, \quad \forall K \in \mathcal{K} \quad (2.11)$$

$$\Delta D_{K,\Sigma}(\mathbf{x}, \mathbf{y}, \mathbf{q}) = \max_{\substack{(\mathbf{a}, \mathbf{d}, \mathbf{w}) \in \mathcal{U}_{\Sigma, K}^{\mathbf{a}, \mathbf{d}, \mathbf{w}}, \\ \boldsymbol{\mu} \in \mathcal{Z}^D}} \mathbf{b}(\mathbf{x}, \mathbf{y}, \mathbf{q}, \mathbf{a}, \mathbf{d}, \mathbf{w})^\top \boldsymbol{\mu}, \quad \forall K \in \mathcal{K}. \quad (2.12)$$

Similarly to [17, 44], the worst-case imbalance function $\Delta D_{K,\Sigma}(\mathbf{x}, \mathbf{y}, \mathbf{q})$ (which is a recourse function) is the maximum of affine functions of the first-level variables parameterized on the second-level feasible solutions. Therefore, it is a convex function. Under this assumption, model (2.10)–(2.12) is suitable for both Benders decomposition (dual approach) and column-and-row generation (primal approach) algorithms, which ensure convergence to a near-global-optimal solution. Finally, following the findings of [44] and [42], bilinear terms in the objective function (2.12) (due to the product between $\boldsymbol{\mu}$ and the middle-level variables, $\mathbf{a}, \mathbf{d}, \mathbf{w}$) can be linearized. Thus, (2.10)–(2.12) can be solved by means of available mixed integer linear programming (MILP) commercial solvers [47]. The detailed solution methodology is presented in appendix B.

2.4 Case Studies

The performance of the proposed model and solution methodology is illustrated in this section. Three cases are utilized to do so. The first one comprises a small 3 (existing) + 2 (candidate)-bus test system that illustrates the impact of considering multiple security criteria under the presence of correlated-renewable injection uncertainty. The second case, based on the main Chilean power system, demonstrates the effectiveness of the proposed methodology in a realistic case study. Finally, the third one, based on the standard IEEE 118-bus system, analyses the performance of the solution algorithm for a meshed topology with more than hundred buses.

The presented methodology was implemented on a computer with two Intel® Xeon® E5-2697 v2 processors at 2.7 GHz and 512 GB of RAM, using Xpress-MP 7.8 under MOSEL [47].

2.4.1 (3e+2c)-Bus System Case Study

As depicted in Fig. 2.2, this system has three existing buses with eight conventional generation units and two candidate buses with potential wind generation. The system comprises two existing transmission assets and twenty-one candidates, which are represented by the dashed lines. Each dashed line corresponds to several candidate circuits. In this case study, we set the standard deviation of the renewable generation of buses 4 and 5 to 23.11% of their maximum output and we consider s^w equal to 1. Then, we perform a sensitivity analysis on the correlation factor ρ . The dashed line between buses 1 and 2 comprises 9 candidate circuits, whereas each dashed lines between buses 2 and 3, 4 and 2, and 5 and 2 refers to 4 candidate circuits. Detailed data for this case study can be found in the data document [48].

To depict the impact of considering multiple security criteria under the presence of correlated-renewable injection uncertainty, four different combined security criteria

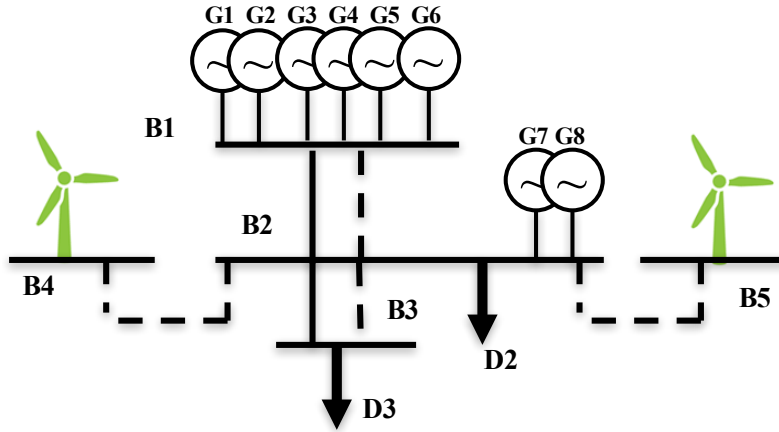


Figure 2.2: 3(existing)+2(candidate)-nodes power system

are considered in each study: 1) pure ($n - 0$), where only renewable variability is addressed, 2) combined ($n - 0$) and ($n - 1$), 3) combined ($n - 0$), ($n - 1$), and ($n - 2$), and 4) combined ($n - 0$), ($n - 1$), ($n - 2$) and ($n - 3$). Hereinafter, we use the acronym $K(0)$ to represent a single ($n - 0$) security criterion, whereas $K(0 \rightarrow 3)$ refers to a compound security criterion ranging from ($n - 0$) to ($n - 3$). For all of the composed criteria, renewable variability is considered as described in the previous section. For simplicity purposes, demand variability is neglected.

In this case study, a sensitivity analysis is performed to investigate the impact of correlation between renewable sources under combined security criteria on spinning reserve costs and transmission expansion investments. For the individual security criteria ($n - 0$), ($n - 1$), and ($n - 2$) comprised in the aforementioned combined criteria, we consider the penalization cost $C_{K=0,1,2}^I$ equal to $4 \times 10^3 \$/MWh$, and for the individual ($n - 3$), the penalization $C_{K=3}^I$ is set to $600 \$/MWh$. The tolerance for convergence is 5×10^{-3} . In addition, the available renewable nominal generation in the two candidate buses corresponds to 63.1% of the total energy demand. Finally, the spillage factor γ^{Spil} is set to 10^{-2} .

In Table 2.1, the costs associated with reserve levels for each considered correlation and combined security criteria are shown. There is a clear pattern of increase in

Table 2.1: Total Reserve Cost (\$/hour)

| Correlation | Security Criteria | | | |
|-------------|-------------------|----------------------|----------------------|----------------------|
| | $K(0)$ | $K(0 \rightarrow 1)$ | $K(0 \rightarrow 2)$ | $K(0 \rightarrow 3)$ |
| -100% | 0.00 | 162.00 | 349.00 | 1069.22 |
| -50% | 95.99 | 282.19 | 492.79 | 6992.92 |
| 0% | 111.38 | 300.88 | 515.38 | 7945.11 |
| 50% | 177.50 | 384.60 | 654.30 | 11336.40 |
| 100% | 248.50 | 480.50 | 3693.50 | 14845.60 |

reserve needs when the security criterion becomes tighter. In addition, as correlation increases, the required levels of spinning reserves become higher.

Table 2.2: Total Investment in Lines (\$/hour)

| Correlation | Security Criteria | | | |
|-------------|-------------------|----------------------|----------------------|----------------------|
| | $K(0)$ | $K(0 \rightarrow 1)$ | $K(0 \rightarrow 2)$ | $K(0 \rightarrow 3)$ |
| -100% | 6704.62 | 13760.30 | 21477.00 | 29307.80 |
| -50% | 7916.44 | 15064.90 | 22652.90 | 28361.10 |
| 0% | 7954.40 | 15122.20 | 22791.30 | 28043.30 |
| 50% | 7990.86 | 15159.90 | 22859.90 | 29151.10 |
| 100% | 9319.00 | 16374.50 | 22947.00 | 29330.40 |

Table 2.2 displays the investments in transmission lines undertaken for each correlation and combined security criteria. As we can see, a correlation increase leads to higher investments in transmission lines for combined security criteria up to $K(0 \rightarrow 2)$. Two reasons are behind this effect. The first is due to the fact that usually additional line capacity is needed to accommodate positively correlated peaks of renewable injection. The second is related to the ability to deliver reserves. The higher the correlation between RES buses, the higher the required reserve level to ensure system reliability. Since the cheapest conventional generators are located at bus 1, a higher correlation implies in more investment to bring cheap reserves from bus 1, i.e., an extra investment is needed to ensure reserve deliverability. However, for the $K(0 \rightarrow 3)$ criterion, the pattern for investments in lines is broken since the available candidate lines are not sufficient to bring the required levels of cheap reserves from bus 1. This is reflected in the faster rate of growth of reserve costs

for $K(0 \rightarrow 3)$ from correlation equal to -100% up to correlation equal to 100%, as reported in Table 2.1.

2.4.2 Main Chilean Power System Case Study

We illustrate the proposed model using a stylized representation of the main Chilean power system (Sistema Interconectado Central, or its acronym SIC). The stylized SIC comprises 27 nodes, 52 existing lines, and 282 generating units. The data (transmission lines, generating units, locations, demands, etc) is obtained from the Chilean Regulatory Authority [49] and SIC System Operator [50]. We have chosen 66 candidates lines for expansion. Full generation, lines and demand data are available in [48]. Our study focuses on the year 2025, for which Chilean Law has set a 20% renewable energy generation target. Nodal demand is projected according to the CNE's technical report [49]. We have considered here that renewable generation targets are reached with wind and solar energy resources only. Potential future RES generation data are obtained from the MAPS-Chile initiative project [51].

We have imposed simultaneous security criteria with different thresholds. System power imbalance is limited in terms of the total demand to 0% for the individual security criteria $(n - 0)$, $(n - 1)$, and $(n - 2)$ and to 2.5% for the individual $(n - 3)$. In addition, load shedding is penalized with a cost of 4×10^4 \$/MWh, and the convergence gap is set to 5×10^{-3} for imbalances associated with up to two outages, while imbalances associated with three outages are penalized by 40\$/MWh, with a convergence gap of 3×10^{-2} . Finally, the spillage factor γ^{Spil} is set to 10^{-3} in this case study.

The model outcomes are summarized in Table 2.3. In columns 2 to 5, results for different security criteria are provided. In rows 2 to 5, we present the costs related to operation of and investment in new transmission lines and renewable energy capacity

Table 2.3: Results for the Chilean Power System

| Security Criteria | $K(0)$ | $K(0 \rightarrow 1)$ | $K(0 \rightarrow 2)$ | $K(0 \rightarrow 3)$ |
|----------------------------------|--------|----------------------|----------------------|----------------------|
| Total Sys. Cost(10^3 \$) | 236.89 | 250.70 | 261.96 | 268.79 |
| Total Ope. Cost(10^3 \$) | 201.41 | 215.12 | 222.72 | 228.98 |
| Inv. in Trans. Lines(10^3 \$) | 6.69 | 6.77 | 10.43 | 11.00 |
| Inv. in New Buses(10^3 \$) | 28.80 | 28.80 | 28.80 | 28.80 |
| Down Spinning Reserve(MW) | 0 | 1511.88 | 2932.13 | 3035.17 |
| Up Spinning Reserve(MW) | 114.00 | 1161.91 | 1526.06 | 2287.67 |
| No. of Lines Built | 14 | 14 | 25 | 27 |
| RES Penetration (%) | 20.25 | 20.25 | 20.25 | 20.25 |
| Aver. Inv.&Ope. Cost(\$/MWh) | 20.94 | 22.16 | 23.16 | 23.76 |
| WC LOL for $K = 0$ (%) | - | - | - | - |
| WC LOL for $K = 1$ (%) | 12.16 | - | - | - |
| WC LOL for $K = 2$ (%) | 20.48 | 5.56 | - | - |
| WC LOL for $K = 3$ (%) | 23.76 | 13.29 | 7.82 | 1.82 |
| Time of resolution (s) | 88.01 | 1408.28 | 47226.90 | 78358.40 |

expansion in thousands of dollars¹. As it is expected, operation costs increase while the imposed security criteria becomes tighter. However, investment costs in new RES nodes as well as RES penetration remain equal for all security criteria, as shown in rows 5 and 9. In order to accomplish identical RES penetration with different and more stringent security criteria, it is necessary to undertake higher investments in transmission lines. Thus, if the expansion is planned without security criteria, the number of constructed lines is 14, with a cost of 6.69 thousand dollars. However, under the combined $K(0 \rightarrow 3)$ security criterion, the number of built lines increases to 27, resulting in a cost of more than 11 thousand dollars. It is worth mentioning that costs presented in Table 2.3 refer to one hour of operation. Thus, the value of 6.69 thousand dollars per hour associated with line investments for $K(0)$ is actually equivalent to approximately 58.60 million dollars per year. Assuming a 30 years life time, this is equivalent to 1.80 billion dollars. Similar results have been reported

¹These results are associated with a single time interval, i.e., a representative worst-case hour obtained by the two lowermost optimization problem. This is consistent with previously reported works on the subject of static planning, [23, 43, 44], and sufficient to capture the effect of the new features proposed in this study.

previously in [52] for the Chilean system. Levels of up- and down-spinning reserves are shown in rows 6 and 7. Such levels of up and down reserves rise from light to rigorous security criteria.

The optimal number of lines to build, the percentage of renewable penetration, and the total average cost per MWh of demand for each security criterion are respectively shown in rows 8, 9, and 10 of Table 2.3. Note that the average cost of the energy supply is calculated by taking into account operational, RES capacity, and transmission expansion costs. In this study, for a renewable penetration equal to 20.25% of the demand share, for all cases, the average cost slightly increases as the imposed security criteria become tighter. It should be noted that the investment in new lines to comply with $K(0 \rightarrow 1)$ criterion is slightly higher than the necessary investment required by pure $K(0)$. In this case, most of the increase in reliability is addressed by significantly higher levels of allocated reserves. However, under a $K(0 \rightarrow 2)$ criterion, both investment plan and reserve levels notably differ from the $K(0 \rightarrow 1)$ case due to the quasi-radial characteristics of the Chilean power system. Nevertheless, since more lines are built for $K(0 \rightarrow 3)$ than for $K(0)$ and these lines are strategically chosen to guarantee security at minimum cost, the delivery of cheaper reserves is facilitated. As a consequence, although the up-spinning reserve requirements rise from 114MW for $K(0)$ to 2287.67MW for $K(0 \rightarrow 3)$, the operational cost only increases less than 14% from $K(0)$ to $K(0 \rightarrow 3)$. This effect reinforces the importance of considering reserve deliverability while planning system expansion as it is proposed in the methodology presented in this work.

The worst-case load shedding for contingencies with up to 3 outages is shown in rows 11 to 14. According to these results, an expansion plan without any security criteria could lead to severe costs of load shedding. More specifically, 12.16% of the load demand may be curtailed by a single outage, while up to 23.76% of the load demand may be non-served due to a combination of 3 simultaneous outages.

However, an increase in the security requirement implies in significant reduction of the worst-case load shedding, which drops under the given threshold at the expense of having higher system operational and investment costs, as expected. Finally, CPU times to achieve the solutions are shown in row 14.

In order to assess the reliability of the solutions provided by the proposed methodology, we performed an out-of-sample Monte Carlo simulation test. This test aims to analyze the reliability and cost for the solutions obtained using different compound security criteria. To do that, after running the model, we generated 10,000 scenarios assuming independently generated Bernoulli trials for each line and generator state (1 for on-service and 0 for out-of-service state), with 0.1% and 1% probability for the out-of-service states, respectively, according to [53]. Renewable generation output scenarios are obtained by means of multivariate Gaussian random samples with mean equal to the estimated values for the nominal outputs and covariance matrix used in the uncertainty set definition. Therefore, it is worth mentioning that this out-of-sample numerical testing is based on scenarios generated under higher uncertainty than that used to construct the optimization problem.

Table 2.4 shows the load shedding level, or loss of load (LOL), for different solutions, each of them obtained for different security criteria. The expected value (average among all the 10,000 scenarios) and the conditional value at risk (CVaR) with 95% confidence (average among the highest 500 scenarios) for the LOL are shown in rows 11 and 12 of Table 2.4.

In the $K(0)$ case, where no security criterion is enforced and only renewable variability is taken into account through $\mathcal{U}_{\Sigma,K}^{\mathbf{a},\mathbf{d},\mathbf{w}}$ (column 2 of Table 2.4), there is a significant probability of observing a deep LOL. According to column 2, the probability of an event in which a LOL of 5 to 10% of the overall system demand takes place exceeds 20%. Also for the $K(0)$ case, although the expected LOL corresponds to 3.49%

Table 2.4: Out-of-sample Monte Carlo Simulation Test for the Chilean Power System

| Security Criteria | $K(0)$ | $K(0 \rightarrow 1)$ | $K(0 \rightarrow 2)$ | $K(0 \rightarrow 3)$ |
|-------------------------------|--------------------------|--|--|--|
| LOL Interval (% of demand) | LOL Probability | | | |
| =0% | 11.77% | 85.72% | 93.72% | 96.88% |
| (0-1]% | 7.65% | 2.94% | 2.22% | 0.87% |
| (1-2]% | 15.99% | 4.35% | 1.92% | 1.10% |
| (2-3]% | 15.44% | 2.94% | 1.10% | 0.60% |
| (3-4]% | 13.84% | 1.86% | 0.56% | 0.24% |
| (4-5]% | 10.25% | 1.12% | 0.23% | 0.19% |
| (5-10]% | 21.81% | 1.04% | 0.25% | 0.12% |
| >10% | 3.25% | 0.03% | 0.00% | 0.00% |
| Expected LOL (% of demand) | 3.49% | 0.34% | 0.12% | 0.06% |
| CVaR of the LOL (% of demand) | 11.13% | 4.20% | 2.16% | 1.23% |
| Expected Total Costs [K\$] | 410.01 | 268.82 | 269.19 | 272.46 |
| CVaR of the Total Costs [K\$] | 746.52 | 442.48 | 361.11 | 330.38 |

of the demand, the 95%-CVaR reaches the amount of 11.13%. If the $K(0 \rightarrow 1)$ security criterion (column 3 of Table 2.4) is chosen, the reliability of the system significantly increases in comparison to $K(0)$ criterion. For instance, the probability of having zero LOL increases from 11.77% to 85.72% (row 1 of Table 2.4). However, for the $K(0 \rightarrow 1)$ case, more than 6% of the scenarios still imply in LOL higher than 2%. For the compound security criteria $K(0 \rightarrow 2)$ and $K(0 \rightarrow 3)$, the levels of 95%-CVaR of LOL significantly decrease to 2.16% and 1.23% of the system demand, respectively. Also, according to the fourth and fifth columns of Table 2.4, the probability of experiencing scenarios in which the loss of load is higher than 2% of the system demand falls to 2.14% and 1.15%, respectively.

The last two rows of Table 2.4 show the expected and 95%-CVaR of total (first and second stage) costs for the four planning solutions associated with the security levels under consideration. Observe that, as a result of the protection provided, the more stringent security criteria, the lower the CVaR of the total costs (transmission investments plus operation costs plus system power imbalance costs). It should be noted that the expansion plan without any security criteria results in the most

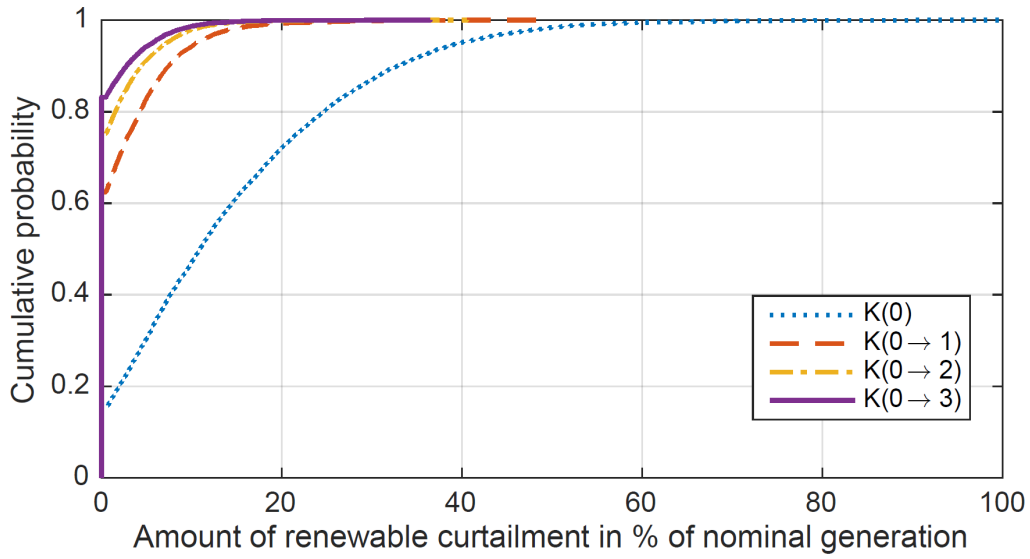


Figure 2.3: Empirical CDF of renewable curtailment from Monte Carlo simulation

expensive aggregate cost due to its corresponding high load shedding and renewable curtailment.

Figure 2.3 shows the cumulative distribution function of the renewable curtailment. This curtailment is measured in terms of percentage of the total nominal RES generation capacity after investment. Although all optimal expansion plans reach 20.25% of renewable penetration (see Table 2.3), there is significant renewable curtailment depending on the assumed security level requirement. For instance, if no security criterion is imposed, only less than 20% of the scenarios do not incur in renewable curtailment. On the other hand, if $K(0 \rightarrow 3)$ security criterion is enforced, more than 80% of the scenarios do not have renewable curtailment.

2.4.3 (118e+4c)-Bus System Case Study

In this case study, we apply the proposed methodology for a modified version of the standard IEEE 118-bus test system. Here, we consider this system with 118 existing buses, 4 candidates buses with potential renewable generation sources, and 53 candidate transmission lines. Such candidate sources, if connected to the system, can contribute together to meet up to 24.81% of the system demand with their nominal

output. Each of these potential renewable sites is considered to have a standard deviation equivalent to 17% of its maximum generation output. In addition, the correlation factors between the outputs of candidate buses 119 and 120 and between the outputs of candidate buses 121 and 122 are set to 0.75. For the $(n - 0)$, $(n - 1)$, and the $(n - 2)$ security criteria, null load shedding is imposed, whereas, 3.5% of load shedding is allowed in the worst case of triple contingencies. In this case study, the target to meet at least 20% of demand by renewable generation is also imposed. Full data for this case study can be accessed in [48].

Table 2.5: Results for the (118e+4c)-Bus System

| Security Criteria | $K(0)$ | $K(0 \rightarrow 1)$ | $K(0 \rightarrow 2)$ | $K(0 \rightarrow 3)$ |
|-------------------------------|--------|----------------------|----------------------|----------------------|
| Total System Cost(10^3 \$) | 18.93 | 21.72 | 36.86 | 37.50 |
| Down Spinning Reserve(MW) | 12.00 | 28.00 | 28.00 | 29.00 |
| Up Spinning Reserve(MW) | 28.00 | 301.02 | 245.28 | 275.29 |
| Number of Lines Built | 6 | 8 | 21 | 21 |
| Time of resolution (s) | 14.09 | 898.76 | 18,934.50 | 20,393.70 |

Table 2.5 summarizes the attained results for this system. Total (operation and investments) system cost increases with the stringency of the security criterion. The renewable generation expansion solution reaches the maximum level (24.81%) available for all criteria. The level of down-spinning reserves grows with the safety of the system. However, the required level of up-spinning reserves decreases from the $K(0 \rightarrow 1)$ to the $K(0 \rightarrow 2)$ security criteria since there is a major investment in the transmission network. This investment enables the procurement of cheaper reserves to meet the security requirement. In addition, the deliverability of reserves is improved, therefore eliminating the need for redundant amounts of reserves. This optimal balance between reserves and transmission expansion is only possible due to the explicit consideration of reserves into the RG-TEP problem. Time of resolution is shown in the last row for all criteria.

CHAPTER 3

A Five-Level MILP Model for Flexible Transmission Network Planning under Uncertainty: A Min-Max Regret Approach

Transmission expansion plays a key role in integrating growing volumes of renewable energy sources (RES) and thus in decarbonizing power systems. Planning new transmission assets to integrate RES, however, has become increasingly difficult due to mid- and long-term uncertainties associated with the amount and location of deployment of renewable generation [28,54,55]. Additionally, network design has to be secured [44,56] which refers to the need to withstand outages of components through an efficient portfolio of preventive and corrective actions. As a consequence, there is growing interest in system models that can inform future transmission network

planning in order to accommodate the forthcoming renewable generation (that is uncertain) in an economically efficient and secured fashion. In this context, this chapter proposes a novel optimization model for transmission expansion planning (TEP) based on the concept of min-max regret [57] that considers uncertainties associated with future generation expansion while taking into account deterministic security standards.

Recent works have addressed transmission expansion planning to comply with reliability standards [56], [44]. In [56], a trilevel model to plan transmission investments under uncertain demand and wind generation is proposed. In order to tackle the problem of expanding transmission infrastructure while complying with deterministic $n - K$ security criterion, [44] proposed a two-stage robust optimization model to consider all possible generation and transmission contingencies in the transmission expansion planning framework. Despite the relevance of the aforementioned works, they did not consider opportunities for investment in flexible alternating current transmission system (FACTS) devices, which can improve the flexibility of the transmission network to deal with uncertainty and also support delivery of system security requirements at efficient cost.

In effect, the role of FACTS devices has received considerable attention in recent literature [58–62]. In [58], the DC optimal power flow (DC-OPF) problem is formulated as a non-linear model, which is then recast as a MILP, effectively representing the role of FACTS in providing flexibility and hence reducing operating costs. In [59], an approach for deciding day-ahead dispatch that considers FACTS devices to facilitate corrective actions is proposed. In [60], the authors provide an assessment of the benefits of flexible DC and AC transmission assets when considering post-contingency control of FACTS setpoints. On the transmission planning side, [61] presents a MILP model to address the TEP problem considering series compensation devices among the candidate transmission assets without imposing security

criteria. In [62], a stochastic TEP model is proposed to assess the value of incorporating flexible assets to the grid. The importance of the aforementioned progresses notwithstanding, determining optimal portfolios of conventional and flexible network investments while optimizing pre- and post-fault operational measures (from generation and network components) to efficiently and securely deal with long-term uncertainties (volume and location of future generation) and system failures has not yet been addressed.

Under a contingency state, besides deciding the set of post-contingency corrective actions, system operators must also ensure deliverability of scheduled reserves in order to match supply and demand post-fault without overloading network infrastructure. In some conditions, however, it may be difficult to guarantee deliverability of reserves while respecting Kirchhoff's laws due to the presence of network loop flows as shown in [63]. In this case, the flexibility provided by FACTS devices may play a fundamental role, offering the necessary leeway to ensure supply-demand balance while complying with network constraints following the occurrence of an outage of any generation plant or transmission circuit. Thus, this chapter analyses the possibility of investing in phase-shifters alongside transmission lines to reinforce the grid.

The value of the notion of regret as an approach to measure risk in decision making under uncertainty has already been recognized in the classical academic literature [64, 65]. In the context of expansion planning models for power systems, approaches based on the minimization of the maximum regret have been proposed in the nineties [66] for generation expansion planning and recently for transmission expansion planning [55, 67]. In addition, in industry, the min-max regret has also been already accepted as the most appropriate metric for transmission expansion planning by the major player of the power sector in the UK, namely National Grid [68, 69]. Despite the relevance of the aforementioned academic works, they do

not consider all the features that are simultaneously included in our proposed methodology. These features are: (i) the determination of the transmission expansion plan that minimizes the regret of the system planner under uncertainty in future generation expansion; (ii) the inclusion of deterministic security criterion ($n - K$) to better characterize the operational side while planning the transmission expansion; (iii) the incorporation of flexible devices among the candidate transmission assets to provide better controllability of the transmission grid; (iv) and the consideration of the balance between scheduling spinning reserves and investing in transmission assets. The simultaneous inclusion of all the aforementioned features in a single methodology is a key factor that allows in the planning stage the consideration of the value of investing in transmission assets that increase operational flexibility. The benefit of considering these features in the transmission expansion problem notwithstanding, it implies significant challenges mostly due to computational burden since the number of constraints to represent them may render the problem intractable. To circumvent these challenges, in this chapter, we propose a five-level formulation for the TEP problem considering features (i) to (iv), which precisely reproduce the decision process hierarchy faced by the decision maker, and a solution methodology based on a decomposition scheme capable to provide near-optimal solutions with moderate computational effort.

Regarding the min-max regret approach utilized by National Grid, it should be noted that such approach is a heuristic process that cannot guarantee optimality. As described in [69], National Grid considers only a few candidate transmission plans. Each of these plans is obtained by selecting an individual scenario of generation expansion and identifying the best transmission expansion plan for this particular scenario under perfect information. Then, the regret of using the best solution of one particular scenario is evaluated under the realization of the other scenarios. This process is repeated for each candidate transmission plan (there is one candidate

transmission plan per scenario under perfect information). The preferred option is then chosen in [69] as the option that leads to the minimum maximum regret. This approach may be narrow in scope since it may disregard investments that have potential to minimize the maximum regret but do not appear in any of the solutions under perfect information. The need for considering in the planning model many operational details, which significantly affect the investment plan and therefore need to be considered, imposes computational challenges that justify the use of a heuristic process. However, this choice also imposes sub optimality. Hence, we propose a methodology that more comprehensively minimizes the maximum regret by considering all possible transmission plans (i.e. all possible combinations of candidate transmission assets) to minimize the maximum regret in our proposed optimization model while considering relevant details from the operational side that affect the evaluation of the resulting operational cost.

The concept of minimizing the maximum regret in the TEP problem under uncertainty in future generation capacity has already been addressed in [55], which also provides a comprehensive comparison between min-max cost and min-max regret approaches.

Likewise, the methodology proposed in the present work also considers the TEP problem under uncertainty in future generation capacity. However, this chapter is different to [55] in four remarkable aspects. Firstly, unlike [55], we consider industry reliability practices and model deterministic $n - 1$ security criterion, i.e., the resulting transmission plan effectively provides system operators with necessary set of preventive and corrective actions to withstand any credible outage while planning the system dispatch. Secondly, flexible network investment is considered through phase-shifters that are included in the array of candidate transmission assets, and this is critical to efficiently deal with contingencies and long-term uncertainty in volume and location of RES. Thirdly, the scheduling of spinning reserves is taken

into account so that the trade-off between operational measures (scheduling reserves) and installing new transmission assets can be truly optimized. Finally, instead of considering continuous intervals of future newly added capacity, our proposition accounts for a set of discrete, credible expansion scenarios¹. Regarding the discrete set of generation expansion scenarios, it is worth mentioning that we do not claim that this proposed approach to represent the uncertainty in generation expansion is more (or less) appropriate than that proposed in [55]. Instead, we argue that our approach constitutes an interesting alternative that is in line with current industry practices. Moreover, it is important to highlight that the consideration of security criteria in the min-max regret model implies significant changes in the modeling structure as compared to [55], regardless of the scenarios considered for generation expansion. Hence, the 5-level optimization model and the solution algorithm proposed in this chapter are required to deal with the improvements carried out.

The remainder of the chapter is organized as follows. Section 3.1 specifies the nomenclature associated with this chapter. Section 3.2 presents the 5-level framework proposed; Section 3.3 shows the mathematical formulation; and Section 3.4 describes the proposed solution methodology. Finally, in Section 3.5, we present the case studies.

3.1 Nomenclature

The mathematical symbols used throughout this chapter and its corresponding appendix are classified below as follows.

Sets

I Set of indexes of all generators, equal to $(I_c \cup I_w)$.

¹In the UK, for instance as explained in [69], National Grid represents uncertainty in future energy capacity by means of four representative plausible scenarios. These scenarios are developed after an extensive consultation of industry experts. In this chapter, we also use a discrete set of scenarios following this industry practice. However, the generation of such scenarios is out of the scope of this thesis. We aim to provide a methodology for which these scenarios are an input. The scenarios used in this chapter are illustrative.

I_b Set of indexes of generators connected to bus b .

I_c Set of indexes of conventional power plants.

I_w Set of indexes of potential new renewable generators.

\mathcal{L} Set of indexes of all transmission lines, equal to $(\mathcal{L}^C \cup \mathcal{L}^F \cup \mathcal{L}^{PS})$.

\mathcal{L}^C Set of indexes of transmission lines that are candidate to be built.

\mathcal{L}^F Set of indexes of fixed existing transmission lines, i.e, existing lines that are not candidate for placement of phase shifters.

\mathcal{L}^{PS} Set of indexes of existing transmission lines that are candidate for placement of phase shifters.

N Set of indexes of buses.

Functions

$I(\cdot)$ Investment cost function.

$MaxReg(\cdot)$ Maximum regret function.

Parameters

$\bar{\psi}$ Capacity limit of phase shifters.

C_l^{Cap} Annual cost per MW of candidate line l .

C_i^D Reserve-down cost of generator i .

C_l^{fix} Annual fixed cost of installation of candidate transmission asset l .

C^I Cost of system power imbalance.

C_i^P Production cost of generator i .

C^S Cost of wind spillage.

C_i^U Reserve-up cost of generator i .

D_{bt} Demand at bus b , during snapshot t .

d_t Number of hours of snapshot t .

\bar{F}_l Power flow capacity of existing line l .

\bar{f}_l^C Maximum power flow capacity of candidate line l .

$fr(l)$ Sending or origin bus of line l .

\bar{P}_i Capacity of generator i .

R_i^D Reserve-down limit of generator i .

R_i^U Reserve-up limit of generator i .

$to(l)$ Receiving or destination bus of line l .

\bar{W}_{its} Available capacity of renewable generator i at snapshot t in scenario s .

x_l Reactance of line l .

Decision Variables

Δ_t System power imbalance at snapshot t under the worst-case contingency given a transmission expansion plan, a generation expansion realization, and a scheduling of power and reserves.

ΔD_t^{wc} System power imbalance at snapshot t under the worst-case contingency given a transmission expansion plan, a generation expansion realization, and a scheduling of power and reserves.

ΔD_{bt}^+ Power surplus at bus b , at snapshot t .

ΔD_{bt}^- Power deficit at bus b , at snapshot t .

θ_{bt} Phase angle at bus b , at snapshot t , in the pre-contingency state.

θ_{bt}^{wc} Phase angle at bus b , at snapshot t , under the worst-case contingency given a transmission expansion plan, a generation expansion realization, and a scheduling of power and reserves.

ψ_{lt} Phase-shifting angle in line l , at snapshot t , in the pre-contingency state.

ψ_{lt}^{wc} Phase-shifting angle in line l , at snapshot t , under the worst-case contingency given a transmission expansion plan, a generation expansion realization, and a scheduling of power and reserves.

a_{it}^G Binary variable that is equal to 0 if generator i is unavailable at snapshot t under the worst-case contingency, given a transmission expansion plan, a generation expansion realization, and a scheduling of power and reserves, being 1 otherwise.

a_{lt}^L Binary variable that is equal to 0 if line l is unavailable at snapshot t under the worst-case contingency, given a transmission expansion plan, a generation expansion realization, and a scheduling of power and reserves, being 1 otherwise.

f_{lt} Power flow of line l , at snapshot t , in the pre-contingency state.

f_l^C Power flow capacity of candidate line l .

f_{lt}^{wc} Power flow of line l , at snapshot t , under the worst-case contingency given a transmission expansion plan, a generation expansion realization, and a scheduling of power and reserves.

- p_{it} Power output of generator i , at snapshot t , in the pre-contingency state.
- p_{it}^{wc} Power output of generator i , at snapshot t , under the worst-case contingency given a transmission expansion plan, a generation expansion realization, and a scheduling of power and reserves.
- r_{it}^d Down-spinning reserve provided by generator i , at snapshot t .
- r_{it}^u Up-spinning reserve provided by generator i , at snapshot t .
- v_l Binary variable that is equal to 1 if candidate transmission asset l is installed, being 0 otherwise.

Dual Variables

- β_{bt} Dual variable associated with the power balance equation at bus b , at snapshot t , under the worst-case contingency given a transmission expansion plan, a generation expansion realization, and a scheduling of power and reserves.
- $\gamma_{it}^+, \gamma_{it}^-$ Dual variables associated with the constraints imposing the lower and upper bounds on p_{it}^{wc} for generating unit i .
- η_{it}^+, η_{it}^- Dual variables associated with the constraints imposing the lower and upper bounds on ψ_{lt}^{wc} for line l .
- ξ_{lts}^+, ξ_{lts}^- Dual variables associated with the lower- and upper-bound constraints for transmission in candidate line l , at snapshot t , in scenario s of generation expansion.
- π_{lt}^+, π_{lt}^- Dual variables associated with the constraints imposing the lower and upper bounds on f_{lt}^{wc} for existing line l .

$\rho_{lts}^+, \rho_{lts}^-$ Dual variables associated with the lower- and upper-bound constraints relating power flow and phase angles for candidate line l , at snapshot t , in scenario s of generation expansion.

$\sigma_{lt}^+, \sigma_{lt}^-$ Dual variables associated with the lower- and upper-bound constraints relating power flow and phase angles for candidate line l , at snapshot t , under the worst-case contingency given a transmission expansion plan, a generation expansion realization, and a scheduling of power and reserves.

$\phi_{lts}^+, \phi_{lts}^-$ Dual variables associated with the lower- and upper-bound constraints for phase-shifting in candidate line l , at snapshot t , in scenario s of generation expansion.

χ_{lt}^+, χ_{lt}^- Dual variables associated with the constraints imposing the lower and upper bounds on f_{lt}^{wc} for candidate line l .

ω_{lt} Dual variable associated with the equation relating power flow and phase angles for existing line l , at snapshot t , under the worst-case contingency given a transmission expansion plan, a generation expansion realization, and a scheduling of power and reserves.

3.2 5-level framework

As discussed in [70], the time required to install new renewable generation can be considerably shorter than that required to build new network infrastructure. As a result, network planners may have to take transmission expansion decisions in advance of generation investments (and therefore under uncertainty). In this context, the proposed framework minimizes exposure to the two following conditions that may lead to increased regret: (i) cost of stranded network assets in case that

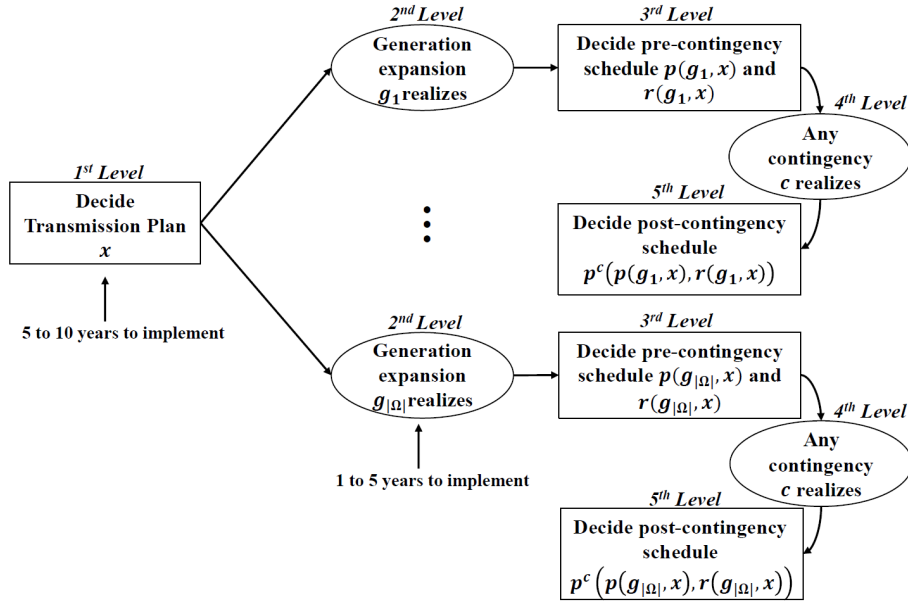


Figure 3.1: Framework diagram.

future generation is not fully deployed, and (ii) increased congestion and renewable resource curtailment costs in case that new RES is deployed without the adequate network investment. In order to minimize the exposure to these regrets, the proposed framework explicitly considers the uncertainty associated with future generation expansion in terms of amount and location. Additionally, our framework plans secured network infrastructure since it considers all credible $(n - 1)$ outages and contingencies of system components. Hence, we propose a methodology to minimize the maximum regret in the TEP problem while securing network operation. In order to do so, this methodology determines an optimal portfolio of conventional and flexible network investments. The determination of this portfolio takes into account the optimization of pre- and post-fault operational measures (from generation and network assets, e.g. reserves and phase shifters). In this manner, we can efficiently and securely deal with long term uncertainties (capacity and location of future generation) while meeting system security criteria. Flexible network investments are modeled since they can support integration of RES by alleviating network congestion pre- and post-fault and therefore reducing the need for new transmission lines.

Fig. 3.1 illustrates the five-level structure of the proposed methodology. In the first level, the min-max regret transmission plan is determined. In the second level, generation expansion realizes. In the third level, the pre-contingency schedule of power and reserves is determined considering the previously obtained transmission plan and the realized generation expansion (from first and second level). In the fourth level, any single outage or contingency realizes. Finally, in the fifth level the post-contingency schedule is determined.

3.3 Mathematical Formulation

The methodology proposed in this chapter aims to determine the transmission expansion plan (comprising conventional and flexible transmission assets) under generation expansion uncertainty while imposing deterministic security criterion. This objective is itself challenging since it involves the solution of a highly combinatorial problem. Hence, the representation of this problem in a single level formulation can become computationally intractable even for a system with a relatively small number of nodes. Therefore we present in this section a model decomposed in five levels in order to achieve our objectives with moderate computational effort.

The minimization of the maximum regret in the TEP problem under generation expansion uncertainty can be written as:

$$\text{Minimize } \underset{(\mathbf{v}, \mathbf{f}^C) \in \mathcal{X}}{\text{MaxReg}(\mathbf{v}, \mathbf{f}^C)} \quad (3.1)$$

subject to:

$$\text{MaxReg}(\mathbf{v}, \mathbf{f}^C) = \max_{s \in \Omega} \left\{ I(\mathbf{v}, \mathbf{f}^C) + \sum_{t \in T} d_t \left[\min_{(\mathbf{p}, \mathbf{r}) \in \mathcal{D}(\mathbf{v}, \mathbf{f}^C, \mathbf{g}_{ts})} \{c^{op}(\mathbf{p}, \mathbf{r})\} \right] - c_s^* \right\}, \quad (3.2)$$

where

$$\mathcal{X} = \left\{ \begin{array}{l} \mathbf{v} \in \{0, 1\}^{|\mathcal{L}^{PS} \cup \mathcal{L}^C|}, \\ \mathbf{f}^C \in \mathbb{R}^{|\mathcal{L}^C|} \end{array} \left| \begin{array}{l} 0 \leq f_l^C \leq \bar{f}_l^C v_l; \\ \forall l \in \mathcal{L}^C \end{array} \right. \right\}.$$

In (3.1)–(3.2), the objective function to be minimized (3.1) is the maximum regret among all scenarios of future generation capacity. In our case, each scenario corresponds to a potential generation expansion plan, represented by vector \mathbf{g}_{ts} , which captures the possible evolution pathways of RES capacity in the future. The total cost of each scenario represents the sum of investment and operation costs across all the operating conditions (or snapshots) that belong to set T , where duration of each snapshot d_t is specified (i.e. number of hours). The investment cost is given by $I(\mathbf{v}, \mathbf{f}^C)$, where \mathbf{v} is a vector of binary investment decision variables associated with new lines and phase shifters, and vector \mathbf{f}^C comprises the continuous decision variables associated with the capacity of new transmission lines. Similarly to [71] and [72], we represent the capacities of candidate lines as continuous decision variables. Nevertheless, it should be emphasized that, with very slight modification in the input data, our proposed methodology can also replicate the binary approach undertaken for transmission investment as in [23, 28, 44, 55, 56], and [24], to mention a few. More specifically, in \mathcal{X} , the user can limit the value of each of these continuous decision variables related to capacity through adequate upper and lower capacity bounds which will be multiplied by the binary decision variable associated with line investment. In this manner, if the binary variable associated with a candidate line investment results equal to one (i.e., if the line is built), the capacity of this line will be equal to the bounded predefined value set in \mathcal{X} , following exactly the binary approach undertaken in [23, 28, 44, 55, 56], and [24]. Hence, by choosing appropriate values of lower and upper bounds for line capacity, the user is able to decide whether newly built lines can have a single, fixed specific predefined capacity value or one

that can be optimized within a range as a continuous decision variable. Sets \mathcal{L}^{PS} and \mathcal{L}^C refer to indexes of existing lines that are candidates for placement of phase shifters and new transmission lines, respectively. The operation cost, $c^{op}(\mathbf{p}, \mathbf{r})$, is a function of the vectors \mathbf{p} and \mathbf{r} , which represent the power and spinning reserves scheduled, respectively across all possible operating points $\mathcal{P}(\mathbf{v}, \mathbf{f}^C, \mathbf{g}_{ts})$. The regret of a scenario is defined as the difference between (i) the cost (investment and operation) incurred in the decision obtained under uncertainty and (ii) the cost of the decision obtained under that particular scenario when assuming perfect information (i.e. full certainty about evolution of future generation capacity), given by c_s^* . Note that the $n - 1$ security criterion is enforced for both cases, namely uncertain future and perfect information. Hence, the maximum regret is the largest regret value among all considered scenarios, as defined in (3.2). It is important to highlight that the scenario that would lead to the maximum regret is not defined a priori, being decision-dependent and thus a result of the optimization.

Expression (3.2) can be rewritten as:

$$MaxReg(\mathbf{v}, \mathbf{f}^C) = \max_{s \in \Omega} \left\{ I(\mathbf{v}, \mathbf{f}^C) + \sum_{t \in T} d_t C_{ts}^O - c_s^* \right\}, \quad (3.3)$$

where

$$C_{ts}^O = \min_{(\mathbf{p}, \mathbf{r}) \in \mathcal{P}(\mathbf{v}, \mathbf{f}^C, \mathbf{g}_{ts})} \{c^{op}(\mathbf{p}, \mathbf{r})\}.$$

As in [17], the inner problem shown in (3.3) that schedules generation power outputs and reserves can be written as:

$$C_{ts}^O = \underset{\substack{\Delta D_t^{wc}, \theta_{bt}, \psi_{lt}, f_{lt}, \\ p_{it}, r_{it}^d, r_{it}^u}}{\text{Minimize}} \sum_{i \in I_w} C^S (\bar{W}_{its} - p_{it}) + \sum_{i \in I_c} C_i^P p_{it} + \sum_{i \in I_c} C_i^U r_{it}^u + \sum_{i \in I_c} C_i^D r_{it}^d + C^I \Delta D_t^{wc} \quad (3.4)$$

subject to:

$$\sum_{i \in I_b} p_{it} + \sum_{l \in \mathcal{L} | to(l)=b} f_{lt} - \sum_{l \in \mathcal{L} | fr(l)=b} f_{lt} = D_{bt}; \forall b \in N \quad (3.5)$$

$$f_{lt} = \frac{1}{x_l} (\theta_{fr(l),t} - \theta_{to(l),t}); \forall l \in \mathcal{L}^F \quad (3.6)$$

$$f_{lt} = \frac{1}{x_l} (\theta_{fr(l),t} - \theta_{to(l),t} + \psi_{lt}); \forall l \in \mathcal{L}^{PS} \quad (3.7)$$

$$-M_l(1-v_l) \leq f_{lt} - \frac{1}{x_l} (\theta_{fr(l),t} - \theta_{to(l),t}) \leq M_l(1-v_l) : (\rho_{lts}^+, \rho_{lts}^-); \quad \forall l \in \mathcal{L}^C \quad (3.8)$$

$$-v_l \bar{\psi} \leq \psi_{lt} \leq v_l \bar{\psi} : (\varphi_{lts}^+, \varphi_{lts}^-); \forall l \in \mathcal{L}^{PS} \quad (3.9)$$

$$-\bar{F}_l \leq f_{lt} \leq \bar{F}_l; \forall l \in (\mathcal{L}^F \cup \mathcal{L}^{PS}) \quad (3.10)$$

$$-f_l^C \leq f_{lt} \leq f_l^C : (\xi_{lts}^+, \xi_{lts}^-); \forall l \in \mathcal{L}^C \quad (3.11)$$

$$0 \leq p_{it} \leq \bar{P}_i; \forall i \in I_c \quad (3.12)$$

$$0 \leq p_{it} \leq \bar{W}_{its}; \forall i \in I_w \quad (3.13)$$

$$p_{it} + r_{it}^u \leq \bar{P}_i; \forall i \in I_c \quad (3.14)$$

$$p_{it} - r_{it}^d \geq 0; \forall i \in I_c \quad (3.15)$$

$$r_{it}^u \leq R_i^U; \forall i \in I_c \quad (3.16)$$

$$r_{it}^d \leq R_i^D; \forall i \in I_c \quad (3.17)$$

$$r_{it}^u = 0; \forall i \in I_w \quad (3.18)$$

$$r_{it}^d \leq p_{it}; \forall i \in I_w \quad (3.19)$$

$$\Delta D_t^{wc} = \max_{\Delta_t, a_{it}^G, a_{it}^L} \left\{ \Delta_t \right. \quad (3.20)$$

subject to:

$$f(\{a_{it}^G\}_{i \in I}, \{a_{it}^L\}_{l \in \mathcal{L}}) \geq \mathbf{0} \quad (3.21)$$

$$a_{it}^G \in \{0, 1\}; \forall i \in I \quad (3.22)$$

$$a_{it}^L \in \{0, 1\}; \forall l \in \mathcal{L} \quad (3.23)$$

$$\Delta_t = \min_{\substack{\Delta D_{bt}^+, \Delta D_{bt}^-, \\ \theta_{bt}^{wc}, \psi_{lt}^{wc}, f_{lt}^{wc}, p_{it}^{wc}}} \left[\sum_{b \in N} (\Delta D_{bt}^+ + \Delta D_{bt}^-) \right] \quad (3.24)$$

subject to:

$$\sum_{i \in I_b} p_{it}^{wc} + \sum_{l \in \mathcal{L} | to(l)=b} f_{lt}^{wc} - \sum_{l \in \mathcal{L} | fr(l)=b} f_{lt}^{wc} - \Delta D_{bt}^+ + \Delta D_{bt}^- = D_{bt} : \quad (\beta_{bt}); \forall b \in N \quad (3.25)$$

$$f_{lt}^{wc} = \frac{a_{lt}^L}{x_l} (\theta_{fr(l),t}^{wc} - \theta_{to(l),t}^{wc}) : (\omega_{lt}); \forall l \in \mathcal{L}^F \quad (3.26)$$

$$f_{lt}^{wc} = \frac{a_{lt}^L}{x_l} (\theta_{fr(l),t}^{wc} - \theta_{to(l),t}^{wc} + \psi_{lt}^{wc}) : (\omega_{lt}); \forall l \in \mathcal{L}^{PS} \quad (3.27)$$

$$-M_l(1 - v_l a_{lt}^L) \leq f_{lt}^{wc} - \frac{1}{x_l} (\theta_{fr(l),t}^{wc} - \theta_{to(l),t}^{wc}) \leq M_l(1 - v_l a_{lt}^L) : \quad (\sigma_{lt}^+, \sigma_{lt}^-); \forall l \in \mathcal{L}^C \quad (3.28)$$

$$-\bar{F}_l \leq f_{lt}^{wc} \leq \bar{F}_l : (\pi_{lt}^+, \pi_{lt}^-); \forall l \in (\mathcal{L}^F \cup \mathcal{L}^{PS}) \quad (3.29)$$

$$-a_{lt}^L f_l^C \leq f_{lt}^{wc} \leq a_{lt}^L f_l^C : (\chi_{lt}^+, \chi_{lt}^-); \forall l \in \mathcal{L}^C \quad (3.30)$$

$$a_{it}^G (p_{it} - r_{it}^d) \leq p_{it}^{wc} \leq a_{it}^G (p_{it} + r_{it}^u) : (\gamma_{it}^+, \gamma_{it}^-); \forall i \in I \quad (3.31)$$

$$-v_l \bar{\psi} \leq \psi_{lt}^{wc} \leq v_l \bar{\psi} : (\eta_{lt}^+, \eta_{lt}^-); \forall l \in \mathcal{L}^{PS} \quad (3.32)$$

$$\left. \Delta D_{bt}^+, \Delta D_{bt}^- \geq 0; \forall b \in N \right\} \quad (3.33)$$

Formulation (3.4)–(3.33) is a tri-level model, where the upper-level (3.4)–(3.19) refers to the pre-contingency generation dispatch of power and reserves. The decision variables of the upper-level are voltage angles, θ_{bt} , phase-shifting angles, ψ_{lt} , power flows, f_{lt} , power outputs, p_{it} , up- and down-spinning reserves, r_{it}^u and r_{it}^d , as well as the system power imbalance, ΔD_t^{wc} . Coefficients C^S , C_i^P , C_i^U , C_i^D , and C^I represent cost of wind spillage, generation, up- and down-spinning reserves, and system power imbalance (which is penalized by a large number to avoid infeasible solutions), respectively. Parameters D_{bt} , M_l , x_l , $\bar{\psi}$, \bar{F}_l , \bar{P}_i , R_i^U , and R_i^D correspond to demand, sufficiently large constants (associated with the disjunctive approach, also used in [55] and [61]),

reactances of lines, and capacity limits of phase shifters, transmission, generation and reserves, respectively, while \overline{W}_{its} represents the available capacity of renewable generator i at snapshot t in scenario s . Note that $\mathbf{g}_{ts} = [\overline{\mathbf{P}}^T | \mathbf{R}^U | \mathbf{R}^D | \mathbf{W}_{ts}^T]^T$. Sets I , I_w , I_c , I_b , N , \mathcal{L} , and \mathcal{L}^F include (in this order) all generating units, renewable generators, conventional power plants, generators attached to bus b , buses, all transmission lines, and existing transmission lines that cannot accommodate a new phase shifter. Dual variables ρ_{lts}^+ , ρ_{lts}^- , φ_{lts}^+ , φ_{lts}^- , ζ_{lts}^+ , and ζ_{lts}^- reflect the impact of the transmission plan on operating cost. The middle-level (3.20)–(3.23) is associated with the identification of the worst-case contingency state for the schedule determined in the pre-contingency state, and thus decision variables of the middle-level are the availability of generators, a_{it}^G , and lines, a_{lt}^L as well as the auxiliary variable Δ_t , which is an output of the lower-level problem. Finally, the lower-level (3.24)–(3.33) represents the system redispatch actions (or corrective actions) to deal with the worst-case contingency state, and thus decision variables of the lower-level are θ_{bt}^{wc} , ψ_{lt}^{wc} , f_{lt}^{wc} , and p_{it}^{wc} that represent post-contingency control of generation and network assets. ΔD_{bt}^+ and ΔD_{bt}^- are the nodal power violations. Note that dual variables are written within parenthesis after colons.

The objective function (3.4) of the upper-level formulation includes costs of wind spillage, generation, up- and down-spinning reserves as well as the system power imbalance cost. Constraints (3.5) refer to the nodal power balance. In a DC load flow fashion, constraints (3.6), (3.7), and (3.8) represent power transfers through existing lines, existing lines that are candidate to have a phase-shifter installed, and candidate lines to be built, respectively. Constraints (3.9) limit the control actions of phase-shifters. Constraints (3.10) and (3.11) limit power transfers through existing and candidate lines, respectively. Similarly, capacities associated with generating units are enforced by (3.12) on existing units and by (3.13) on coming units under a given generation expansion scenario s . Limits to up- and down-spinning reserves

are modeled by constraints (3.14)–(3.19).

The middle-level problem (3.20)–(3.23) finds the maximum system power imbalance associated with the pre-contingency schedule obtained by the upper-level. This identification is undertaken by optimizing vectors \mathbf{a}_t^G and \mathbf{a}_t^L , whose components indicate the availability of each element, e.g., a_{it}^G represents the availability of the generating unit i , i.e., it assumes a value equal to 1 if generator i is available and 0 otherwise. Likewise, a_{lt}^L is related to the availability of transmission line l . Constraint (3.21) ensures the prescribed levels of security, which can be written as $\sum_{i \in I} a_{it}^G + \sum_{l \in \mathcal{L}} a_{lt}^L \geq |I| + |\mathcal{L}| - 1$ for the $n - 1$ criterion. Constraints (3.22) and (3.23) describe the binary nature of vectors \mathbf{a}_t^G and \mathbf{a}_t^L .

The lower-level problem (3.24)–(3.33) describes the system response against the worst-case contingency identified by the middle-level. The objective function (3.24) represents the system power imbalance, which corresponds to the summation of nodal power violations (in absolute value), ΔD_{bt}^+ (generation curtailment) and ΔD_{bt}^- (demand curtailment), across all buses. Expressions (3.25)–(3.30) represent post-contingency network constraints. Constraints (3.31) impose the limits to generation redispatch actions according to the levels of power and reserves scheduled by the upper-level. Constraints (3.32) limit phase-shifting actions. Finally, constraints (3.33) ensure that ΔD_{bt}^+ and ΔD_{bt}^- are positive.

In summary, the model presented in this Section is a 5-level optimization problem. The first level optimizes variables v_l and f_l^C , which are related to the transmission expansion plan. The second level identifies the generation expansion scenario (represented by \bar{W}_{its}) that leads to the maximum regret given the decided transmission plan. Once first and second level decisions are taken, v_l , f_l^C , and \bar{W}_{its} arrive as parameters for the trilevel model composed by third, fourth, and fifth levels. The purpose of this trilevel model is to assess the minimum operation cost of the system

under a predefined deterministic security criterion given a transmission expansion (represented by v_l and f_l^C) and a generation expansion (represented by \overline{W}_{its}). To do so, a system dispatch (represented by θ_{bt} , ψ_{lt} , f_{lt} , p_{it} , r_{it}^d , and r_{it}^u) is decided in the third level so that any contingency (represented by a_{it}^G and a_{it}^L) contained in the feasible region of the fourth level can be circumvented in the redispatch (represented by θ_{bt}^{wc} , ψ_{lt}^{wc} , f_{lt}^{wc} , and p_{it}^{wc}) of the fifth level.

3.4 Solution Methodology

The formulation shown through (3.1) and (3.3) corresponds to a MILP with five levels, where the first-level problem determines the transmission expansion plan, the second level problem identifies the scenario associated with the maximum regret, and the inner tri-level optimization model determines the system operation and its corresponding costs under each scenario of future installed generation capacity. In this section, we propose a procedure that iteratively identifies (for each snapshot of each scenario of generation expansion) the umbrella set of contingencies [73] and recasts the inner tri-level formulation (that determines system operation in each snapshot) to a linear program which is convex with respect to the main first-level decision. Due to the aforementioned convexity property, the operation cost can be approximated via cutting planes in a Benders-type outer algorithm. Next, we present in detail the proposed solution methodology.

3.4.1 Obtaining Operation Costs

Once a transmission expansion plan (defined by the vectors $\boldsymbol{v}^{(j)}$ and $\boldsymbol{f}^{C(j)}$) is proposed in iteration j of the outer algorithm, power and reserves in each period $t \in T$ and $s \in \Omega$ are scheduled in order to obtain $C_{ts}^{O(j)}$, $\forall t \in T, s \in \Omega$, i.e., the trilevel

formulation (3.4)–(3.33) must be solved for all snapshots and scenarios. Hence we propose to solve the problem (3.4)–(3.33) through the solution methodology presented in [17], which presents the two following steps. Firstly, we develop a MILP associated with the middle- and lower-level operation models, hereinafter referred to as the oracle, to identify the worst-case contingency for a given set of power outputs and reserves scheduled. To do so, we replace the middle-level objective function by the dual representation of the lower-level objective function subject to the middle-level constraints and dual representation of the lower-level constraints, while linearizing some bilinear products. The formulation of the oracle is provided in the Appendix C. Secondly, we formulate the following operation master problem.

$$C_{ts}^{O(j)} = \underset{\substack{\alpha_t, \Delta D_{bt}^{c+}, \Delta D_{bt}^{c-}, \\ \theta_{bt}, \theta_{bt}^c, \psi_{lt}, \psi_{lt}^c, \\ f_{lt}, f_{lt}^c, p_{it}, p_{it}^c, r_{it}^d, r_{it}^u}}{\text{Minimize}} \sum_{i \in I_w} C^S (\bar{W}_{its} - p_{it}) + \sum_{i \in I_c} C_i^P p_{it} + \sum_{i \in I_c} C_i^U r_{it}^u + \sum_{i \in I_c} C_i^D r_{it}^d + C^I \alpha_t \quad (3.34)$$

subject to:

$$\text{Constraints (3.5)–(3.19)} \quad (3.35)$$

$$\sum_{i \in I_b} p_{it}^c + \sum_{l \in \mathcal{L} | to(l)=b} f_{lt}^c - \sum_{l \in \mathcal{L} | fr(l)=b} f_{lt}^c - \Delta D_{bt}^{c+} + \Delta D_{bt}^{c-} = D_{bt}; \forall b \in N, \quad c \in \mathcal{C}^{(j)} \quad (3.36)$$

$$f_{lt}^c = \frac{a_{lt}^{L(c)}}{x_l} (\theta_{fr(l),t}^c - \theta_{to(l),t}^c); \forall l \in \mathcal{L}^F, c \in \mathcal{C}^{(j)} \quad (3.37)$$

$$f_{lt}^c = \frac{a_{lt}^{L(c)}}{x_l} (\theta_{fr(l),t}^c - \theta_{to(l),t}^c + \psi_{lt}^c); \forall l \in \mathcal{L}^{PS}, c \in \mathcal{C}^{(j)} \quad (3.38)$$

$$-M_l(1 - v_l^{(j)}) \leq f_{lt}^c - \frac{a_{lt}^{L(c)}}{x_l} (\theta_{fr(l),t}^c - \theta_{to(l),t}^c) \leq M_l(1 - v_l^{(j)}); \quad (\rho_{lts}^{c+(j)}, \rho_{lts}^{c-(j)}); \forall l \in \mathcal{L}^C, c \in \mathcal{C}^{(j)} \quad (3.39)$$

$$-\bar{F}_l \leq f_{lt}^c \leq \bar{F}_l; \forall l \in (\mathcal{L}^F \cup \mathcal{L}^{PS}), c \in \mathcal{C}^{(j)} \quad (3.40)$$

$$-f_l^{C(j)} \leq f_{lt}^c \leq f_l^{C(j)}; (\xi_{lts}^{c+(j)}, \xi_{lts}^{c-(j)}); \forall l \in \mathcal{L}^C, c \in \mathcal{C}^{(j)} \quad (3.41)$$

$$a_{it}^{G(c)}(p_{it} - r_{it}^d) \leq p_{it}^c \leq a_{it}^{G(c)}(p_{it} + r_{it}^u); \forall i \in I, c \in \mathcal{C}^{(j)} \quad (3.42)$$

$$-v_l^{(j)}\bar{\psi} \leq \psi_{lt}^c \leq v_l^{(j)}\bar{\psi} : (\varphi_{lts}^{c+(j)}, \varphi_{lts}^{c-(j)}); \forall l \in \mathcal{L}^{PS}, c \in \mathcal{C}^{(j)} \quad (3.43)$$

$$\alpha_t \geq \sum_{b \in N} \left[\Delta D_{bt}^{c+} + \Delta D_{bt}^{c-} \right]; c \in \mathcal{C}^{(j)} \quad (3.44)$$

$$\Delta D_{bt}^{c+}, \Delta D_{bt}^{c-} \geq 0; \forall b \in N, c \in \mathcal{C}^{(j)}. \quad (3.45)$$

The formulation (3.34)–(3.45) is a relaxation of (3.4)–(3.33) since it only comprises a subset of the contingency set associated with the security criterion imposed in (3.21). Nevertheless, (3.34)–(3.45) and (3.4)–(3.33) provide equivalent results of operation cost as well as power and reserves schedule when $\mathcal{C}^{(j)}$ includes the umbrella contingency set, which is the set with the smallest number of contingencies capable to preserve the feasible region.

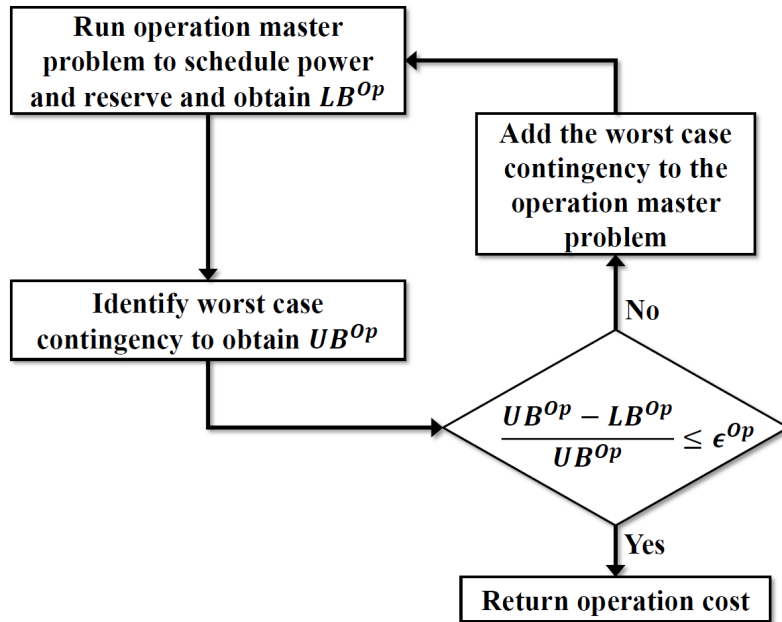


Figure 3.2: Procedure to obtain operation cost for each snapshot.

As depicted in Fig. 3.2, in the first iteration of the algorithm to obtain the operation cost, we solve model (3.34)–(3.35) since the set of contingencies $\mathcal{C}^{(j)}$ begins empty. Once the worst-contingency for the proposed schedule of power and reserves is identified, a convergence test is performed. If convergence is not achieved, the

contingency c identified is included in $\mathcal{C}^{(j)}$. Therefore, in the next iteration of the algorithm to obtain the operation cost, new variables ΔD_{bt}^{c+} , ΔD_{bt}^{c-} , θ_{bt}^c , ψ_{lt}^c , f_{lt}^c , and p_{it}^c are included. The inclusion of these new variables generates new columns in (3.34)–(3.45). In addition, in order to describe the feasible region for the newly added variables, a new block of expressions (3.36)–(3.45) is included and this inclusion generates new constraints. The model (3.34)–(3.45) is then solved again and new contingencies c are iteratively included in set $\mathcal{C}^{(j)}$ (therefore new columns and constraints are included) until convergence is achieved. While no formal convergence analysis is provided to investigate circumstances that may incur in slow execution of the proposed algorithm, convergence in test cases is always achieved.

Within this context, the solution algorithm associated with the operation model is the following:

- (i) Solve the optimization model (3.34)–(3.45) with $\mathcal{C}^{(j)} = \emptyset$, store \mathbf{p}_t as well as \mathbf{r}_t , and calculate $LB^{Op} = \sum_{i \in I_w} C^S(\bar{W}_{its} - p_{it}) + \sum_{i \in I_c} C_i^P p_{it} + \sum_{i \in I_c} C_i^U r_{it}^u + \sum_{i \in I_c} C_i^D r_{it}^d$.
- (ii) Identify the worst case contingency for stored \mathbf{p}_t and \mathbf{r}_t by running the oracle and calculate $UB^{Op} = \sum_{i \in I_w} C^S(\bar{W}_{its} - p_{it}) + \sum_{i \in I_c} C_i^P p_{it} + \sum_{i \in I_c} C_i^U r_{it}^u + \sum_{i \in I_c} C_i^D r_{it}^d + C^I \Delta D_t^{wc}$, where ΔD_t^{wc} is the worst case system power imbalance determined by the oracle.
- (iii) If $(UB^{Op} - LB^{Op})/UB^{Op} \leq \epsilon^{Op}$, then STOP and return C_{ts}^O ; else, CONTINUE.
- (iv) Include the worst-case contingency identified by the oracle in $\mathcal{C}^{(j)}$ (this generates new columns and constraints in the master problem).
- (v) Solve the optimization model (3.34)–(3.45), store \mathbf{p}_t as well as \mathbf{r}_t , calculate $LB^{Op} = \sum_{i \in I_w} C^S(\bar{W}_{its} - p_{it}) + \sum_{i \in I_c} C_i^P p_{it} + \sum_{i \in I_c} C_i^U r_{it}^u + \sum_{i \in I_c} C_i^D r_{it}^d + C^I \alpha_t$,

and go to step 2.

3.4.2 Obtaining Transmission Expansion Plan

The formulation (3.34)–(3.45) is a linear program where the right hand side is parameterized through vectors $\mathbf{f}^{C(j)}$ and $\mathbf{v}^{(j)}$, and therefore the operation cost $C_{ts}^{O(j)}$ is a convex function of the transmission expansion plan which and can be approximated via cutting planes at each iteration j . Hence we propose a Benders-type solution algorithm that iteratively calculates lower and upper bounds for the minimum maximum regret and finitely converges to the optimal solution.

A lower bound can be calculated for the minimum maximum regret at iteration j by solving the following model:

$$LB^{Reg(j)} = \underset{\delta_{ts}, (\mathbf{v}, \mathbf{f}^C) \in \mathcal{X}, MaxRegret}{\text{Minimize}} \quad MaxRegret \quad (3.46)$$

subject to:

$$MaxRegret \geq I(\mathbf{v}, \mathbf{f}^C) + \sum_{t \in T} d_t \delta_{ts} - c_s^*; \forall s \in \Omega \quad (3.47)$$

$$\begin{aligned} \delta_{ts} \geq & C_{ts}^{O(m)} + \sum_{l \in \mathcal{L}^C} (v_l - v_l^{(m)}) M_l \left[\rho_{lts}^{+(m)} + \rho_{lts}^{- (m)} + \sum_{c \in \mathcal{C}^{(m)}} \left(\rho_{lts}^{c+(m)} + \rho_{lts}^{c-(m)} \right) \right] \\ & + \sum_{l \in \mathcal{L}^{PS}} (v_l - v_l^{(m)}) \bar{\psi} \left[-\varphi_{lts}^{+(m)} - \varphi_{lts}^{- (m)} - \sum_{c \in \mathcal{C}^{(m)}} \left(\varphi_{lts}^{c+(m)} + \varphi_{lts}^{c-(m)} \right) \right] \\ & + \sum_{l \in \mathcal{L}^C} (f_l^C - f_l^{C(m)}) \left[-\xi_{lts}^{+(m)} - \xi_{lts}^{- (m)} - \sum_{c \in \mathcal{C}^{(m)}} \left(\xi_{lts}^{c+(m)} + \xi_{lts}^{c-(m)} \right) \right]; \\ & \forall t \in T, s \in \Omega, m = 1, \dots, j-1 \end{aligned} \quad (3.48)$$

$$\delta_{ts} \geq 0; \forall t \in T, s \in \Omega, \quad (3.49)$$

where the objective function (3.46) is identical to (3.1), constraints (3.47) correspond to (3.3) where δ_{ts} is the approximation of the operation costs per snapshot and scenario via cutting planes shown in (3.48) in terms of the dual variables obtained

from (3.34)–(3.45). Finally, constraints (3.49) ensure that δ_{ts} is non-negative. On the other hand, an upper bound to the minimum maximum regret can be obtained as follows:

$$UB^{Reg(j)} = \max_{s \in \Omega} \left\{ I(\mathbf{v}^{(j)}, \mathbf{f}^{C(j)}) + \sum_{t \in T} d_t C_{ts}^{O(j)} - c_s^* \right\}. \quad (3.50)$$

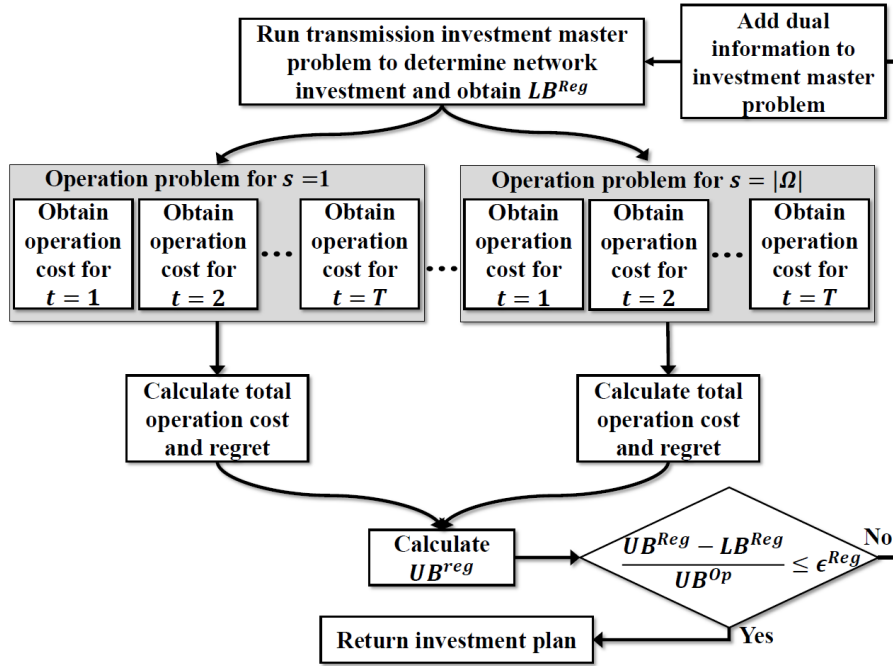


Figure 3.3: Solution algorithm to determine the optimal transmission plan.

The steps of the proposed solution algorithm, as depicted in Fig. 3.3, can be summarized as follows:

- (i) *Initialization*: Set the iteration counter: $j \leftarrow 0$.
- (ii) Solve the optimization model defined by (3.46), (3.47), and (3.49), store $\mathbf{v}^{(j)}$, $\mathbf{f}^{C(j)}$, and $LB^{Reg(j)}$.
- (iii) Obtain $C_{ts}^{O(j)} \forall t \in T, s \in \Omega$ by running the procedure described in Section 3.4.1. Calculate $UB^{Reg(j)}$ through (3.50) and store it.

-
- (iv) If $(UB^{Reg(j)} - LB^{Reg(j)}) / UB^{Reg(j)} \leq \epsilon^{Reg}$, then STOP and return the transmission plan; else, CONTINUE.
 - (v) Update the iteration counter: $j \leftarrow j + 1$.
 - (vi) Solve the optimization model defined by (3.46)–(3.49), store $\mathbf{v}^{(j)}$, $\mathbf{f}^{C(j)}$, and $LB^{Reg(j)}$. Go to step 3.

It should be emphasized that not only the so-called worst contingency is comprised but all credible contingencies (in the case of $n - 1$ security, all single outages) are taken into account. As illustrated in Fig. 3.3, once a transmission plan is proposed by the master problem, the operation cost under each scenario of generation expansion is evaluated in order to compute the upper-bound for the maximum regret. This operation cost, as customary in power systems operation, comprises the cost to provide security of supply under contingencies of system elements. In order to efficiently comprise these contingencies, instead of explicitly and exhaustively representing all of them by means of constraints in the operation problem, we just represent a subset of contingencies that includes the umbrella set of contingencies (which is the set of contingencies that needs to have null imbalance imposed so that all the other considered contingencies will also lead to null imbalance). This subset of contingencies is built by identifying the worst case contingency for each proposed power and reserves dispatch at each iteration of the algorithm that minimizes the operation cost (see Fig. 3.2). Clearly, each dispatch may have a different worst-case contingency. Within this framework, since the goal at this point is to identify the least expensive dispatch and system power imbalance is highly penalized, the system power imbalance will be minimized as much as possible. If it is not possible to avoid system power imbalance for a particular scenario, the operation cost of such scenario will be very high as well as its corresponding regret. Therefore, in the next iteration of the algorithm that determines the expansion plan, given the

additional dual information, the master problem will naturally select a transmission plan that provides the system with necessary leeway to circumvent the system power imbalance recognized in the previous iteration. Finally deliverability of reserves is guaranteed since post-contingency constraints are imposed in the fifth level of the formulation.

3.5 Case Studies

In this section, the key objectives of the studies carried out are: (i) validate the model, (ii) analyze the results and the main features of transmission plans against various sources of uncertainty, and finally (iii) examine the computational performance and scalability of the proposed solution algorithm. In order to achieve this, we use a tailor-made 6-bus system and the standard IEEE 118-bus system whose data can be found in [74]. In the presented case studies, we use a linear investment cost function of the form $I(\mathbf{v}, \mathbf{f}^C) = \sum_{l \in (\mathcal{L}^C \cup \mathcal{L}^{PS})} C_l^{fix} v_l + \sum_{l \in \mathcal{L}^C} C_l^{Cap} f_l^C$, where C_l^{fix} and C_l^{Cap} are annual fixed investment cost to install a candidate transmission asset l and annual investment cost of transmission capacity of a candidate transmission line l , respectively. The proposed methodology has been implemented in a computer with two Intel[®] Xeon[®] E5-2697 v2 processors (2.7 GHz) and 512 GB of RAM, using Xpress-MP 7.8 [47].

3.5.1 6-Bus System

As shown in Fig. 3.4, this system is composed of four existing buses and two potential new buses where wind generation might be connected in the future. In addition, there are three existing lines and six candidate lines. We also consider two candidate phase shifters (in lines L2 and L3) that can be installed to provide flexibility to net-

work investment options and thus deal with uncertainty from generation expansion and outages more efficiently.

There are four scenarios (S1, S2, S3, and S4) under consideration to represent uncertainty in future wind generation capacity. In S1, no generator is built/realized. In S2, generator G5 is built. In S3, generator G6 is built. Finally, in S4, generation expansion includes realization of both G5 and G6. Each scenario consists of three snapshots (each of 2920 hours) which represent combinations of demand and wind power outputs that may occur during a year.

In order to analyze the effects of security of supply, we obtain transmission expansion plans with and without $n - 1$ security criterion. We also study the savings achieved when phase-shifters are applied. In addition, we compare the min-max regret solution against plans that assume perfect information about future generation installed capacity. For this case study, we have set convergence tolerance parameters ϵ^{Op} and ϵ^{Reg} equal to 10^{-3} . The branch and bound relative gap to solve MILP problems at each iteration was set equal to 10^{-4} . For the case without security

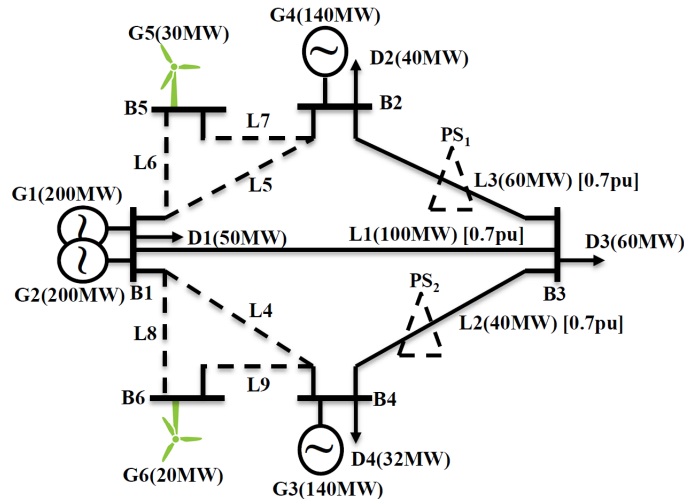


Figure 3.4: Generation, network, and demand data of 6-Bus system, where continuous lines refer to existing infrastructure and dashed lines refer to candidate infrastructure. Normal brackets refer to generation and network capacities and peak demand conditions, while square brackets refer to reactances.

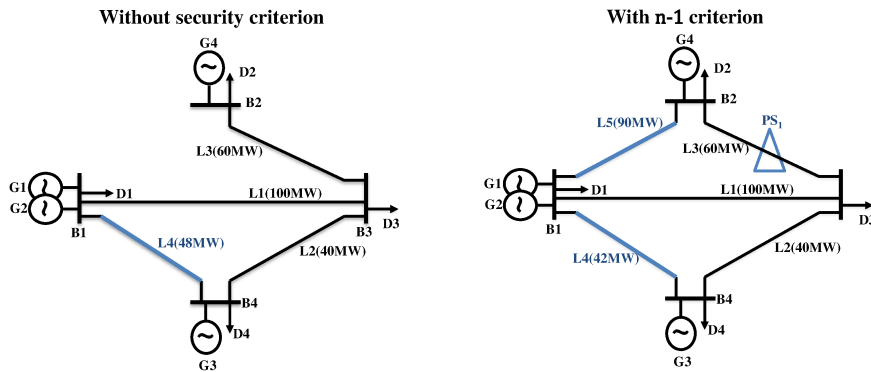


Figure 3.5: Solution under perfect information for scenario 1 with and without $n - 1$ security criterion.

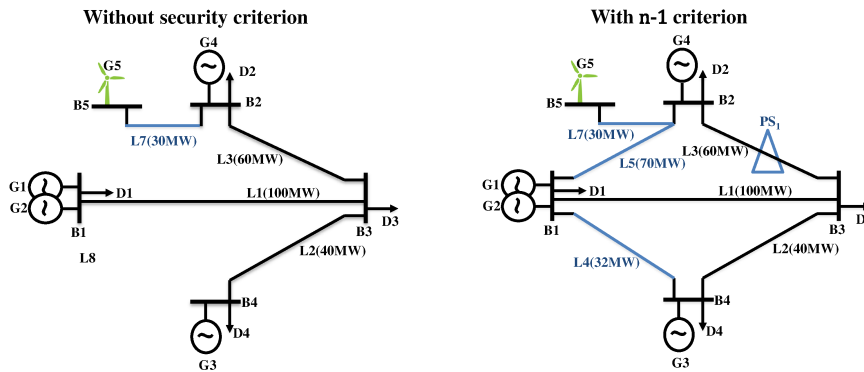


Figure 3.6: Solution under perfect information for scenario 2 with and without $n - 1$ security criterion.

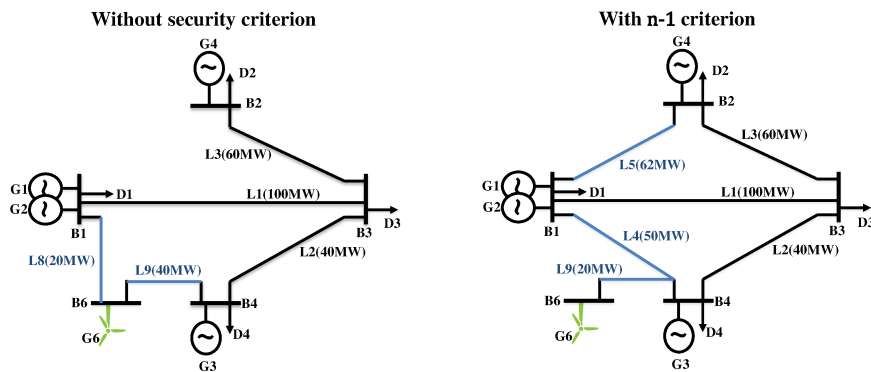


Figure 3.7: Solution under perfect information for scenario 3 with and without $n - 1$ security criterion.

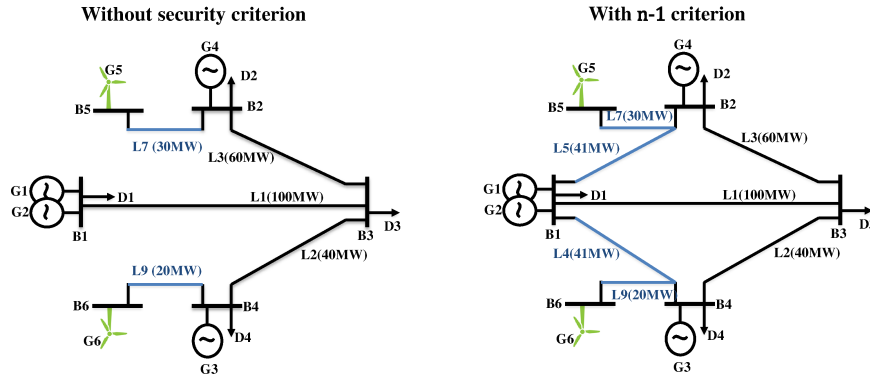


Figure 3.8: Solution under perfect information for scenario 4 with and without $n - 1$ security criterion.

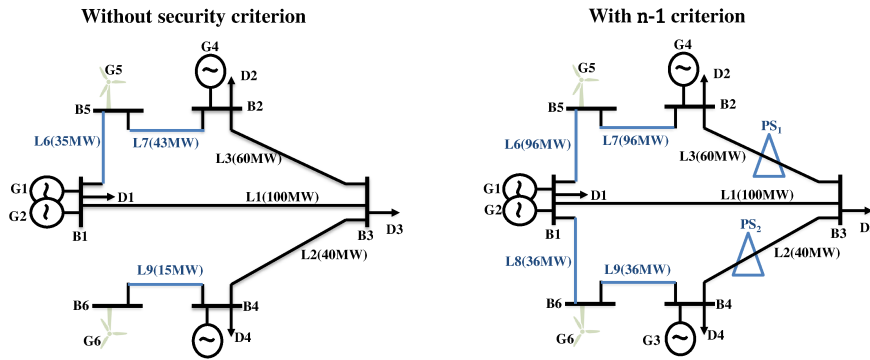


Figure 3.9: Min-max regret solution under generation expansion uncertainty with and without $n - 1$ security criterion.

criterion, 12 iterations of the algorithm (illustrated in Fig. 3.3) were required. In each iteration (except the last one when convergence is achieved) the number of cutting planes added to the transmission investment master problem is equal to the number of snapshots multiplied by the number of scenarios. Therefore, 132 cutting planes were included in the block of constraints (3.48) in this case. For the case with $n - 1$ security criterion and with candidate phase-shifters, 21 iterations were needed. Consequently, 240 cutting planes were added to the master in this case. Finally, for the case with $n - 1$ security criterion and without candidate phase-shifters, 26 iterations were required, resulting in the inclusion of 300 cutting planes.

Table 3.1: 6-Bus System – Costs of alternative expansion plans under perfect information and under uncertainty (MMR solution) and regrets of the MMR solution under each scenario.

| | | Scenario 1 | Scenario 2 | Scenario 3 | Scenario 4 | |
|---|--|------------------------------------|------------|------------|------------|-------|
| Without security criterion | Under Perfect Information about future generation capacity | Total Cost (MM\$/year) | 12.48 | 11.09 | 11.62 | 10.10 |
| | | Operation Cost (MM\$/year) | 11.56 | 10.55 | 10.54 | 9.02 |
| | | Investment Cost (MM\$/year) | 0.92 | 0.54 | 1.08 | 1.08 |
| | | Total Cost (MM\$/year) | 13.19 | 11.80 | 12.32 | 10.81 |
| | | Operation Cost (MM\$/year) | 11.56 | 10.17 | 10.69 | 9.18 |
| | Under Uncertainty in future generation capacity (MMR solution) | Investment Cost (MM\$/year) | 1.63 | 1.63 | 1.63 | 1.63 |
| | | Regret of MMR solution (MM\$/year) | 0.71 | 0.71 | 0.70 | 0.71 |
| | | Total Cost (MM\$/year) | 17.25 | 15.79 | 16.09 | 14.63 |
| | | Operation Cost (MM\$/year) | 15.03 | 13.06 | 13.70 | 11.73 |
| | | Investment Cost (MM\$/year) | 2.22 | 2.73 | 2.39 | 2.90 |
| With $n - 1$ security criterion (with candidate phase-shifters) | Under Perfect Information about future generation capacity | Total Cost (MM\$/year) | 17.97 | 16.00 | 16.65 | 14.67 |
| | | Operation Cost (MM\$/year) | 15.03 | 13.06 | 13.71 | 11.73 |
| | | Investment Cost (MM\$/year) | 2.94 | 2.94 | 2.94 | 2.94 |
| | | Regret of MMR solution (MM\$/year) | 0.72 | 0.21 | 0.56 | 0.04 |
| | | Total Cost (MM\$/year) | 17.96 | 16.40 | 16.09 | 14.63 |
| | Under Perfect Information about future generation capacity | Operation Cost (MM\$/year) | 15.04 | 13.31 | 13.70 | 11.73 |
| | | Investment Cost (MM\$/year) | 2.92 | 3.09 | 2.39 | 2.90 |
| | | Total Cost (MM\$/year) | 18.94 | 17.03 | 17.16 | 15.70 |
| | | Operation Cost (MM\$/year) | 15.48 | 13.57 | 13.70 | 12.24 |
| | | Investment Cost (MM\$/year) | 3.46 | 3.46 | 3.46 | 3.46 |
| Under Uncertainty in future generation capacity (MMR solution) | Regret of MMR solution (MM\$/year) | 0.98 | 0.63 | 1.07 | 1.07 | |
| | Total Cost (MM\$/year) | 18.94 | 17.03 | 17.16 | 15.70 | |
| | Operation Cost (MM\$/year) | 15.48 | 13.57 | 13.70 | 12.24 | |
| | Investment Cost (MM\$/year) | 3.46 | 3.46 | 3.46 | 3.46 | |
| | Regret of MMR solution (MM\$/year) | 0.98 | 0.63 | 1.07 | 1.07 | |

Table 3.2: 6-Bus System – New infrastructure of alternative expansion plans. Decisions under perfect information (S1,S2,S3,S4) and under uncertainty (MMR).

| Assumption | Case | Decision |
|--|------------|---|
| $n - 0$ with candidate PS | S1 | L4(48MW) |
| | S2 | L7(30MW) |
| | S3 | L8(20MW), L9(40MW) |
| | S4 | L7(30MW), L9(20MW) |
| | MMR | L6(35MW), L7(43MW), L9(15MW) |
| $n - 1$ with candidate PS | S1 | L3(PS), L4(42MW), L5(90MW) |
| | S2 | L3(PS), L4(32MW), L5(70MW), L7(30MW) |
| | S3 | L4(50MW), L5(62MW), L9(20MW) |
| | S4 | L4(41MW), L5(41MW), L7(30MW), L9(20MW) |
| | MMR | L2(PS), L3(PS), L6(96MW), L7(96MW), L8(36MW), L9(36MW) |
| $n - 1$ without candidate PS | S1 | L4(48MW), L5(61MW), L8(24MW), L9(24MW) |
| | S2 | L5(51MW), L6(13MW), L7(40MW), L8(40MW), L9(40MW) |
| | S3 | L4(50MW), L5(62MW), L9(20MW) |
| | S4 | L4(41MW), L5(41MW), L7(30MW), L9(20MW) |
| | MMR | L4(47MW), L5(59MW), L6(17MW), L8(24MW), L9(24MW) |

3.5.2 Solutions under perfect information and MMR solution

Table 3.1 presents the cost associated with the solution under perfect information for each scenario. In addition, also for each scenario, this table displays the regret associated with the min-max regret (MMR) solution, which is obtained when facing uncertainty in the forthcoming generation expansion. Moreover, Table 3.2 provides the details of expansion plans obtained (i) without security criterion, (ii) with $n - 1$ security criterion and no candidate phase-shifters, and (iii) with both $n - 1$ criterion and candidate phase-shifters.

Figs. 3.5, 3.6, 3.7, and 3.8 illustrate expansion plans under perfect information with and without security criterion for scenarios S1, S2, S3, and S4, respectively, whereas Fig.3.9 depicts the expansion plans also with and without security criterion

obtained under generation expansion uncertainty via the proposed min-max regret approach. We can observe that, when the security requirement is imposed, more transmission assets are built. In addition, note that, when the $n - 1$ security criterion is imposed, expansion plans are more prone to install phase-shifters (see L3 in S1 and S2) and this is exacerbated in the min-max regret solution under uncertainty when two phase-shifters are installed (see Fig.3.9). This demonstrates that increased levels of flexibility are needed to deal with high levels of uncertainty. Furthermore, holding levels of spinning reserves needed to deal with security provision against single outages is reduced in the case where phase-shifters are installed. On the contrary, preventing installation of flexible devices drives more transmission redundancy for the provision of security, increasing investment costs. Therefore, overall costs (investment plus operation) and regrets can be reduced by allowing investments in phase-shifters that can efficiently provide flexibility to deal with short- and long-term uncertainties.

3.5.3 Role played by the phase shifter under perfect information of generation expansion

In order to understand the importance of the role played by the phase-shifter installed in line L3 in scenario S1 under perfect information of future generation expansion, we provide a comparison between the operation costs under $n - 1$ security criterion with and without the phase-shifter in L3 while supposing that scenario S1 has realized. Table 3.3 displays power and spinning reserves scheduling with and without the phase shifter to comply with the $n - 1$ security criterion, whereas Table 3.4 reports the optimal system redispatch under eventual failures in generators G1 and G2 and line L1. Figs. 3.10, 3.11, 3.12, and 3.13 present the power flow with and without the phase for the pre-contingency scheduling, redispatch under outage

of generator G1, redispatch under outage of generator G2, and redispatch under outage of transmission line L1, respectively.

Table 3.3: Scheduling with and without PS1 under realization of S1

| Generator | Without PS1 | | | With PS1 | | |
|-----------|-------------|------------|------------|----------|------------|------------|
| | p (MW) | r^u (MW) | r^d (MW) | p (MW) | r^u (MW) | r^d (MW) |
| G1 | 100 | 48 | 0 | 100 | 82 | 0 |
| G2 | 48 | 100 | 0 | 82 | 100 | 0 |
| G3 | 30 | 0 | 0 | 0 | 0 | 0 |
| G4 | 4 | 0 | 0 | 0 | 0 | 0 |

Table 3.4: Redispatch (in MW) under the considered outages of G1, G2, and L1 with and without PS1

| Generator | Without PS1 | | | With PS1 | | |
|-----------|--------------|--------------|--------------|--------------|--------------|--------------|
| | Outage of G1 | Outage of G2 | Outage of L1 | Outage of G1 | Outage of G2 | Outage of L1 |
| G1 | Out | 148 | 100 | Out | 182 | 100 |
| G2 | 148 | Out | 48 | 182 | Out | 82 |
| G3 | 30 | 30 | 30 | 0 | 0 | 0 |
| G4 | 4 | 4 | 4 | 0 | 0 | 0 |

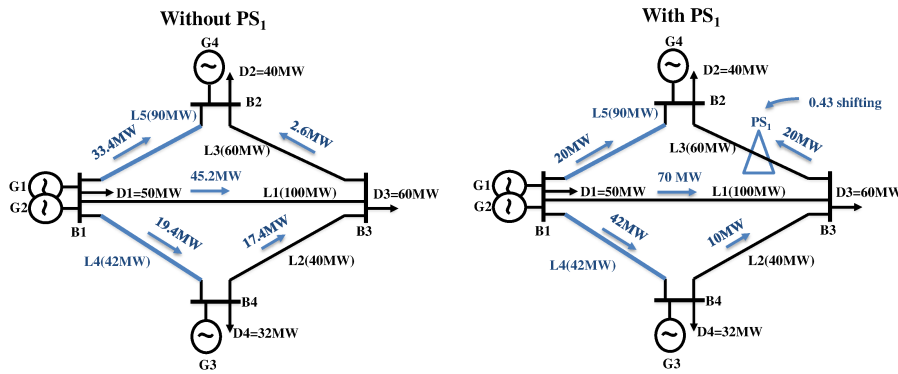


Figure 3.10: Power flow with and without PS1 under the realization of S1 considering $n - 1$ security criterion.

As can be seen in Table 3.3, without the installation of the phase shifter, generators G3 and G4, which are the most expensive units, are required to provide power to supply demand while complying with the $n - 1$ security criterion. The need to schedule power from all generators instead of only requiring two units to generate is

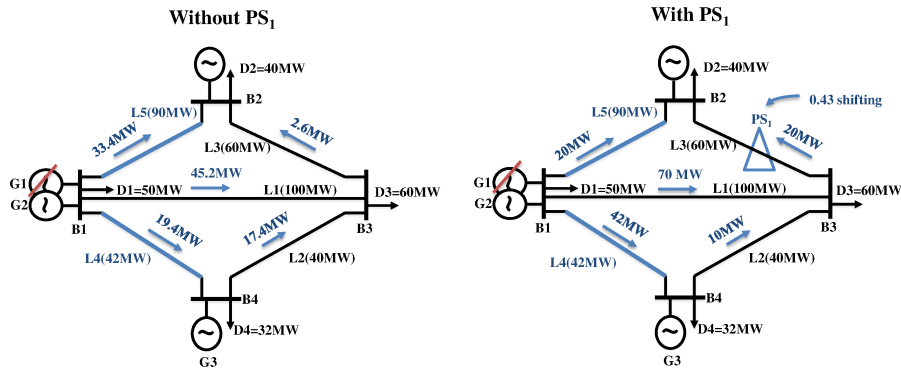


Figure 3.11: Power flow with and without PS_1 under the realization of S_1 considering a failure in G_1 .

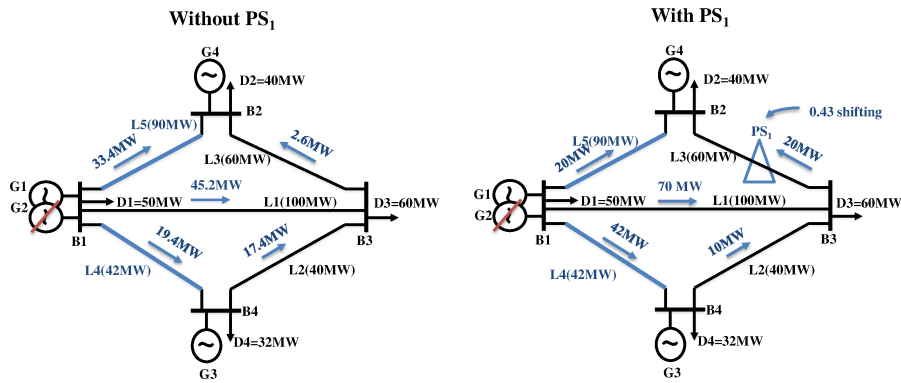


Figure 3.12: Power flow with and without PS_1 under the realization of S_1 considering a failure in G_2 .

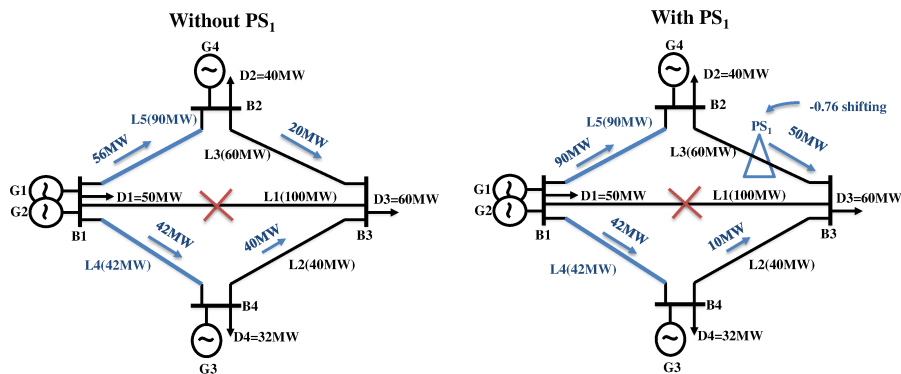


Figure 3.13: Power flow with and without PS_1 under the realization of S_1 considering a failure in L_1 .

significantly reflected in the operation costs. While the cost to operate the system with the phase shifter installed is equal to \$2396.00, the operation cost without the phase shifter is equal to \$5218.00, which represents 118% of increase.

The reason behind the savings in operation costs achieved in consequence of the installation of the phase shifter relies on the flexibility in terms of power flow provided by such device. As shown in Fig. 3.10, the installation of the phase shifter in L3 allows a significant increase from 36% to 49% in the overall utilization of the transmission network in the pre-contingency schedule. In some lines, namely L1, L3, and L4, the power flow rose by at least 25% in terms of the capacity of each line. The same pattern can be identified when outages of generators G1 and G2 and of line L1 arise. As depicted in Figs. 3.11 and 3.12, the power flow keeps the same if a failure occurs in either generator G1 or G2. Nevertheless, if line L1 becomes out of service, as illustrated in Fig. 3.13, the power flow is rearranged both with and without the phase shifter to keep supply-demand balance. As in the pre-contingency case, under contingency states, the installed phase shifter plays a fundamental role in ensuring deliverability for the power generated by units G1 and G2, therefore preventing the undesirable use of the most expensive generators G3 and G4.

3.5.4 Role played by the phase shifter under uncertainty of generation expansion

The installation of the two candidate phase shifters proposed by the min-max regret solution can be interpreted as counter-intuitive since such an investment does not appear in any of the solutions under perfect information of generation expansion. In order to investigate this particular decision, in Table 3.5, we compare costs and regrets associated with the min-max regret solution under the realization of each comprised scenario considering (i) the installation of both proposed phase shifters,

(ii) the installation of the proposed phase shifter in L3 only, (iii) the installation of the proposed phase shifter in L2 only, and (iv) the non-installation of both phase shifters proposed by the min-max regret solution.

Table 3.5: 6-Bus System – Overall costs and regrets per scenario (in MM\$/year) of implementing the min-max regret solution (i) with its two proposed phase shifters, (ii) with only one of its proposed phase shifters, and (iii) without any of its proposed phase shifters. Costs and regrets are indicated without and within brackets, respectively.

| MMR Decision | Realization | | | |
|-------------------------------|------------------|------------------|------------------|------------------|
| | S1 | S2 | S3 | S4 |
| With 2 phase shifters | 17.97 (0.72) | 16.00 (0.21) | 16.65 (0.56) | 14.67 (0.04) |
| With PS1 (L3) only | 23.22 (5.97) | 19.11 (3.32) | 21.89 (5.80) | 17.78 (3.15) |
| With PS2 (L2) only | 23.22 (5.97) | 19.11 (3.32) | 21.89 (5.80) | 17.78 (3.15) |
| Without phase shifters | 35.60 (18.35) | 28.92 (13.13) | 34.27 (18.18) | 27.60 (12.96) |

As can be seen in Table 3.5, costs and regrets significantly increase without the installation of one or both of the phase shifters proposed by the min-max regret solution. To be more precise, if just one of the proposed phase shifters is installed, overall costs (investment plus operation) would rise by 29.20%, 19.43%, 31.53%, and 21.20% under the realization of S1, S2, S3, and S4, respectively, whereas regrets would increase by 724.95%, 1489.01%, 944.37%, and 7650.65%. In case the min-max regret solution is implemented without any of its proposed phase shifters, overall costs would jump by 98.08%, 80.77%, 105.91%, and 88.09%, whereas regrets would dramatically rise by 2435.13%, 6188.46%, 3172.13%, 31795.91%. Therefore, in light of the aforementioned figures, once uncertainty of generation expansion is recognized and explicitly modeled in this case, the installation of both candidate phase shifters is required regardless the fact that at most only one of them is placed under perfect information.

3.5.5 Comparison with industry practice

Table 3.6: 6-Bus System – Overall costs and regrets per scenario (in MM\$/year) of implementing decisions under perfect information (S1, S2, S3 and S4) and under uncertainty (MMR). Costs and regrets are indicated without and within brackets, respectively.

| Decision | Realization | | | |
|------------|------------------|-----------------|------------------|-----------------|
| | S1 | S2 | S3 | S4 |
| S1 | 17.25 (0.00) | 17.40 (1.61) | 17.35 (1.26) | 17.50 (2.87) |
| S2 | 25.04 (7.79) | 15.79 (0.00) | 25.14 (9.05) | 15.89 (1.26) |
| S3 | 22.35 (5.10) | 22.50 (6.71) | 16.09 (0.00) | 16.24 (1.61) |
| S4 | 34.90 (17.65) | 22.02 (6.23) | 27.01 (10.92) | 14.63 (0.00) |
| MMR | 17.97 (0.72) | 16.00 (0.21) | 16.65 (0.56) | 14.67 (0.04) |

Table 3.6 shows a comparison between the proposed methodology and a heuristic procedure typically applied in the power industry. This heuristic method identifies the transmission plan that minimizes the maximum regret among the investment options found under perfect information [75]. As Table 3.6 shows, both costs and regrets associated with this method are significantly larger than those obtained by the proposed model, since the latter appropriately captures the uncertainties under consideration when determining the transmission investment. Clearly, when uncertainty is formally considered, a different solution to any of those obtained under perfect information may emerge. This demonstrates that flexible investment solutions against uncertainty include investment options that are not possible to observe in the solutions obtained under perfect information, which ultimately underestimate the value of flexibility and robustness. In contrast, investment options determined by the min-max regret problem adequately value flexibility levels that are needed to hedge against various potential future scenarios of generation expansion and outages. Hence it is important to recognize that current planning approach adopted in

Table 3.7: 118-Bus System – New infrastructure of alternative expansion plans (no security) and the associated computing time. Decisions under perfect information (S1, S2,...,S7) and under uncertainty (MMR).

| Case | Decision | Computing Time(s) |
|------------|---|-------------------|
| S1 | 32-113(100MW) | 9.86 |
| S2 | 114-115(50MW) | 9.52 |
| S3 | 109-110(100MW) | 12.55 |
| S4 | 100-101(100MW) | 12.26 |
| S5 | 17-113(100MW), 114-115(50MW) | 12.35 |
| S6 | 108-109(100MW), 101-102(100MW) | 13.66 |
| S7 | 17-113(100MW), 114-115(50MW), 109-110(100MW), 100-101(100MW) | 14.75 |
| MMR | 32-113(100MW), 114-115(50MW), 108-109(100MW), 100-101(100MW) | 74.08 |

the power industry may neglect network investments that are only valuable to deal with uncertainty and may underestimate the value of technologies such as FACTS to efficiently provide flexibility and robustness to transmission plans and this is critical in the light of increasing uncertainty levels that characterize future generation deployments.

3.5.6 IEEE 118-Bus System

This case study illustrates the scalability of the proposed methodology to a larger network based on the IEEE 118-Bus System, which comprises 118 buses, 181 existing transmission lines, 23 candidate transmission assets (7 candidate phase-shifters and 16 candidate lines), 54 conventional generators, and 4 potential new renewable units to be located in buses 101, 109, 113, and 115. We consider 7 scenarios of future generation capacity expansion. S1, S2, S3, and S4 involve the construction of new generating units in bus 113, 115, 109, and 101, respectively. In S5, generators in buses 113 and 115 are built, while in S6, generators in buses 109 and 101 are built. In S7, all new generating units are built. For this case study, we have set convergence tolerance parameters ϵ^{Op} and ϵ^{Reg} equal to 5×10^{-3} and 10^{-2} ,

Table 3.8: 118-Bus System – Costs of alternative expansion plans under perfect information and under uncertainty (MMR solution) and regrets of the MMR solution under each scenario.

| | | Scenario 1 | Scenario 2 | Scenario 3 | Scenario 4 | Scenario 5 | Scenario 6 | Scenario 7 | |
|---------------------------------|--|------------------------------------|------------|------------|------------|------------|------------|------------|--------|
| Without security criterion | Under Perfect Information about future generation capacity | Total Cost (MM\$/year) | 80.29 | 82.34 | 80.39 | 80.38 | 85.29 | 83.29 | 92.17 |
| | | Operation Cost (MM\$/year) | 71.51 | 73.64 | 71.61 | 71.60 | 67.81 | 65.72 | 57.12 |
| | | Investment Cost (MM\$/year) | 8.78 | 8.70 | 8.78 | 8.78 | 17.48 | 17.57 | 35.05 |
| | Under Uncertainty in future generation capacity (MMR solution) | Total Cost (MM\$/year) | 106.64 | 108.69 | 106.74 | 106.73 | 104.57 | 100.94 | 93.33 |
| | | Operation Cost (MM\$/year) | 71.59 | 73.64 | 71.69 | 71.68 | 69.52 | 65.89 | 58.28 |
| | | Investment Cost (MM\$/year) | 35.05 | 35.05 | 35.05 | 35.05 | 35.05 | 35.05 | 35.05 |
| | | Regret of MMR solution (MM\$/year) | 26.35 | 26.35 | 26.35 | 26.35 | 19.28 | 17.65 | 1.16 |
| With $n - 1$ security criterion | Under Perfect Information about future generation capacity | Total Cost (MM\$/year) | 125.60 | 110.41 | 125.61 | 125.56 | 110.36 | 125.97 | 114.29 |
| | | Operation Cost (MM\$/year) | 96.36 | 98.67 | 96.37 | 96.32 | 89.76 | 87.93 | 76.19 |
| | | Investment Cost (MM\$/year) | 29.24 | 11.74 | 29.24 | 29.24 | 20.60 | 38.03 | 38.10 |
| | Under Uncertainty in future generation capacity (MMR solution) | Total Cost (MM\$/year) | 152.75 | 147.54 | 162.56 | 146.50 | 147.50 | 156.32 | 151.41 |
| | | Operation Cost (MM\$/year) | 103.78 | 98.57 | 113.59 | 97.53 | 98.53 | 107.35 | 102.44 |
| | | Investment Cost (MM\$/year) | 48.97 | 48.97 | 48.97 | 48.97 | 48.97 | 48.97 | 48.97 |
| | | Regret of MMR solution (MM\$/year) | 27.15 | 37.13 | 36.95 | 20.94 | 37.14 | 30.35 | 37.12 |

Table 3.9: 118-Bus System – New infrastructure of alternative expansion plans (with $n - 1$ security) and the associated computing time. Decisions under perfect information (S1, S2,...,S7) and under uncertainty (MMR).

| Case | Decision | Computing Time(s) |
|------------|---|-------------------|
| S1 | 31-32(PS), 11-117(13MW), 17-113(100MW), 27-114(50MW) | 9948.05 |
| S2 | 11-117(11MW), 114-115(50MW) | 3880.77 |
| S3 | 31-32(PS), 11-117(14MW), 27-114(50MW), 109-110(100MW) | 10499.80 |
| S4 | 31-32(PS), 11-117(12MW), 27-114(50MW), 100-101(100MW) | 11295.50 |
| S5 | 11-117(18MW), 17-113(141MW), 114-115(50MW) | 3832.68 |
| S6 | 31-32(PS), 11-117(30MW), 27-114(50MW), 109-110(100MW), 101-102(100MW) | 9607.17 |
| S7 | 11-117(17MW), 17-113(100MW), 114-115(50MW), 108-109(100MW), 100-101(100MW) | 6361.07 |
| MMR | 31-32(PS), 11-117(21MW), 32-113(98MW), 27-115(50MW), 114-115(100MW), 108-109(94MW), 101-102(100MW) | 45314.70 |

respectively. The branch and bound relative gap to solve MILP problems at each iteration was set equal to 10^{-4} . For the case without security criterion, convergence of the algorithm (illustrated in Fig. 3.3) was achieved in 9 iterations. Therefore, 168 cutting planes were included in the transmission investment master. For the case with $n - 1$ security criterion, 45 iterations were required. Consequently, 924 cutting planes were added to the master in this case.

Tables 3.7, 3.8, and 3.9 present the results that demonstrate the need for further transmission assets to provide security of supply and the need for further investment options to deal with uncertainty (which are not revealed in the solutions under perfect information). For the sake of comparison, we developed an equivalent single-level MILP that explicitly enumerates all scenarios and contingencies to obtain the

same min-max regret solutions reported in Table 3.8. Although this model could be used to obtain investment plans without security criterion, no feasible solution was found (after a week) when $n - 1$ criterion is imposed. The proposed methodology, instead, can effectively find the min-max regret solution under $n - 1$ criterion for all tested cases as reported in Table 3.9.

Table 3.10: Results of the contingency analysis for the MMR transmission plan without security criterion.

| Scenario | Probability of Imbalance (%) | Exp. Value of Imbalance (% of demand) | CVaR of Imbalance (% of demand) |
|-----------------|---|--|--|
| S1 | 8.08% | 1.19% | 21.96% |
| S2 | 7.84% | 1.26% | 23.62% |
| S3 | 7.30% | 1.13% | 21.20% |
| S4 | 7.20% | 1.10% | 20.82% |
| S5 | 8.61% | 1.16% | 21.48% |
| S6 | 8.30% | 1.14% | 20.83% |
| S7 | 9.81% | 1.10% | 18.51% |

Table 3.11: Results of the contingency analysis for the MMR transmission plan with $n - 1$ security criterion.

| Scenario | Probability of Imbalance (%) | Exp. Value of Imbalance (% of demand) | CVaR of Imbalance (% of demand) |
|-----------------|---|--|--|
| S1 | 0.45% | 0.03% | 0.68% |
| S2 | 0.47% | 0.03% | 0.60% |
| S3 | 0.33% | 0.02% | 0.46% |
| S4 | 0.35% | 0.03% | 0.63% |
| S5 | 0.42% | 0.03% | 0.51% |
| S6 | 0.42% | 0.03% | 0.60% |
| S7 | 0.46% | 0.03% | 0.53% |

Finally, we performed an out of sample contingency analysis in order to compare the performance of the solutions with and without security criterion ($n - 1$). This comparison is in terms of reliability. Thus, we generated via Monte Carlo simulation 10,000 contingency states for each snapshot of each possible scenario of future generation capacity. Each contingency state was generated by simulating independent Bernoulli trials for the availability of each line and generator state (1 for available

and 0 for unavailable state). As in [53], we set to 0.1% and 1% the probability of outage for lines and generators, respectively. For each simulated contingency state, we assessed the system imbalance for (i) the min-max regret transmission plan that was obtained without imposing security criterion and for (ii) the min-max regret transmission plan that was obtained while imposing the $n - 1$ security criterion. Tables 3.10 and 3.11 summarize the results of this experiment. As can be seen from these results, by considering a security criterion while planning the system expansion, we are able to dramatically decrease levels of probability of system imbalance, expected value of system imbalance, and CVaR (with 95% confidence) of system imbalance.

CHAPTER 4

An Ambiguity Averse Approach for Transmission Expansion Planning

The levels of renewable penetration recently established by most countries around the globe will permanently change the way that power systems are planned, operated and controlled [76]. Every year, the share of energy consumption supplied by renewable energy sources (RES) increases rapidly. It is estimated that close to 20% of total worldwide consumption are currently addressed by renewables. Additionally, several countries have already committed to cover 50% of demand through renewable sources in the near future [77]. However, the environmental and financial benefits of a cleaner and cheaper power matrix come with a critical technical challenge of how to deal in day-by-day operation with the increasing variability in energy production due to a high penetration of RES.

To start tackling this issue, it is of utmost importance to adequately plan and redesign the transmission system network to cope with this new uncertain environment [78]. It is well recognized that transmission systems are costly infrastructures. Hence, it is critically important to be assertive in both technical and economical terms while planning a network extension. From a methodological point-of-view, the transmission expansion planning (TEP) problem has been broadly studied in technical literature from many different angles [79], with its uncertain decision process usually based on either stochastic [80] or robust [81] optimization. On the one hand, within the stochastic TEP models, the uncertainty factors are assumed to be precisely characterized via a known underlying stochastic process, usually represented by a set of exogenous scenarios. For instance, in [82], the expansion plan is devised so that the system can have leeway to circumvent deliberate attacks against its transmission lines, which are represented via a set of scenarios of potential attack plans. In [62], a stochastic model is used to evaluate the benefits of incorporating flexible assets into the power system. In [83], the authors proposed a three-level filter to reduce the number of considered contingencies of transmission lines in a two-stage stochastic TEP model. The objective in [83] is to identify the transmission plan that minimizes the expected value of system operation cost under wind and load uncertainty. Moreover, in [84], the TEP problem is tackled via a Benders-decomposition approach, in which both wind and load uncertainties are described by a set of scenarios chosen by an improved forward selection algorithm. From a robust TEP perspective, on the other hand, the underlying stochastic process is assumed to be unknown, and the dynamics of the uncertain factors are endogenously characterized by an *a priori* specified uncertainty set along with a worst-case metric. In [43], a robust model is proposed to address the TEP problem, modeling RES output and load uncertainties with a box uncertainty set. In [44], a two-stage robust formulation is developed to determine a transmission expansion plan that complies with deterministic $n - K$ security criterion. In [23], the authors present a

methodology to devise the expansion plan under variation of available generation capacity and load in different regions. In [24], the TEP problem is addressed under uncertainty in retirement of coal plants as well as in future investments in generation capacity.

Following industry and academic guidelines, system outages and RES output uncertainties are two critical concerns while expanding the transmission system. In this work, both uncertainties are comprised within a hybrid stochastic and robust optimization framework. More precisely, on the one hand, failures of system elements (conventional power units and/or transmission lines) are addressed by imposing deterministic security standards in an adjustable robust optimization fashion. On the other hand, uncertainty in RES output is represented via a scenario-based approach. Essentially, the methodology proposed in this chapter aims at determining the optimal transmission expansion plan while limiting the system imbalance to a maximum allowed level. Due to its uncertain nature, a risk-constrained formulation, based on the conditional value-at-risk (CVaR) [85], is adapted aiming at ensuring system reliability.

The adequate characterization of the forthcoming renewable production dynamics is a critical aspect to properly accommodate and utilize RES potentials. In this matter, a determinant factor on the uncertainty characterization associated with RES output is the identification of a stochastic process that accurately represents its future behaviour. Several methodologies have been proposed over the last years [86, 87], but still no unanimous solution has been devised. This issue is of particular relevance in the TEP context, since the expansion plan is made ahead enough (usually, 5 to 10 years) so that a non-negligible portion of uncertainty is of difficult modeling. As a consequence, the expansion decision under uncertainty on RES output is made under ambiguity. To cope with this modeling issue, the proposed methodology places at disposal the possibility of simultaneously taking into account different RES

probability distributions, thus being, simultaneously, risk- and ambiguity-averse. It is worth mentioning that, within the context of the TEP problem, [88] has considered ambiguity in the probability distribution of loads. However, despite of its relevant contribution, [88] does not take into account the occurrence of system outages, which increases the modeling and computational challenges.

Another key challenge in daily power systems operation is the allocation of system's resources at least cost in order to meet the constantly growing demand for electricity, thus continually keeping the system balanced [89]. To overcome this challenge, an adequate design of the transmission network plays a crucial role since it allows the operator to efficiently and cost-effectively flow energy through the network, therefore making better use of available resources. Such well-designed networks become even more relevant in the presence of significant renewable energy sources (RES) in the system for two main reasons. Firstly, areas with potential RES are usually located in remote regions (consequently distant from the bulk power system) and therefore transmission lines are required to access this potential [90]. Secondly, as discussed in technical literature [91–93], the production variability inherent to RES impose the scheduling and utilization of higher levels of spinning and eventually non-spinning reserves. Hence, in this chapter, the scheduling of spinning reserves is also taken into account while planning the system expansion.

In light of the aforementioned observations, this chapter proposes a novel transmission expansion planning methodology capable of determining a renewable-oriented network expansion aiming to properly accommodate the extensive forthcoming renewable penetration while meeting security standards in daily operation. Structurally, the proposed TEP formulation is a particular instance of the risk-constrained adjustable robust optimization (R-ARO) framework, modelled as a (hierarchical) three-level system of optimization problems. To solve the multi-level problem, an algorithm based on column-and-constraint generation (CCG) [94] is proposed.

The chapter is laid out as follows. Section 4.1 specifies the nomenclature associated with this chapter. Section 4.2 presents the proposed three-level ambiguity averse formulation for the TEP problem, whereas Section 4.3 provides a solution methodology. Finally, in Section 4.4, the effectiveness of the proposed model is demonstrated through an illustrative example and a case study based on the IEEE 118-bus test system.

4.1 Nomenclature

The mathematical symbols used throughout this chapter are classified below as follows.

Sets

\mathcal{L} Set of indexes of all transmission lines.

\mathcal{L}^C Set of indexes of candidate transmission lines.

\mathcal{L}^E Set of indexes of existing transmission lines.

\mathcal{L}^{PS} Set of indexes of existing transmission lines where phase shifters can be installed (subset of \mathcal{L}^E).

N Set of bus indexes.

\mathcal{I} Set of conventional generator indexes.

Functions

$C_i(\cdot)$ Energy cost function offered by generator i .

Parameters

$\bar{\psi}_l$ Capacity limit of phase shifter in line l .

c_l^L Construction cost of a candidate line l .

c_l^{PS} Installment cost of a phase shifter in line l .

b_l Susceptance of line l .

d_n Demand at bus n .

\bar{F}_l Power flow capacity of line l .

$fr(l)$ Sending or origin bus of line l .

\hat{g}_n Expected or best estimation for renewable production at bus n .

\bar{P}_i Capacity of conventional generator i .

\underline{P}_i Minimum power output of conventional generator i .

\bar{R}_i^D Upper bound for the down-spinning reserve contribution of conventional generator i .

\bar{R}_i^U Upper bound for the up-spinning reserve contribution of conventional generator i .

$to(l)$ Receiving or destination bus of line l .

Decision Variables

ψ_l Phase-shifting angle in line l .

θ_b Phase angle at bus b in the pre-contingency state.

a_i^G Binary variable that is equal to 0 if generator i is unavailable, being 1 otherwise.

a_l^L Binary variable that is equal to 0 if line l is unavailable, being 1 otherwise.

f_l Power flow of line l in the pre-contingency state.

p_i Power output of generator i in the pre-contingency state.

r_i^D Down-spinning reserve provided by generator i .

r_i^U Up-spinning reserve provided by generator i .

v_l Binary variable that is equal to 1 if candidate transmission line l is constructed, being 0 otherwise.

w_l Binary variable that is equal to 1 if a phase shifter is installed in line l , being 0 otherwise.

4.2 Mathematical Formulation

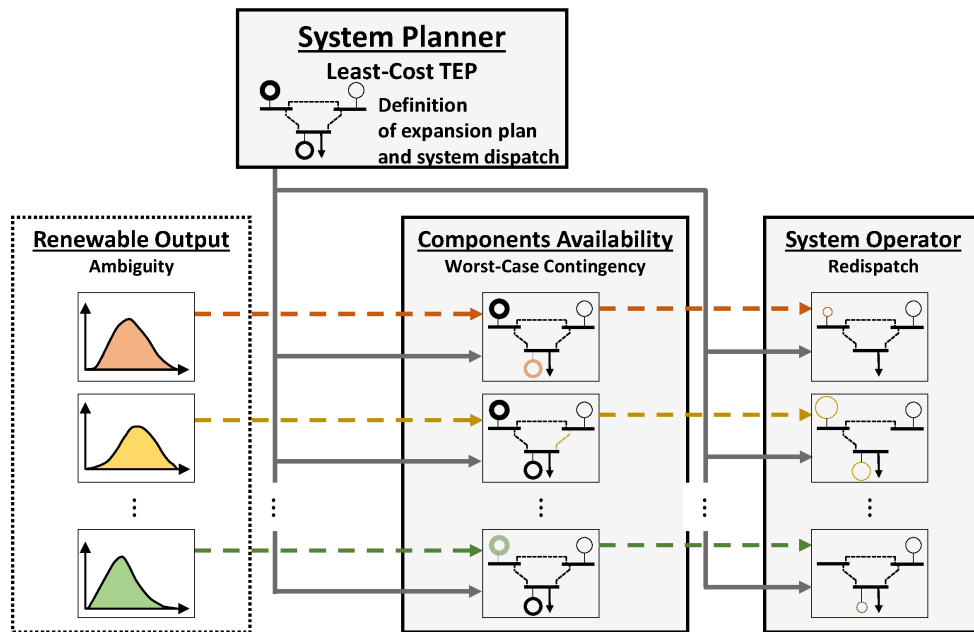


Figure 4.1: Model scheme.

In a centralized network expansion, a transmission planner aims at identifying a set of candidate assets to be built so that both expansion and daily operation costs are jointly minimized. As depicted in 4.1, on the one hand, we are particularly interested in a least-cost transmission expansion with optimal placement of phase shifters in

the system. On the other hand, given the expansion planning, the daily operation seeks for a dispatch of power and up-/down-spinning reserves from conventional sources – referred to as an *operating point* – to meet system’s demand at lowest cost under uncertainty in equipment failure and ambiguity on RES output.

Mathematically, let \mathcal{L}^C be the set of candidate lines and $\mathbf{v} = \{v_l\}_{l \in \mathcal{L}^C}$ a binary vector indicating if line $l \in \mathcal{L}^C$ has been chosen to be built. Analogously, let $\mathcal{L}^{PS} \subset \mathcal{L}^E$ be the subset of existing lines (\mathcal{L}^E) where phase shifters can be placed and $\mathbf{w} = \{w_l\}_{l \in \mathcal{L}^{PS}}$ the respective binary vector indicating if a phase shifter has been placed in line $l \in \mathcal{L}^{PS}$. From the system operation perspective, let $(\mathbf{p}, \mathbf{r}^U, \mathbf{r}^D)$ denote an operating point with $\mathbf{p} = \{p_i\}_{i \in \mathcal{I}}$ being the power dispatch of each conventional generator $i \in \mathcal{I}$, and $\mathbf{r}^U = \{r_i^U\}_{i \in \mathcal{I}}$ and $\mathbf{r}^D = \{r_i^D\}_{i \in \mathcal{I}}$ the respective up and down reserves. Before presenting the proposed expansion model, we discuss the characterization of uncertainty considered in this work.

4.2.1 RES Output and Equipment Availability Uncertainties

Two sources of uncertainty mostly impact the daily operation of power systems: unplanned equipment halt and RES output. To address the former, we follow current industry practices and consider a deterministic approach [95, 96]. More specifically, let $\mathbf{a}^G = \{a_i^G\}_{i \in \mathcal{I}}$ and $\mathbf{a}^L = \{a_l^L\}_{l \in \mathcal{L}}$ be two binary vectors whose components indicate the availability of each conventional generating unit $i \in \mathcal{I}$ and each existing/candidate transmission line $l \in \mathcal{L} = \mathcal{L}^E \cup \mathcal{L}^C$, respectively. A set of possible outages $(\mathbf{a}^G, \mathbf{a}^L) \in \mathcal{A}$ is thus assumed given and a worst-case analysis is performed over \mathcal{A} . For generality purposes, we assume \mathcal{A} is a binary set ($\mathcal{A} \subseteq \{0, 1\}^{|\mathcal{I}|} \times \{0, 1\}^{|\mathcal{L}|}$).

With respect to RES output uncertainty, the standard scenario-based representation is considered in this chapter. However, despite the significant effort devoted

to appropriately characterize the future behavior of renewable production, still no consensus has been reached. Therefore, the usual method based on sampling from a unique probability distribution may not be sufficient due to the difficulty to precisely identify the probability distribution which properly characterizes the behaviour of the renewable output [97]. Therefore, in this chapter, we extend the standard approach and consider an ambiguity set of credible RES output probability distributions to account for ambiguity in renewable production probabilistic characterization. More precisely, let $(\Omega, \Sigma, \mathbb{P})$ be a probability space with a finite sample space Ω as usual in standard scenario-based uncertainty representations [80], $\tilde{\mathbf{g}} = \{\tilde{g}_n\}_{n \in \mathcal{N}}$ be the uncertain power injection from renewable sources in node $n \in \mathcal{N}$ and \mathcal{F} a set of probability distribution functions $F_{\tilde{\mathbf{g}}}$ of the uncertain RES output $\tilde{\mathbf{g}}$. For presentation purposes, we identify the ambiguity set \mathcal{F} to a set of random vectors \mathcal{G} representing the uncertain power injection from renewable sources using the probability measure \mathbb{P} .

We make the following modeling assumption over \mathcal{G} .

Assumption 1. *The set of random vectors \mathcal{G} is assumed finite with dimension J , i.e. $\mathcal{G} = \{\tilde{\mathbf{g}}_1, \dots, \tilde{\mathbf{g}}_j, \dots, \tilde{\mathbf{g}}_{|J|}\}$ and we associate to each $\tilde{\mathbf{g}}_j \in \mathcal{G}$ the index set $\mathcal{J} = \{1, \dots, J\}$.*

4.2.2 Transmission Expansion Planning Model

The objective of this chapter is to present an ambiguity averse transmission expansion formulation, which models the decision on investing in new transmission lines and/or phase shifters. The full mathematical formulation is presented in equations (4.1)–(4.29).

$$\min_{\substack{\theta, \psi, f, \\ p, r^D, r^U, \\ v, w}} \sum_{l \in \mathcal{L}^C} c_l^L v_l + \sum_{l \in \mathcal{L}^{PS}} c_l^{PS} w_l + \sum_{i \in \mathcal{I}} C_i(\mathbf{p}, \mathbf{r}^U, \mathbf{r}^D) \quad (4.1)$$

subject to:

$$\sum_{i \in \mathcal{I}_n} p_i + \sum_{l \in \mathcal{L} | \text{to}(l)=n} f_l - \sum_{l \in \mathcal{L} | \text{fr}(l)=n} f_l = d_n - \hat{g}_n; \forall n \in \mathcal{N} \quad (4.2)$$

$$f_l = b_l (\theta_{\text{fr}(l)} - \theta_{\text{to}(l)}); \forall l \in \mathcal{L}^E \setminus \mathcal{L}^{\text{PS}} \quad (4.3)$$

$$f_l = b_l (\theta_{\text{fr}(l)} - \theta_{\text{to}(l)} + \psi_l); \forall l \in \mathcal{L}^{\text{PS}} \quad (4.4)$$

$$-w_l \bar{\psi}_l \leq \psi_l \leq w_l \bar{\psi}_l; \forall l \in \mathcal{L}^{\text{PS}} \quad (4.5)$$

$$-\bar{F}_l \leq f_l \leq \bar{F}_l; \forall l \in \mathcal{L}^E \quad (4.6)$$

$$f_l \geq b_l (\theta_{\text{fr}(l)} - \theta_{\text{to}(l)}) - M(1 - v_l); \forall l \in \mathcal{L}^C \quad (4.7)$$

$$f_l \leq b_l (\theta_{\text{fr}(l)} - \theta_{\text{to}(l)}) + M(1 - v_l); \forall l \in \mathcal{L}^C \quad (4.8)$$

$$-v_l \bar{F}_l \leq f_l \leq v_l \bar{F}_l; \forall l \in \mathcal{L}^C \quad (4.9)$$

$$\underline{P}_i \leq p_i \leq \bar{P}_i; \forall i \in \mathcal{I} \quad (4.10)$$

$$0 \leq r_i^U \leq \bar{R}_i^U; \forall i \in \mathcal{I} \quad (4.11)$$

$$0 \leq r_i^D \leq \bar{R}_i^D; \forall i \in \mathcal{I} \quad (4.12)$$

$$p_i + r_i^U \leq \bar{P}_i; \forall i \in \mathcal{I} \quad (4.13)$$

$$p_i - r_i^D \geq \underline{P}_i; \forall i \in \mathcal{I} \quad (4.14)$$

$$v_l \in \{0, 1\}; \forall l \in \mathcal{L}^C \quad (4.15)$$

$$w_l \in \{0, 1\}; \forall l \in \mathcal{L}^{\text{PS}} \quad (4.16)$$

$$\text{CVaR}_\alpha \left(\mathcal{L}(\mathbf{p}, \mathbf{r}^U, \mathbf{r}^D, \mathbf{v}, \mathbf{w}, \tilde{\mathbf{g}}_j) \right) \leq \bar{\mathcal{L}}; \forall j \in \mathcal{J} \quad (4.17)$$

$$\mathcal{L}(\mathbf{p}, \mathbf{r}^U, \mathbf{r}^D, \mathbf{v}, \mathbf{w}, \mathbf{g}_{j,\omega}) = \max_{(\mathbf{a}_{j,\omega}^G, \mathbf{a}_{j,\omega}^L) \in \mathcal{A}} \left\{ \min_{\substack{\delta_{j,\omega}^+, \delta_{j,\omega}^-, \theta_{j,\omega}^c \\ \psi_{j,\omega}^c, f_{j,\omega}^c, p_{j,\omega}^c}} \sum_{n \in \mathcal{N}} (\delta_{n,j,\omega}^+ + \delta_{n,j,\omega}^-) \right\} \quad (4.18)$$

subject to:

$$\sum_{i \in \mathcal{I}_n} p_{i,j,\omega}^c + \sum_{l \in \mathcal{L} | \text{to}(l)=n} f_{l,j,\omega}^c - \sum_{l \in \mathcal{L} | \text{fr}(l)=n} f_{l,j,\omega}^c = d_n - g_{n,j,\omega} + \delta_{n,j,\omega}^+ - \delta_{n,j,\omega}^- : (\beta_{n,j,\omega}); \forall n \in \mathcal{N} \quad (4.19)$$

$$f_{l,j,\omega}^c = a_{l,j,\omega}^L b_l (\theta_{\text{fr}(l),j,\omega}^c - \theta_{\text{to}(l),j,\omega}^c) : (\gamma_{l,j,\omega}); \forall l \in \mathcal{L}^E \setminus \mathcal{L}^{\text{PS}} \quad (4.20)$$

$$f_{l,j,\omega}^c = a_{l,j,\omega}^L b_l (\theta_{fr(l),j,\omega}^c - \theta_{to(l),j,\omega}^c + \psi_{l,j,\omega}^c) : (\zeta_{l,j,\omega}); \forall l \in \mathcal{L}^{PS} \quad (4.21)$$

$$-w_l \bar{\psi}_l \leq \psi_{l,j,\omega}^c \leq w_l \bar{\psi}_l : (\eta_{l,j,\omega}^-, \eta_{l,j,\omega}^+); \forall l \in \mathcal{L}^{PS} \quad (4.22)$$

$$-\bar{F}_l \leq f_{l,j,\omega}^c \leq \bar{F}_l : (\pi_{l,j,\omega}^-, \pi_{l,j,\omega}^+); \forall l \in \mathcal{L}^E \quad (4.23)$$

$$f_{l,j,\omega}^c \geq b_l (\theta_{fr(l),j,\omega}^c - \theta_{to(l),j,\omega}^c) - M(1 - a_{l,j,\omega}^L v_l) : (\phi_{l,j,\omega}^-); \forall l \in \mathcal{L}^C \quad (4.24)$$

$$f_{l,j,\omega}^c \leq b_l (\theta_{fr(l),j,\omega}^c - \theta_{to(l),j,\omega}^c) + M(1 - a_{l,j,\omega}^L v_l) : (\phi_{l,j,\omega}^+); \forall l \in \mathcal{L}^C \quad (4.25)$$

$$-\bar{F}_l v_l a_{l,j,\omega}^L \leq f_{l,j,\omega}^c \leq \bar{F}_l v_l a_{l,j,\omega}^L : (\chi_{l,j,\omega}^-, \chi_{l,j,\omega}^+); \forall l \in \mathcal{L}^C \quad (4.26)$$

$$p_{i,j,\omega}^c \geq a_{i,j,\omega}^G (p_i - r_i^D) : (\sigma_{i,j,\omega}^-); \forall i \in \mathcal{I} \quad (4.27)$$

$$p_{i,j,\omega}^c \leq a_{i,j,\omega}^G (p_i + r_i^U) : (\sigma_{i,j,\omega}^+); \forall i \in \mathcal{I} \quad (4.28)$$

$$\left. \delta_{n,j,\omega}^+, \delta_{n,j,\omega}^- \geq 0; \forall n \in \mathcal{N} \right\}, \forall j \in \mathcal{J}, \omega \in \Omega. \quad (4.29)$$

The idea of (4.1)–(4.29) is to identify a least-cost expansion plan such that the CVaR $_{\alpha}$ of the system imbalance satisfies the maximum level requirement ($\bar{\mathcal{L}}$) for each “credible” renewable distribution $j \in \mathcal{J}$ with a minimum operation cost. More specifically, equation (4.1) jointly minimizes the expansion and daily operation costs, with $\mathbf{c}^L = \{c_l^L\}_{l \in \mathcal{L}^C}$ representing the construction cost of a candidate line $l \in \mathcal{L}^C$, $\mathbf{c}^{PS} = \{c_l^{PS}\}_{l \in \mathcal{L}^{PS}}$ the installment cost of a phase shifter in line $l \in \mathcal{L}^{PS}$ and $C_i(\cdot)$ the cost function of a conventional energy producer $i \in \mathcal{I}$. For each node $n \in \mathcal{N}$, constraint (4.2) assures power balance considering an inelastic demand $\mathbf{d} = \{d_n\}_{n \in \mathcal{N}}$ and a RES output estimative $\hat{\mathbf{g}} = \{\hat{g}_n\}_{n \in \mathcal{N}}$. The set of equations (4.3)–(4.9) define a DC approximation of the Kirchhoff voltage law and bounds for each line in the system (both existing and candidate) with $\mathbf{b} = \{b_l\}_{l \in \mathcal{L}}$ denoting the susceptance of transmission lines and $\bar{\mathbf{F}} = \{\bar{F}_l\}_{l \in \mathcal{L}}$ the respective flow capacities. Note that in equation (4.4), the phase shifting ($\boldsymbol{\psi} = \{\psi_l\}_{l \in \mathcal{L}^{PS}}$) is considered and bounded by $\bar{\boldsymbol{\psi}} = \{\bar{\psi}_l\}_{l \in \mathcal{L}^{PS}}$ in (4.5). Constraints (4.10)–(4.12) establish bounds for the operating point, with $\underline{\mathbf{P}} = \{\underline{P}_i\}_{i \in \mathcal{I}}$ and $\bar{\mathbf{P}} = \{\bar{P}_i\}_{i \in \mathcal{I}}$ representing the minimum and maximum power production of each conventional generator $i \in \mathcal{I}$, and $\bar{\mathbf{R}}^U = \{\bar{R}_i^U\}_{i \in \mathcal{I}}$ and

$\bar{\mathbf{R}}^D = \{\bar{R}_i^D\}_{i \in \mathcal{I}}$ the maximum up-/down-spinning reserve limit. Moreover, constraints (4.13) ensure that the up-spinning reserve do not exceed the capacity left in each conventional generating unit and equation (4.14) assures that the down-spinning reserve is less than the scheduled power. Equations (4.15) and (4.16) ensures the binary nature of line investment and phase shifter placement variables. Finally, (4.17) establishes that, for each renewable production distribution function $j \in \mathcal{J}$, the system imbalance CVaR $_{\alpha}$ is lower than a maximum level ($\bar{\mathcal{L}}$). The system imbalance function ($\mathcal{L}(\cdot)$) is defined by equations (4.18)–(4.29) as a two-level system of optimization problems. Given an expansion planning (\mathbf{v}, \mathbf{w}) , an operating point $(\mathbf{p}, \mathbf{r}^U, \mathbf{r}^D)$ and a scenario $\omega \in \Omega$ of nodal injection from renewable sources $\mathbf{g}_{j,\omega}$, the idea of (4.18)–(4.29) is to identify a feasible redispatch with the lowest power imbalance under the worst possible contingency state within \mathcal{A} . More precisely, equations (4.19) define the power balance for each node $n \in \mathcal{N}$ and (4.20)–(4.26) represent the DC approximation of the Kirchhoff voltage law and power flow bounds, similar to (4.2)–(4.9). Equations (4.27) and (4.28) guarantee that the power redispatch is bounded by the scheduled power and up/down reserves. It is worth to point out that the proposed expansion model (4.1)–(4.29) is a particular instance of the R-ARO framework, thus not suitable for direct implementation on commercial solvers. Nevertheless, in the next section, a solution methodology is devised based on column-and-constraint generation (CCG) techniques [94].

4.3 Solution Methodology

The proposed expansion model (4.1)–(4.29) is a three-level system of optimization problems which cannot be directly solved using commercial solvers. In this section, we devise a solution methodology based on column-and-constraint generation. To ease the presentation, let $\mathbf{y} = (\mathbf{v}, \mathbf{w})$ be the expansion binary vectors, $\mathbf{x} = (\mathbf{p}, \mathbf{r}^U, \mathbf{r}^D)$ be an operating point, $\mathbf{a}_{j,\omega} = (\mathbf{a}_{j,\omega}^G, \mathbf{a}_{j,\omega}^L)$ the vector of contingen-

cies, and $\mathbf{z}_{j,\omega} = (\delta_{j,\omega}^+, \delta_{j,\omega}^-, \boldsymbol{\theta}_{j,\omega}^c, \boldsymbol{\psi}_{j,\omega}^c, \mathbf{f}_{j,\omega}^c, \mathbf{p}_{j,\omega}^c)$ a vector of redispatch variables. The expansion model (4.1)–(4.29) can be compactly written as follows.

$$\min_{\substack{\boldsymbol{\theta}, \boldsymbol{\psi}, \mathbf{f}, \\ \mathbf{x}, \mathbf{y}}} \mathbf{c}^\top \mathbf{y} + \sum_{i \in \mathcal{I}} C_i(\mathbf{x}) \quad (4.30)$$

subject to:

$$(\boldsymbol{\theta}, \boldsymbol{\psi}, \mathbf{f}, \mathbf{x}, \mathbf{y}) \in \mathcal{X} \quad (4.31)$$

$$\text{CVaR}_\alpha(\mathcal{L}(\mathbf{x}, \mathbf{y}, \tilde{\mathbf{g}}_j)) \leq \bar{\mathcal{L}}; \forall j \in \mathcal{J} \quad (4.32)$$

$$\mathcal{L}(\mathbf{x}, \mathbf{y}, \mathbf{g}_{j,\omega}) = \max_{\mathbf{a}_{j,\omega} \in \mathcal{A}} \left\{ \min_{\mathbf{z}_{j,\omega} \in \mathcal{Z}(\mathbf{x}, \mathbf{y}, \mathbf{g}_{j,\omega}, \mathbf{a}_{j,\omega})} \mathbf{h}^\top \mathbf{z}_{j,\omega} \right\}; \forall j \in \mathcal{J}, \omega \in \Omega. \quad (4.33)$$

In (4.30)–(4.33), $\mathbf{c} = (\mathbf{c}^L, \mathbf{c}^{PS})$. In addition, the sets \mathcal{X} and $\mathcal{Z}(\mathbf{x}, \mathbf{y}, \mathbf{g}_{j,\omega}, \mathbf{a}_{j,\omega})$ comprise the feasible region of first and third-level problems, respectively, and \mathbf{h} recovers the third-level objective function. For a given (\mathbf{x}, \mathbf{y}) and renewable distribution function $j \in \mathcal{J}$, the $\text{CVaR}_\alpha(\mathcal{L}(\mathbf{x}, \mathbf{y}, \tilde{\mathbf{g}}_j))$ can be written using its dual form.

$$\text{CVaR}_\alpha(\mathcal{L}(\mathbf{x}, \mathbf{y}, \tilde{\mathbf{g}}_j)) = \max_{\mathbf{q}_j \in \mathcal{Q}} \left\{ \sum_{\omega \in \Omega} q_{j,\omega} \mathcal{L}(\mathbf{x}, \mathbf{y}, \mathbf{g}_{j,\omega}) \right\}, \quad (4.34)$$

with

$$\mathcal{Q} = \left\{ \mathbf{q} \in \mathbb{R}^{|\Omega|} \left| \begin{array}{l} \sum_{\omega \in \Omega} q_\omega = 1; \\ 0 \leq q_\omega \leq \rho_\omega / (1 - \alpha), \quad \omega \in \Omega; \end{array} \right. \right\}, \quad (4.35)$$

where $\rho_\omega = \mathbb{P}(\{\omega\})$ is the probability of scenario $\omega \in \Omega$. Therefore, using (4.34)–(4.35), the proposed trilevel model can be written as the following single-level optimization problem,

$$\min_{\substack{\boldsymbol{\theta}, \boldsymbol{\psi}, \mathbf{f}, \\ \mathbf{x}, \mathbf{y}, \mathbf{z}_{j,\omega}}} \mathbf{c}^\top \mathbf{y} + \sum_{i \in \mathcal{I}} C_i(\mathbf{x}) \quad (4.36)$$

subject to:

$$(\boldsymbol{\theta}, \boldsymbol{\psi}, f, \mathbf{x}, \mathbf{y}) \in \mathcal{X} \quad (4.37)$$

$$\sum_{\omega \in \Omega} q_{j,\omega} \mathbf{h}^\top \mathbf{z}_{j,\omega} \leq \bar{\mathcal{L}}; \forall q_j \in \mathcal{Q}, j \in \mathcal{J} \quad (4.38)$$

$$\mathbf{z}_{j,\omega} \in \mathcal{Z}(\mathbf{x}, \mathbf{y}, \mathbf{g}_{j,\omega}, \mathbf{a}_{j,\omega}); \forall \mathbf{a}_{j,\omega} \in \mathcal{A}, \omega \in \Omega, j \in \mathcal{J}. \quad (4.39)$$

Problem (4.36)–(4.39) is suitable for column-and-constraint generation. Roughly speaking, the solution proposal aims at iteratively recovering a subset of constraints necessary to represent their counterpart (4.38)–(4.39). In other words, identify a set of vectors $\{\{q_{j,\omega}^{(k)}, \mathbf{a}_{j,\omega}^{(k)}\}_{\omega \in \Omega, j \in \mathcal{J}}\}_{k=1}^m$ sufficient to represent constraints (4.38)–(4.39). The proposed CCG algorithm is described next.

Algorithm 1 Column-and-Constraint Generation Algorithm

Initialization:

Set $m \leftarrow 1$;

Solve (4.36)–(4.37) and store its optimal solution $(\mathbf{x}^{(m)}, \mathbf{y}^{(m)})$;

Iteration $m \geq 1$

Step 1: For each $\omega \in \Omega$ and $j \in \mathcal{J}$, compute $\mathcal{L}(\mathbf{x}^{(m)}, \mathbf{y}^{(m)}, \mathbf{g}_{j,\omega})$ solving (4.33). Store $\{\mathbf{a}_{j,\omega}^{(m)}\}_{\omega \in \Omega, j \in \mathcal{J}}$;

Step 2: For each $j \in \mathcal{J}$, compute $\text{CVaR}_\alpha(\mathcal{L}(\mathbf{x}^{(m)}, \mathbf{y}^{(m)}, \tilde{\mathbf{g}}_j))$ solving (4.34)–(4.35). Store $\{q_{j,\omega}^{(m)}\}_{\omega \in \Omega, j \in \mathcal{J}}$;

Step 3: If $\text{CVaR}_\alpha(\mathcal{L}(\mathbf{x}^{(m)}, \mathbf{y}^{(m)}, \tilde{\mathbf{g}}_j)) \leq \bar{\mathcal{L}}, \forall j \in \mathcal{J}$, then stop and return $(\mathbf{x}^{(m)}, \mathbf{y}^{(m)})$. Otherwise, go to **Step 4**;

Step 4: Solve (4.36)–(4.39) with the smaller set $\{\{q_{j,\omega}^{(k)}, \mathbf{a}_{j,\omega}^{(k)}\}_{\omega \in \Omega, j \in \mathcal{J}}\}_{k=1}^m$ fixed in (4.38)–(4.39). Set $m \leftarrow m + 1$ and store its optimal solution $(\mathbf{x}^{(m)}, \mathbf{y}^{(m)})$.

Two key points are important to mention. Firstly, note that (4.34)–(4.35) can be viewed as a constrained knapsack problem. Thus, the solution vector \mathbf{q} usually is composed by several null values. The idea is that the CVaR_α can be interpreted as the average of the $(1 - \alpha)$ worst-valued scenarios and the vector \mathbf{q} represents precisely the conditional probability to compute such average [85]. Therefore, a significant portion of \mathbf{q} is set at zero at the optimal solution which represents those scenarios that are not involved in the computation of the conditional average. As a consequence, in order to enhance the computational capability of the proposed methodology, in **Step 2–Step 3** of every iteration m of the CCG algorithm, we only need to store the variables $\{q_{j,\omega}^{(m)}, \mathbf{a}_{j,\omega}^{(m)}\}_{\omega \in \Omega, j \in \mathcal{J}}$ associated with scenarios such that $q_{j,\omega}^{(m)} > 0$, thus significantly reducing the size of the problem to be solved in **Step 4**.

Secondly, in **Step 1**, we need to solve the two-level system of optimization problems (4.18)–(4.29) (concisely written as (4.33) for presentation purposes) at each iteration m in order to obtain the contingency vector $\mathbf{a}_{j,\omega}^{(m)}$. However, this problem cannot be directly solved using commercial solvers. Nevertheless, we can rewrite the bilevel optimization problem into a single-level counterpart with the following three steps.

- (i) Derive the dual problem of the inner (minimization) problem (4.18)–(4.29).
- (ii) Consolidate both maximization problems into a single one.
- (iii) Linearize the bilinear terms of continuous and binary variables using disjunctive constraints.

4.4 Case Studies

In this section, the effectiveness of the proposed methodology is illustrated through two test systems: (i) an illustrative 5-bus case and (ii) a 128-bus network derived

from the standard IEEE 118-bus test system. In both cases, we set the confidence level to $\alpha = 0.95$ and we assume that generators offer linear cost functions of the form $C_i(\mathbf{p}, \mathbf{r}^U, \mathbf{r}^D) = c_i^p p_i + c_i^U r_i^U + c_i^D r_i^D$. Furthermore, we consider a widely-used $n - K$ security criteria [95] to define the contingency set:

$$\mathcal{A} = \left\{ (\mathbf{a}^G, \mathbf{a}^L) \in \{0, 1\}^{|\mathcal{I}|} \times \{0, 1\}^{|\mathcal{L}|} \mid \sum_{i \in \mathcal{I}} a_i^G + \sum_{l \in \mathcal{L}} a_l^L \geq |\mathcal{I}| + |\mathcal{L}| - K \right\}. \quad (4.40)$$

The proposed solution approach was implemented on a Dell Precision[®] T7600 Xeon[®] E5-2687W 3.10 GHz with 128 GB of RAM, using Xpress-MP 8.2 under MOSEL [47]. The data used in the following case studies can be found in [98].

4.4.1 5-Bus System: Illustrative Example

The illustrative system considered in this section consists of five buses with three (existing) transmission lines, four conventional generators and four demand sites. Eight candidate lines are considered for construction, four of which connecting a disconnected bus with a wind farm¹. We also consider that each existing transmission line is qualified for the placement of a phase shifter. The illustrative 5-bus system is depicted in Figure 4.2, where solid and dotted lines represent, respectively, existing and candidate transmission lines.

Table 4.1: 5-bus system – Data of conventional generators.

| Generator | Capacity (MW) | Generation Cost (\$/MWh) | Up/Down Reserve Cost (\$/MWh) |
|-----------|---------------|--------------------------|-------------------------------|
| G1 | 200 | 10 | 5 |
| G2 | 200 | 10 | 5 |
| G3 | 140 | 50 | 40 |
| G4 | 140 | 50 | 40 |

¹A situation commonly observed in most power systems nowadays since new renewable plants have been constructed at remote sites and must be connected to the main grid.

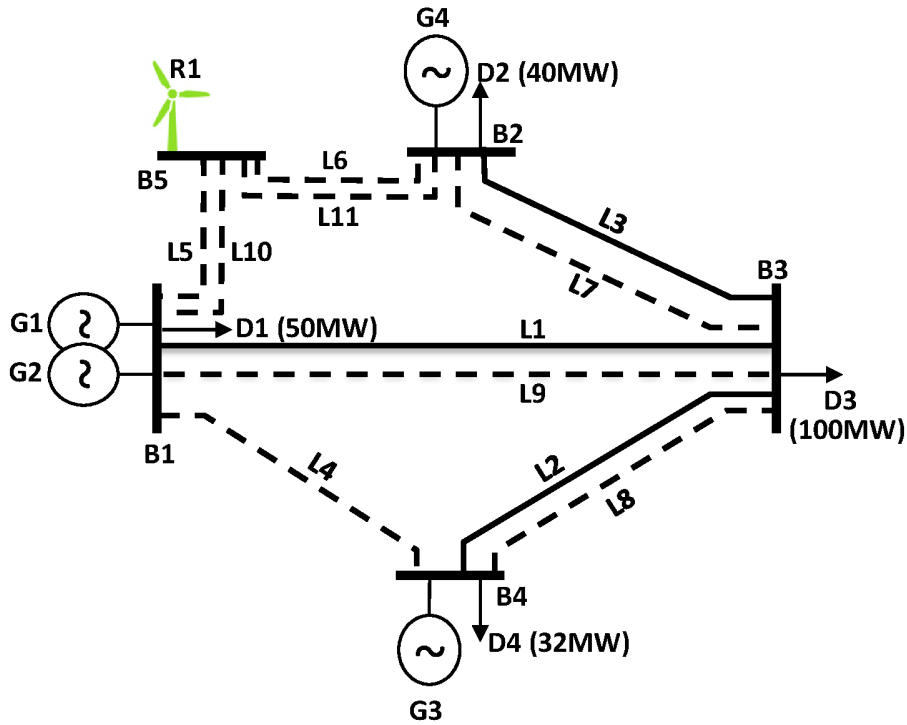


Figure 4.2: 5-bus illustrative system.

Table 4.2: 5-bus system – data of transmission lines.

| Line | from (bus) | to (bus) | Capacity (MW) | Reactance (pu) | Construction Cost (MM\$/year) |
|------|---------------|-------------|------------------|-------------------|----------------------------------|
| L1 | 1 | 3 | 50 | 0.7 | - |
| L2 | 3 | 4 | 40 | 0.7 | - |
| L3 | 3 | 2 | 60 | 0.7 | - |
| L4 | 1 | 4 | 50 | 0.7 | 17.52 |
| L5 | 1 | 5 | 100 | 0.7 | 35.04 |
| L6 | 5 | 2 | 100 | 0.7 | 35.04 |
| L7 | 3 | 2 | 30 | 0.7 | 18.40 |
| L8 | 3 | 4 | 60 | 0.7 | 18.40 |
| L9 | 1 | 3 | 50 | 0.7 | 35.04 |
| L10 | 1 | 5 | 80 | 0.7 | 13.14 |
| L11 | 5 | 2 | 80 | 0.7 | 13.14 |

Generation costs and limits, and relevant specifications of transmission lines are presented in Tables 4.1 and 4.2, respectively. Furthermore, we assume that each phase shifter has an annualized installment cost of 4.38 MM\$ and a maximum shifting of 45 degrees.

In this case study, the expansion plan must enable the system to be operated under a $K = 1$ security criterion. For expository purposes, we assume that the probabilistic description of the wind farm R1 follows a Normal distribution with standard deviation equals to 0.08, but with an uncertain mean. Both $\tilde{g}_1 \sim N(0.72, 0.08^2)$ and $\tilde{g}_2 \sim N(0.60, 0.08^2)$ may be credible representations for the wind power output. Hence, in this case, the most likely RES output belongs to the interval $\hat{g} \in [60, 72]$ MW. We set \hat{g} to 66 MW in (4.2) for bus B5 (center of the interval). In order to represent both distributions, a set of 100 scenarios from each distribution is sampled, i.e. $\Omega = \{\omega_1, \dots, \omega_{100}\}$, using the standard Monte Carlo procedure. Finally, the CVaR_{0.95} of the system power imbalance is limited to 0.41% of the total system demand (i.e., $\overline{\mathcal{L}} = 0.91$ MW).

The objective of this case study is to compare the expansion plan obtained when we consider: (i) only the probability distribution $N(0.72, 0.08^2)$, henceforth referred to as “Distribution 1”, (ii) only the probability distribution $N(0.60, 0.08^2)$, henceforth referred to as “Distribution 2”, and (iii) both aforementioned distributions simultaneously, henceforth referred to as “Ambiguity”. Table 4.3 reports the expansion plans (column 2) and corresponding investment (column 3) and operational (column 4) costs for each case analyzed. Note a non-negligible effect the modeling choice has on the optimal expansion plan. The simultaneous consideration of both distributions (case “Ambiguity”) results in a combination of new transmission assets different in comparison to the case when either distributions are considered individually. In fact, only lines L10 and L11 are simultaneously chosen for all three cases. In summary, under “Distribution 2”, no phase shifter is placed in the system, whereas in case “Distribution 1” PS1 and PS3 are chosen, and in “Ambiguity” only PS3 is placed. It also should be noted that the investment cost for the ambiguity-averse solution is higher (as expected) compared to both single-distribution cases. Nevertheless, the resulting operation cost is significantly lower and the dispatch is robust against both distributions.

Table 4.3: 5-bus system – expansion plan and resulting investment and operation costs.

| Case | Expansion Plan | Investment Cost (MM\$/year) | Operation Cost (MM\$/year) |
|-----------------------|----------------------------|--------------------------------|-------------------------------|
| Distribution 1 | PS1, PS3, L6, L7, L10, L11 | 88.48 | 38.54 |
| Distribution 2 | L9, L10, L11 | 61.32 | 46.05 |
| Ambiguity | PS3, L6, L9, L10, L11 | 100.74 | 30.72 |

Table 4.4: 5-bus system – operation costs considering different probability distributions (MM\$/year).

| Decision | Realization | |
|-----------------------|----------------------------------|----------------------------------|
| | Distribution 1 (\tilde{g}_1) | Distribution 2 (\tilde{g}_2) |
| Distribution 1 | 38.54 | 42.98 |
| Distribution 2 | Infeasible | 46.05 |
| Ambiguity | 29.56 | 30.09 |

Lastly, Table 4.4 presents the operation cost induced by the expansion plan obtained for each one of the three cases analyzed under both \tilde{g}_1 and \tilde{g}_2 distributions. In line with the previous analysis, on the one hand, note that the operation cost for the expansion plan obtained under case “Distribution 1” is roughly 42% higher than the “Ambiguity” case assuming \tilde{g}_2 (“Distribution 2”). Furthermore, on the other hand, under case “Distribution 2”, the system operation is not feasible if \tilde{g}_1 (“Distribution 1”) realizes, since there is no operating point that meets the maximum allowed system imbalance ($\overline{\mathcal{L}}$) under the security criterion $K = 1$. We thus highlight that the simultaneous consideration of both distributions in the expansion evaluation is key to guarantee not only feasibility, but also it may imply in lower operation costs.

4.4.2 128-Bus System: Case Study

To illustrate the scalability of the proposed TEP methodology, a 128-bus system designed from the standard IEEE 118-bus test system is considered. It comprises 198 existing branches with 54 thermal units, 10 wind farms, and 91 loads that result in a total demand of 3286 MW. A total of 12 corridors are candidates for

the construction of up to two transmission lines, each of which with an (annualized) investment cost of 3504 k\$. Additionally, 26 existing lines are considered suitable for installing a phase shifter with an individual (annualized) placement cost of 876 [k\$] and shifting limit of 45 degrees.

Within the daily operation stage, wind production uncertainty can be suitably characterized by a Normal distribution around its best output estimative. However, due to the time length required for construction of new network infrastructure, the expansion plan is made ahead enough to induce a high degree of uncertainty in the best wind production output estimation. As a consequence, even though the probability distribution format of the day-ahead wind production can be suitably defined, the TEP is still made under ambiguity due to the uncertainty in its parameters. That being said, in this case study, we follow the standard procedure adopted by practitioners and make use of historical data to point-estimate the Normal distribution parameters for each wind farm². Nevertheless, regardless of the (point-)estimation procedure, a confidence interval (CI) around this estimative can be constructed such that the decision-maker preference relation between the induced Normal distributions with parameters within such interval is not evident. Therefore, in this case study, the ambiguity set comprises Normal distributions with mean equal to the point-estimative, and the upper- and lower-limits of the CI (hereinafter referred to $\tilde{\mathbf{g}}^{(\text{PE})}$, $\tilde{\mathbf{g}}^{(\text{UL})}$, and $\tilde{\mathbf{g}}^{(\text{LL})}$, respectively). For simplicity, the variance are considered certain and equal to the point-estimated value.

The goal of this section is thus to analyze the expansion plan under two cases: (i) the *Nominal Case*, in which only the point-estimated distribution is considered ($\mathcal{G} = \{\tilde{\mathbf{g}}^{(\text{PE})}\}$); and (ii) the *Ambiguity Case*, in which the expansion plan is assessed considering concomitantly all three distributions ($\mathcal{G} = \{\tilde{\mathbf{g}}^{(\text{PE})}, \tilde{\mathbf{g}}^{(\text{UL})}, \tilde{\mathbf{g}}^{(\text{LL})}\}$). We

²For expository purposes, we assume pairwise independence between the wind farm production random variables.

highlight that the Nominal Case stands for the standard practice adopted in most decision under uncertainty frameworks since point-estimators are typically chosen by practitioners to characterize the distribution parameters due to their strong statistical properties [80]. Therefore, seeking for consistency, in both Nominal and Ambiguity Cases, we set $\hat{\mathbf{g}} = \mathbb{E}[\tilde{\mathbf{g}}^{(\text{PE})}]$. Additionally, to represent the wind power variability, we make use of standard Monte Carlo procedure to sample a set of 100 “scenarios” ($\Omega = \{\omega_1, \dots, \omega_{100}\}$) for each Normal Distribution. We also consider a security criterion of $K = 1$ and assume a maximum system imbalance of 0.5% of total demand, i.e., $\overline{\mathcal{L}} = 16.43$ MW.

Table 4.5: 128-bus system – expansion profiles for both Nominal and Ambiguity Cases.

| Corridor | Nominal Case | Ambiguity Case |
|----------|--------------|----------------|
| 15–120 | 0 | 0 |
| 15–120 | 1 | 1 |
| 19–120 | 0 | 0 |
| 19–120 | 1 | 1 |
| 54–122 | 0 | 0 |
| 54–122 | 1 | 1 |
| 55–122 | 0 | 0 |
| 55–122 | 1 | 1 |
| 55–124 | 0 | 0 |
| 55–124 | 1 | 1 |
| 59–124 | 0 | 0 |
| 59–124 | 1 | 1 |
| 60–125 | 0 | 1 |
| 60–125 | 0 | 1 |
| 61–125 | 1 | 0 |
| 61–125 | 1 | 0 |
| 80–127 | 0 | 0 |
| 80–127 | 1 | 1 |
| 90–128 | 0 | 1 |
| 90–128 | 0 | 0 |
| 91–128 | 1 | 0 |
| 91–128 | 1 | 1 |
| 96–127 | 0 | 0 |
| 96–127 | 1 | 1 |

Table 4.5 outlines the expansion profile for both Nominal and Ambiguity cases (columns two and three, respectively). Table 4.6 presents the operational and expansion costs (columns two and three, respectively) resulting from each modeling approach (Nominal and Ambiguity Cases) along with the respective computational time and number of iterations required to solve each instance (columns four and five, respectively). Firstly, we highlight that the expansion plan is different between the two cases. Basically, in the Nominal Case, a double line is indicated for construction in corridor 61–125, whereas in the Ambiguity Case, the chosen corridor was between nodes 60 and 125. Additionally, the Nominal Case signals the construction of a double line between nodes 91 and 128. In the Ambiguity Case, however, only a single line is indicated to be constructed in this corridor, but a single line should be constructed in 90–128. With respect to phase shifters, both cases indicated the instalment of a single device in the existing corridor 55–59.

Effectively, although the expansion plan differs between cases, the total number of lines and phase shifters indicated for construction is the same. Thus, as shown in Table 4.6, the expansion cost is equal both in Nominal and Ambiguity Cases. Furthermore, as expected, the operational cost of the Ambiguity Case is higher than the Nominal one due to the requirement in the former to meet the maximum desired imbalance level for each one of the three distributions, concomitantly. Nevertheless, we highlight that such increase is less than 5%.

Table 4.6: 128-bus system – operational and expansion costs [MM\$/year] from each Nominal and Ambiguity Cases, along with the computational time [s] and number of iterations required to solve each instance.

| Case | Operation Cost (MM\$/year) | Investment Cost (MM\$/year) | Computing Time (s) | Number of iterations |
|-----------|-------------------------------|--------------------------------|-----------------------|-------------------------|
| Nominal | 211.93 | 42.92 | 670067 | 175 |
| Ambiguity | 223.49 | 42.92 | 93124 | 30 |

Next, we evaluate the impact of performing an ambiguity-averse TEP on the system operation. For consistency, a new set of 2000 scenarios (i.e., $\bar{\Omega} = \{\omega_1, \dots, \omega_{2000}\}$)

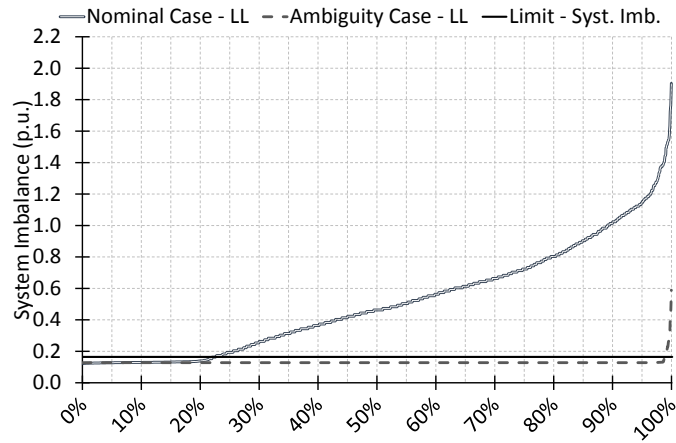


Figure 4.3: Out-of-sample inverse cumulative distributions of the system imbalance under the realization of the lower limit distribution.

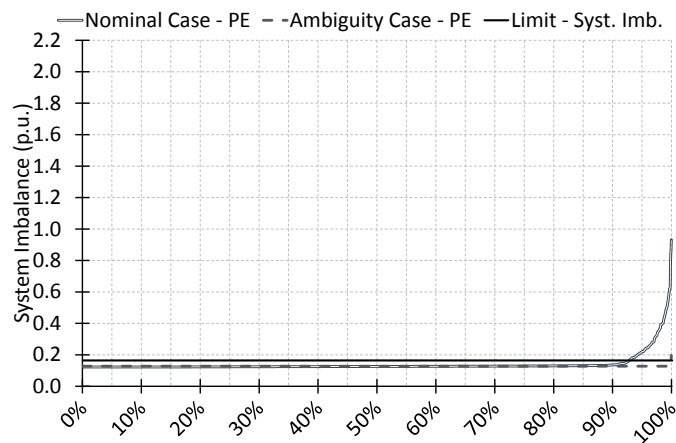


Figure 4.4: Out-of-sample inverse cumulative distributions of the system imbalance under the realization of the point estimative distribution.

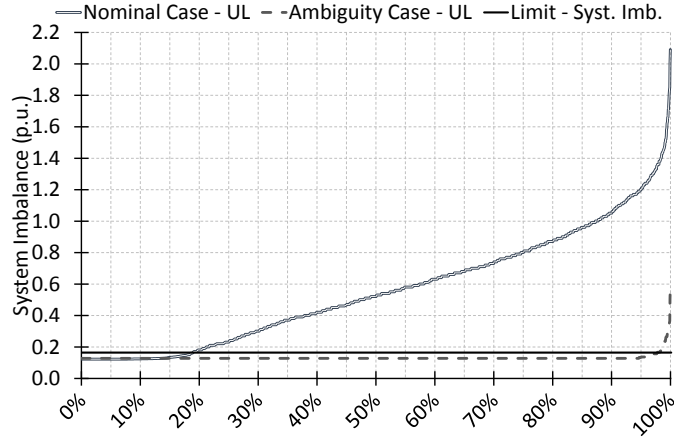


Figure 4.5: Out-of-sample inverse cumulative distributions of the system imbalance under the realization of the upper limit distribution.

were sampled for each distribution $\{\tilde{\mathbf{g}}^{(\text{PE})}, \tilde{\mathbf{g}}^{(\text{UL})}, \tilde{\mathbf{g}}^{(\text{LL})}\}$ and an “out-of-sample” analysis is performed. In Figs. 4.3, 4.4, and 4.5, the distributions of the system imbalance, given the expansion plans for Nominal and Ambiguity Cases, are depicted under the new set of scenarios. Such figures present the inverse cumulative distributions under the realization of lower limit (Fig. 4.3), point estimative (Fig. 4.4) and upper limit (Fig. 4.5) distributions. We firstly highlight that, as expected, both Nominal and Ambiguity expansion plans induce a stable system operation under the PE distribution since a low CVaR of system imbalance is observed (see Fig. 4.4). Nevertheless, under the LL and UL distributions, it is likely that the ambiguity-neutral expansion plan can cause an unstable operation. We argue that, since the system was not prepared to comply with the uncertainty dynamics driven by these two distributions, the resource allocation planned is not sufficient to enable the system operator to satisfy the maximum allowed imbalance in most of the scenarios (78% and 82% for the LL and UL distributions, respectively).

Finally, from a financial point of view, we quantify the impact of the aforementioned power imbalances also using the out-of-sample set of scenarios. For completeness,

Table 4.7: Out-of-sample probability distribution of load shedding cost.

| Interval of Load Shed Cost(k\$/hour) | Nominal Case | | | Amiguity Case | | |
|---|--------------|--------|--------|---------------|---------|--------|
| | LL | PE | UL | LL | PE | UL |
| [0,5) | 0.20% | 17.20% | 18.10% | 96.40% | 100.00% | 99.80% |
| [5,10) | 0.00% | 2.90% | 72.70% | 0.00% | 0.00% | 0.20% |
| [10,30) | 33.20% | 78.80% | 9.20% | 3.20% | 0.00% | 0.00% |
| [30,50) | 20.80% | 0.70% | 0.00% | 0.30% | 0.00% | 0.00% |
| [50,100) | 34.90% | 0.40% | 0.00% | 0.10% | 0.00% | 0.00% |
| [100,∞) | 10.90% | 0.00% | 0.00% | 0.00% | 0.00% | 0.00% |

Table 4.8: Out-of-sample probability distribution of wind spillage cost.

| Interval of Wind Spillage Cost(k\$/hour) | Nominal Case | | | Amiguity Case | | |
|---|--------------|--------|--------|---------------|--------|--------|
| | LL | PE | UL | LL | PE | UL |
| [0,0.5) | 99.90% | 97.10% | 68.60% | 99.70% | 99.50% | 95.20% |
| [0.5,1) | 0.00% | 0.10% | 0.90% | 0.00% | 0.00% | 0.00% |
| [1,3) | 0.10% | 2.20% | 7.70% | 0.30% | 0.50% | 4.50% |
| [3,5) | 0.00% | 0.60% | 9.10% | 0.00% | 0.00% | 0.30% |
| [5,10) | 0.00% | 0.00% | 12.40% | 0.00% | 0.00% | 0.00% |
| [10,∞) | 0.00% | 0.00% | 1.30% | 0.00% | 0.00% | 0.00% |

we split the imbalance in load shedding (loss of load) and wind spillage. The former has a cost of 1000 \$/MWh and the latter a cost of 100 \$/MWh [92]. Tables 4.7 and 4.8 present the distribution of, respectively, load shedding and wind spillage costs. Note that, under the Nominal expansion plan, the probability of a load shedding higher than 30 k\$ is approximately 67% for the LL distribution. We can interpret this result by noting that, for this distribution, the level of wind production is lower than the estimated. Therefore, the system operator should increase conventional generation using up reserves. Since the system was not planned to accommodate this operation, a load shed is induced in most scenarios. Analogously, a probability of a wind spillage cost higher than 3 k\$ (10% of total expansion plus operation costs) is roughly larger than 23% for the UL distribution. A similar argument summarizes this result.

CHAPTER 5

Conclusions

It is well-known that the TEP problem is a complex task. In the technical literature, a great deal of effort has been devoted to deal with various aspects related to this problem [99, 100]. In this thesis, we have addressed three circumstances that a planner may face while devising the expansion of a transmission infrastructure. Following we present a summary of the methodologies proposed in this work and comment possible future directions of research.

5.1 Summary

In chapter 2, we proposed a RG-TEP model to support the efficient achievement of RES share targets while considering the reliability of the system. In this case, the system planner needs to plan the generation and transmission expansion to meet a predefined percentage (or target) of the system demand by means of renewable

sources. In addition, we consider the existence of potential renewable sites that can be connected to the system in order to achieve such targets. Moreover, besides achieving RES targets, the expansion plan should be secure enough to provide the system with necessary flexibility to endure outages and uncertainty in RES generation.

In order to tackle the problem stated in chapter 2, we formulated a two-stage min-max-min optimization model. The first level of this model aims to determine the generation and transmission expansion plan by selecting the most appropriate candidate lines to be built and the best renewable sites to be developed and connected to the system. Also the first level determines a pre-contingency scheduling of power and reserves. The second level identifies worst-case combination of outage and realization of nodal injection uncertainty. Finally, the third level reacts against the worst-case situation by redispatching the system with the resources planned in the first level. An interesting feature of this model is the possibility to combine multiple security criteria simultaneously with different levels of stringency. For instance, the planner has the flexibility to plan the expansion while imposing a maximum system imbalance equal to 0% of the demand for single and double outages while allowing up to 2.5% if three elements of the system fail. Another important feature of the model is the consideration of reserve deliverability.

In order to solve the model proposed in chapter 2, we developed a column and constraint generation algorithm. The simulation results presented for the Chilean case study corroborate the effectiveness of the proposed methodology to find robust solutions and its capability to provide system planners with a flexible tool to measure the trade-off between reliability and cost under reasonable computational effort. The methodology is also tested with the standard IEEE 118-bus system in order to demonstrate its scalability.

In chapter 3, we propose a novel methodology to determine optimal transmission expansion plans through a min-max regret approach. In this case, the system planner has to determine the expansion of the transmission infrastructure under uncertainty in the forthcoming generation expansion. More specifically, the planner does not have a precise picture of where the new generators will be located and how much capacity they will provide to the system. Instead, scenarios of possible future generations expansions are given.

We address the problem faced by planner in chapter 3 by formulating a 5-level model to determine the transmission plan that leads to the minimum maximum regret under uncertainty in future generation expansion. The proposed formulation also considers occurrence of system outages, securing operation through a deterministic $n - 1$ criterion. Candidate infrastructure includes flexible and conventional transmission assets and hence the model can determine optimal portfolios of phase-shifters and transmission lines to deal with both long- and short-term uncertainties. To solve the optimization problem, we developed an algorithm based on column and constraint generation and Benders decomposition techniques to determine the optimal solution of the proposed 5-level model in a finite number of iterations.

Numerical studies in chapter 3 demonstrated that the value of flexible network technologies increases with explicit recognition of uncertainty, and that flexible network portfolios can effectively reduce the regret of investment decisions and improve economic efficiency and security of supply provision. Furthermore, we also demonstrated that there are specific investment decisions which are revealed only when uncertainty is explicitly modeled and that flexible transmission investment options may remain unseen when network infrastructure is planned through considering deterministic scenarios. Decisions that are only taken when uncertainty is properly characterized help to hedge the investment plan against a range of possible uncertainty realizations.

In chapter 4, we propose a novel methodology to address the TEP problem under ambiguity in the probability distribution of RES generation. In this case, the planner needs to take a decision on transmission expansion with limited knowledge of the underlying process behind the realization of the RES output.

To deal with the situation presented in chapter 4, we propose a three-level formulation to determine the optimal transmission expansion plan under ambiguity in renewable probability distribution while considering outages of system elements. Within the set of candidate assets, we consider phase shifters along with transmission lines to provide the system with more flexibility. Contingencies of system elements are addressed via adjustable robust optimization and renewable variability is modeled by means of a scenario-based approach. In order to circumvent the difficulties in the characterization of the uncertainty associated with RES output, the model proposed in this chapter is general enough to accommodate multiple RES probability distributions. To solve the proposed TEP problem, a column and constraint generation algorithm was designed. Numerical studies corroborate and endorse the importance of considering ambiguity in RES probability distribution while planning the expansion of the grid.

5.2 Future Work

Formulations presented in chapters 2 and 4 were devised in a single period fashion. Within this context, extensions of these formulations to the multiperiod setting would be beneficial in order to provide the planner with possibility to consider different load and wind profiles while determining the expansion plan. In addition, in chapter 3, although different snapshots of wind and load are considered, we do not enforce time-coupling in the proposed methodology. The incorporation of such time coupling in the formulation would allow the inclusion of storage devices in the

modeling. Therefore, it would be possible to evaluate the benefits of storage devices while minimizing regret under uncertainty in generation expansion. It should be noted that the main steps used in the proposed solution approaches are readily applicable to the multiperiod instance with time-coupling constraints and some additional notation to properly index variables and parameters over the time periods. However, the computational burdening associated with the multiperiod setting needs to be properly addressed. In this context, parallel computing can be a good starting point.

In chapter 3, we have used a discrete set of scenarios to represent generation expansion uncertainty following industry practices. It is a plausible and reasonable alternative for this kind of uncertainty since it provides industry players, regulators, planners and further stakeholders with the possibility to express their views about uncertainty in generation expansion. This uncertainty is mainly driven by generation companies' investment decisions and thereby significantly affected by policy, political and further macroeconomic conditions that are difficult to model in a real context. Our proposed methodology is therefore highly dependent on the quality of the provided scenarios, which require significant time and effort to be generated since they must properly characterize the set of economic and political structures of possible futures. Within this context, we recognize that it would be interesting to consider, within the proposed framework, stress-test scenarios as those generated by the combinations of up/down deviations within a constrained uncertainty budget. In addition, it would be important to examine more refined regret concepts that attach a greater weight to most probable scenarios (e. g., "expected regret"). These considerations can open up interesting opportunities for future research.

Finally, as customary in TEP models, we simplified the power flow by adopting a DC load fashion. Further research will consider including AC transmission constraints.

Bibliography

- [1] F. Banez-Chicharro, L. Olmos, A. Ramos, and J. M. Latorre, “Estimating the benefits of transmission expansion projects: An aumann-shapley approach,” *Energy*, pp. –, 2016. [Online]. Available: <http://www.sciencedirect.com/science/article/pii/S036054421631581X>
- [2] J. Lu, J. Han, Y. Hu, and G. Zhang, “Multilevel decision-making: A survey,” *Information Sciences*, vol. 346–347, pp. 463 – 487, 2016. [Online]. Available: <http://www.sciencedirect.com/science/article/pii/S0020025516300202>
- [3] F. Plastria and L. Vanhaverbeke, “Discrete models for competitive location with foresight,” *Computers & Operations Research*, vol. 35, no. 3, pp. 683 – 700, 2008, part Special Issue: New Trends in Locational Analysis. [Online]. Available: <http://www.sciencedirect.com/science/article/pii/S0305054806001328>

- [4] H. Küçükaydin, N. Aras, and I. Kuban Altinel, “Competitive facility location problem with attractiveness adjustment of the follower: A bilevel programming model and its solution,” *European Journal of Operational Research*, vol. 208, no. 3, pp. 206 – 220, 2011. [Online]. Available: <http://www.sciencedirect.com/science/article/pii/S0377221710005461>
- [5] T. Kis and A. Kovács, “Exact solution approaches for bilevel lot-sizing,” *European Journal of Operational Research*, vol. 226, no. 2, pp. 237 – 245, 2013. [Online]. Available: <http://www.sciencedirect.com/science/article/pii/S0377221712008715>
- [6] L. dell’Olio, A. Ibeas, and F. Ruisánchez, “Optimizing bus-size and headway in transit networks,” *Transportation*, vol. 39, no. 2, pp. 449–464, 2012.
- [7] S. Wang, Q. Meng, and H. Yang, “Global optimization methods for the discrete network design problem,” *Transportation Research Part B: Methodological*, vol. 50, pp. 42 – 60, 2013. [Online]. Available: <http://www.sciencedirect.com/science/article/pii/S0191261513000179>
- [8] P. Fontaine and S. Minner, “Benders decomposition for discrete–continuous linear bilevel problems with application to traffic network design,” *Transportation Research Part B: Methodological*, vol. 70, pp. 163 – 172, 2014. [Online]. Available: <http://www.sciencedirect.com/science/article/pii/S0191261514001611>
- [9] J. F. Bard, J. Plummer, and J. C. Sourie, “A bilevel programming approach to determining tax credits for biofuel production,” *European Journal of Operational Research*, vol. 120, no. 1, pp. 30 – 46, 2000. [Online]. Available: <http://www.sciencedirect.com/science/article/pii/S0377221798003737>
- [10] M. P. Scaparra and R. L. Church, “A bilevel mixed-integer program for critical infrastructure protection planning,” *Computers & Operations*

- Research*, vol. 35, no. 6, pp. 1905 – 1923, 2008, part Special Issue: {OR} Applications in the Military and in Counter-Terrorism. [Online]. Available: <http://www.sciencedirect.com/science/article/pii/S0305054806002395>
- [11] L. He, G.H. Huang, and H. Lu, “Greenhouse gas emissions control in integrated municipal solid waste management through mixed integer bilevel decision-making,” *Journal of Hazardous Materials*, vol. 193, pp. 112 – 119, 2011. [Online]. Available: <http://www.sciencedirect.com/science/article/pii/S0304389411009174>
- [12] J.-F. Camacho-Vallejo, E. González-Rodríguez, F.-J. Almaguer, and R. G. González-Ramírez, “A bi-level optimization model for aid distribution after the occurrence of a disaster,” *Journal of Cleaner Production*, vol. 105, pp. 134 – 145, 2015, decision-support models and tools for helping to make real progress to more sustainable societies. [Online]. Available: <http://www.sciencedirect.com/science/article/pii/S0959652614010087>
- [13] C. Zhao and Y. Guan, “Unified stochastic and robust unit commitment,” *IEEE Transactions on Power Systems*, vol. 28, no. 3, pp. 3353–3361, Aug 2013.
- [14] Q. Wang, J.-P. Watson, and Y. Guan, “Two-stage robust optimization for N-k contingency-constrained unit commitment,” *IEEE Transactions on Power Systems*, vol. 28, no. 3, pp. 2366–2375, Aug. 2013.
- [15] A. Street, F. Oliveira, and J. M. Arroyo, “Energy and reserve scheduling under an $n - K$ security criterion via robust optimization,” in *Proc. 17th Power Systems Computation Conference (PSCC’11)*, Stockholm, Sweden, Aug. 2011.
- [16] —, “Contingency-constrained unit commitment with $n - K$ security criterion: A robust optimization approach,” *IEEE Transactions on Power Systems*, vol. 26, no. 3, pp. 1581–1590, Aug. 2011.

- [17] A. Street, A. Moreira, and J. M. Arroyo, "Energy and reserve scheduling under a joint generation and transmission security criterion: An adjustable robust optimization approach," *IEEE Transactions on Power Systems*, vol. 29, no. 1, pp. 3–14, Jan. 2014.
- [18] A. Moreira, A. Street, and J. M. Arroyo, "Energy and reserve scheduling under correlated nodal demand uncertainty: An adjustable robust optimization approach," *International Journal of Electrical Power & Energy Systems*, vol. 72, pp. 91 – 98, 2015, the Special Issue for 18th Power Systems Computation Conference. [Online]. Available: <http://www.sciencedirect.com/science/article/pii/S0142061515000988>
- [19] L. P. Garcés, A. J. Conejo, R. García-Bertrand, and R. Romero, "A bilevel approach to transmission expansion planning within a market environment," *IEEE Trans. Power Syst.*, vol. 24, no. 3, pp. 1513–1522, Aug. 2009.
- [20] L. P. Garcés, R. Romero, and J. M. Lopez-Lezama, "Market-driven security-constrained transmission network expansion planning," in *2010 IEEE/PES Transmission and Distribution Conference and Exposition: Latin America (T&D-LA)*, São Paulo, Brazil, 2010, pp. 427–433.
- [21] M. R. Hesamzadeh and M. Yazdani, "Transmission capacity expansion in imperfectly competitive power markets," *IEEE Trans. Power Syst.*, vol. 29, no. 1, pp. 62–71, Jan. 2014.
- [22] D. Pozo, E. E. Sauma, and J. Contreras, "A three-level static MILP model for generation and transmission expansion planning," *IEEE Transactions on Power Systems*, vol. 28, no. 1, pp. 202–210, Feb. 2013.
- [23] C. Ruiz and A. Conejo, "Robust transmission expansion planning," *European Journal of Operational Research*, vol. 242, no. 2, pp. 390–401, 2015.

- [24] B. Chen and L. Wang, "Robust transmission planning under uncertain generation investment and retirement," *IEEE Trans. Power Syst.*, vol. 31, no. 6, pp. 5144–5152, Nov. 2016.
- [25] Directive 2001/77/EC, "On the promotion of electricity produced from renewable energy sources in the internal electricity market." [Online]. Available: <http://eur-lex.europa.eu/>
- [26] M. Madrigal and S. Stoft, *Transmission expansion for renewable energy scale-up: Emerging lessons and recommendations*. World Bank Publications, 2012.
- [27] A. Liu, B. Hobbs, J. Ho, J. D. McCalley, V. Krishnan, M. Shahidehpour, and Q. P. Zheng, "Whitepaper: Co-optimization of transmission and other supply resources," National Association of Regulatory Utility Commissioners, Report, 2013.
- [28] F. D. Munoz, B. F. Hobbs, J. L. Ho, and S. Kasina, "An engineering-economic approach to transmission planning under market and regulatory uncertainties: WECC case study," *IEEE Transactions on Power Systems*, vol. 29, no. 1, pp. 307–317, 2014.
- [29] E. E. Sauma and S. S. Oren, "Proactive planning and valuation of transmission investments in restructured electricity markets," *Journal of Regulatory Economics*, vol. 30, no. 3, pp. 261–290, 2006.
- [30] F. D. Munoz, B. F. Hobbs, and S. Kasina, "Efficient proactive transmission planning to accommodate renewables," in *2012 IEEE Power and Energy Society General Meeting*, July 2012, pp. 1–7.
- [31] A. H. van der Weijde and B. F. Hobbs, "The economics of planning electricity transmission to accommodate renewables: Using two-stage optimisation

- to evaluate flexibility and the cost of disregarding uncertainty,” *Energy Economics*, vol. 34, no. 6, pp. 2089 – 2101, 2012.
- [32] J. H. Roh, M. Shahidehpour, and Y. Fu, “Market-based coordination of transmission and generation capacity planning,” *IEEE Transactions on Power Systems*, vol. 22, no. 4, pp. 1406–1419, 2007.
- [33] IRENA, “Renewable energy integration in power grids,” Technical Report, 2015. [Online]. Available: http://www.irena.org/DocumentDownloads/Publications/IRENA-ETSAP_Tech_Brief_Power_Grid_Integration_2015.pdf.
- [34] NERC, “Potential reliability impacts of epa’s clean power plan,” Technical Report, 2015. [Online]. Available: <http://www.nerc.com>
- [35] J. M. Morales, A. J. Conejo, and J. Perez-Ruiz, “Economic valuation of reserves in power systems with high penetration of wind power,” *IEEE Transactions on Power Systems*, vol. 24, no. 2, pp. 900–910, 2009.
- [36] D. Pozo and J. Contreras, “A chance-constrained unit commitment with an n-K security criterion and significant wind generation,” *IEEE Transactions on Power Systems*, vol. 28, no. 3, pp. 2842–2851, 2013.
- [37] J.D. Lyon, K.W. Hedman, and M. Zhang, “Reserve requirements to efficiently manage intra-zonal congestion,” *IEEE Transactions on Power Systems*, vol. 29, no. 1, pp. 251–258, Jan 2014.
- [38] Y. Chen, P. Gribik, and J. Gardner, “Incorporating post zonal reserve deployment transmission constraints into energy and ancillary service co-optimization,” *IEEE Transactions on Power Systems*, vol. 29, no. 2, pp. 537–549, Mar. 2014.

- [39] A. Ben-Tal and A. Nemirovski, “Robust convex optimization,” *Math. Oper. Res.*, vol. 23, no. 4, pp. 769–805, Nov. 1998.
- [40] R. Jiang, J. Wang, and Y. Guan, “Robust unit commitment with wind power and pumped storage hydro,” *IEEE Transactions on Power Systems*, vol. 27, no. 2, pp. 800–810, May 2012.
- [41] D. Bertsimas, E. Litvinov, X. A. Sun, J. Zhao, and T. Zheng, “Adaptive robust optimization for the security constrained unit commitment problem,” *IEEE Transactions on Power Systems*, vol. 28, no. 1, pp. 52–63, Feb. 2013.
- [42] A. Moreira, A. Street, and J. M. Arroyo, “Energy and reserve scheduling under correlated nodal demand uncertainty: An adjustable robust optimization approach,” in *Proc. 18th Power Systems Computation Conference (PSCC’14)*, Wroclaw, Poland, Aug. 2014.
- [43] R. A. Jabr, “Robust transmission network expansion planning with uncertain renewable generation and loads,” *IEEE Transactions on Power Systems*, vol. 28, no. 4, pp. 4558–4567, Nov. 2013.
- [44] A. Moreira, A. Street, and J. M. Arroyo, “An adjustable robust optimization approach for contingency-constrained transmission expansion planning,” *IEEE Transactions on Power Systems*, vol. 30, no. 4, pp. 2013–2022, July 2015.
- [45] Y. An and B. Zeng, “Exploring the modeling capacity of two-stage robust optimization: Variants of robust unit commitment model,” *IEEE Transactions on Power Systems*, vol. 30, no. 1, pp. 109–122, Jan 2015.
- [46] S. Boyd and L. Vandenberghe, *Convex Optimization*. Cambridge, UK: Cambridge University Press, 2004.
- [47] Xpress Optimization Suite. <http://www.fico.com/>.

- [48] Reliable transmission expansion planning for large renewable energy penetration – Case study input data. <https://drive.google.com/drive/folders/0BxgJO6PuetvKOHRtNGtmMnZkUm8?usp=sharing>.
- [49] CNE, “Fijación de precios de nudo, sistema interconectado central: Informe técnico definitivo,” Report, 2013. [Online]. Available: http://www.cne.cl/archivos_bajar/ITP_SIC_Abr04def.pdf
- [50] CDEC-SIC, “Cálculo de peajes por el sistema de transmisión troncal,” Web Page, 2013. [Online]. Available: <http://www.cdec-sic.cl/>
- [51] “Mitigation options for addressing climate change,” Web Page, 2015. [Online]. Available: <http://mapschile.cl/>
- [52] R. Moreno, G. Strbac, F. Porrua, S. Mocarquer, and B. Bezerra, “Making room for the boom,” *IEEE Power and Energy Magazine*, vol. 8, no. 5, pp. 36–46, Sept 2010.
- [53] A. Papavasiliou, S. Oren, and B. Rountree, “Applying high performance computing to transmission-constrained stochastic unit commitment for renewable energy integration,” *IEEE Transactions on Power Systems*, vol. 30, no. 3, pp. 1109–1120, May 2015.
- [54] G. Strbac, R. Moreno, I. Konstantelos, D. Pudjianto, and M. Aunedi, “Whitepaper: Strategic development of north sea grid infrastructure to facilitate least-cost decarbonisation,” Imperial College London, Technical Report, 2014.
- [55] B. K. Chen, J. H. Wang, L. Z. Wang, Y. Y. He, and Z. Y. Wang, “Robust optimization for transmission expansion planning: Minimax cost vs. minimax regret,” *IEEE Trans. Power Syst.*, vol. 29, no. 6, pp. 3069–3077, 2014.

- [56] N. A. S. Dehghan and A. J. Conejo, "Reliability-constrained robust power system expansion planning," *IEEE Trans. Power Syst.*, vol. PP, no. 99, pp. 1–10, 2015.
- [57] L. J. Savage, "The theory of statistical decision," *Journal of the American Statistical Association*, vol. 46, pp. 55–67, 1951.
- [58] M. Sahraei-Ardakani and K. Hedman, "A fast lp approach for enhanced utilization of variable impedance based facts devices," *IEEE Trans. Power Syst.*, vol. PP, no. 99, pp. 1–10, 2015.
- [59] —, "Day-ahead corrective adjustment of facts reactance: A linear programming approach," *IEEE Trans. Power Syst.*, vol. PP, no. 99, pp. 1–9, 2015.
- [60] R. Moreno, Y. Chen, and G. Strbac, "Evaluation of benefits of coordinated dc ac flexible transmission systems with probabilistic security and corrective control," in *IET International Conference on Resilience of Transmission and Distribution Networks (RTDN) 2015*, Sept 2015, pp. 1–6.
- [61] R. Perez, "Power flow controllability and flexibility in the transmission expansion planning problem: a mixed-integer linear programming approach," Master's thesis, COPPE UFRJ, Rio de Janeiro, Brazil, 2014.
- [62] I. Konstantelos and G. Strbac, "Valuation of flexible transmission investment options under uncertainty," *IEEE Transactions on Power Systems*, vol. 30, no. 2, pp. 1047–1055, March 2015.
- [63] G. Ayala and A. Street, "Energy and reserve scheduling with post-contingency transmission switching," *Electric Power Systems Research*, vol. 111, pp. 133 – 140, 2014. [Online]. Available: <http://www.sciencedirect.com/science/article/pii/S0378779614000510>.

- [64] D. E. Bell, "Regret in decision making under uncertainty," *Oper. Res.*, vol. 30, no. 5, pp. 961–981, Sep./Oct. 1982.
- [65] G. Loomes and R. Sugden, "Regret theory: An alternative theory of rational choice under uncertainty," *Econ. J.*, vol. 92, no. 368, pp. 805–824, Dec. 1982.
- [66] B. G. Gorenstin, N. M. Campodonico, J. P. Costa, and M. V. F. Pereira, "Power system planning under uncertainty," *IEEE Trans. Power Syst.*, vol. 8, no. 1, pp. 129–136, Feb. 1993.
- [67] J. M. Arroyo, N. Alguacil, and M. Carrión, "A risk-based approach for transmission network expansion planning under deliberate outages," *IEEE Transactions on Power Systems*, vol. 25, no. 3, pp. 1759–1766, Aug. 2010.
- [68] K. Bell, P. Roddy, and C. Ward, "The impact of generation market uncertainty on transmission system thermal constraints and plant procurement volumes," in *39th CIGRE Session*, Paris, France, Aug. 2002.
- [69] "Electricity ten year statement 2014," National Grid, Report, 2014. [Online]. Available: <http://www2.nationalgrid.com/UK/Industry-information/Future-of-Energy/Electricity-ten-year-statement/ETYS-Archive/>.
- [70] V. Rious, Y. Perez, and J. Glachant, "Power transmission network investment as an anticipation problem," *Rev. Netw. Econ.*, vol. 10, no. 4, pp. 1–21, 2011.
- [71] J. M. Morales, P. Pinson, and H. Madsen, "A transmission-cost-based model to estimate the amount of market-integrable wind resources," *IEEE Trans. Power Syst.*, vol. 27, no. 2, pp. 1060–1069, May 2012.
- [72] D. Pozo, J. Contreras, and E. Sauma, "If you build it, he will come: Anticipative power transmission planning," *Energy Economics*, vol. 36, pp. 135–146, 2013.

- [73] F. Bouffard, F. D. Galiana, and J. M. Arroyo, “Umbrella contingencies in security-constrained optimal power flow,” in *Proc. 15th Power Systems Computation Conference (PSCC’05)*, Liege, Belgium, Aug. 2005.
- [74] A five-level MILP model for flexible transmission network planning under uncertainty: A min-max regret approach – Case study input data. <https://drive.google.com/open?id=0BxgJO6PuetvKYW9SOG11dVpYekk>.
- [75] “Whitepaper: Electricity capacity report,” National Grid, Report, 2015. [Online]. Available: <https://www.emrdeliverybody.com/Capacity%20Markets%20Document%20Library/Electricity%20Capacity%20Report%202015.pdf>.
- [76] I. J. Pérez-Arriaga and C. Batlle, “Impacts of Intermittent Renewables on Electricity Generation System Operation,” *Economics of Energy & Environmental Policy*, vol. 1, no. 2, pp. 3–8, Mar. 2012.
- [77] REN21, “Renewables 2017 – Global Status Report,” REN21 Secretariat, Tech. Rep.
- [78] M. Madrigal and S. Stoft, “Transmission Expansion for Renewable Energy Scale-Up: Emerging Lessons and Recommendations,” A World Bank Study. Washington, DC: World Bank, Tech. Rep.
- [79] S. Lumberras and A. Ramos, “The New Challenges to Transmission Expansion Planning. Survey of Recent Practice and Literature Review,” *Elect. Power Syst. Res.*, vol. 134, no. 1, pp. 19–29, May 2016.
- [80] A. Shapiro, D. Dentcheva, and A. Ruszczyński, *Lectures on Stochastic Programming: Modeling and Theory*. SIAM-Society for Industrial and Applied Mathematics, Sept. 2009.
- [81] A. Ben-Tal, L. E. Ghaoui, and A. Nemirovski, *Robust Optimization*. Princeton University Press, Aug. 2009.

- [82] M. Carrión, J. M. Arroyo, and N. Alguacil, “Vulnerability-constrained transmission expansion planning: A stochastic programming approach,” *IEEE Transactions on Power Systems*, vol. 22, no. 4, pp. 1436–1445, Nov. 2007.
- [83] M. Majidi-Qadikolai and R. Baldick, “Stochastic transmission capacity expansion planning with special scenario selection for integrating $n - 1$ contingency analysis,” *IEEE Trans. Power Syst.*, vol. 31, no. 6, pp. 4901–4912, Nov 2016.
- [84] J. Zhan, C. Y. Chung, and A. Zare, “A fast solution method for stochastic transmission expansion planning,” *IEEE Trans. Power Syst.*, vol. 32, no. 6, pp. 4684–4695, Nov 2017.
- [85] R. T. Rockafellar and S. P. Uryasev, “Conditional Value-at-Risk for General Loss Distributions,” *Journal of Banking and Finance*, vol. 26, no. 7, pp. 1443–1471, Jul. 2002.
- [86] Y. Zhang, J. Wang, and X. Wang, “Review on Probabilistic Forecasting of Wind Power Generation,” *Renewable and Sustainable Energy Reviews*, vol. 32, no. 1, pp. 255–270, Apr. 2014.
- [87] D. Rani and M. M. Moreira, “Simulation–Optimization Modeling: A Survey and Potential Application in Reservoir Systems Operation,” *Water Resources Management*, vol. 24, no. 6, pp. 1107–1138, Apr. 2010.
- [88] A. Bagheri, J. Wang, and C. Zhao, “Data-driven stochastic transmission expansion planning,” *IEEE Trans. Power Syst.*, vol. 32, no. 5, pp. 3461–3470, Sept 2017.
- [89] A. J. Wood, B. F. Wollenberg, and G. B. Sheblé, *Power Generation, Operation, and Control*. 3rd ed. New York, NY, USA: Wiley, 2014.
- [90] S. Pattanariyankool and L. B. Lave, “Optimizing Transmission from Distant Wind Farms,” *Energy Policy*, vol. 38, no. 6, pp. 2806–2815, Jun. 2010.

- [91] R. Doherty and M. O'Malley, "A New Approach to Quantify Reserve Demand in Systems with Significant Installed Wind Capacity," *IEEE Trans. Power Syst.*, vol. 20, no. 2, pp. 587–595, May 2005.
- [92] J. M. Morales, A. J. Conejo, and J. Pérez-Ruiz, "Economic Valuation of Reserves in Power Systems with High Penetration of Wind Power," *IEEE Trans. Power Syst.*, vol. 24, no. 2, pp. 900–910, May 2009.
- [93] A. Moreira, D. Pozo, A. Street, and E. Sauma, "Reliable Renewable Generation and Transmission Expansion Planning: Co-Optimizing System's Resources for Meeting Renewable Targets," *IEEE Trans. Power Syst.*, vol. 32, no. 4, pp. 3246–3257, Jul. 2017.
- [94] B. Zeng and L. Zhao, "Solving Two-Stage Robust Optimization Problems using a Column-and-Constraint Generation Method," *Operations Research Letters*, vol. 41, no. 5, pp. 457–461, Sept. 2013.
- [95] A. Moreira, B. Fanzeres, and G. Strbac, "Energy and Reserve Scheduling under Ambiguity on Renewable Probability Distribution," *Electric Power Systems Research*, vol. 160, pp. 205–218, Jul. 2018.
- [96] L. Wu, M. Shahidehpour, and T. Li, "Stochastic Security-Constrained Unit Commitment," *IEEE Trans. Power Syst.*, vol. 22, no. 2, pp. 800–811, May 2007.
- [97] L. E. Jones, *Renewable Energy Integration: Practical Management of Variability, Uncertainty, and Flexibility in Power Grids*. Elsevier Inc., 2014.
- [98] An ambiguity averse approach for transmission expansion planning – Case study input data. https://drive.google.com/drive/folders/1sS5qe_F7gE7TOGOdRyRD-5UjzbkiLHAN?usp=sharing.

- [99] G. Latorre, R. D. Cruz, J. M. Areiza, and A. Villegas, “Classification of publications and models on transmission expansion planning,” *IEEE Trans. Power Syst.*, vol. 18, no. 2, pp. 938–946, May 2003.
- [100] R. Hemmati, R.-A. Hooshmand, and A. Khodabakhshian, “Comprehensive review of generation and transmission expansion planning,” *IET Gener. Transm. Distrib.*, vol. 7, no. 9, pp. 955–964, Sep. 2013.
- [101] C. R. Dietrich, “Computationally efficient Cholesky factorization of a covariance matrix with block Toeplitz structure,” *J. Stat. Comput. Simul.*, vol. 45, no. 3–4, pp. 203–218, 1993.
- [102] C. Lee, C. Liu, S. Mehrotra, and M. Shahidehpour, “Modeling transmission line constraints in two-stage robust unit commitment problem,” *IEEE Transactions on Power Systems*, vol. 29, no. 3, pp. 1221–1231, May 2014.
- [103] C. A. Floudas, *Nonlinear and Mixed-Integer Optimization: Fundamentals and Applications*. New York, NY, USA: Oxford University Press, 1995.

APPENDIX A

Detailed formulation of the model presented in Chapter 2

In this appendix we provide the complete formulation for the three-level model (2.7)–(2.9). In the following sections, the decision variables, objective function, and constraints of each of the three optimization levels are described in detail.

A.1 First-level problem: minimization of investment and operative costs

In the first level problem of the trilevel model (2.7)–(2.9), investment decisions in the transmission lines, given by vector \mathbf{x} , comprise the binary decision variables v_l

and continuous decision variables \bar{F}_l^C for all $l \in \mathcal{L}^C$, which is the set of candidate lines. Each decision variable v_l assumes value equal to one if there is investment in the candidate line l or is set to zero otherwise, while \bar{F}_l^C defines the maximum capacity (MW) of each candidate line l . The component y_b of the binary vector \mathbf{y} is determined as one if there is an investment in renewable generation on bus b , being zero otherwise. Finally, vector \mathbf{q} aggregates all the operation variables: p_i – energy scheduled in the pre-contingency state for the generating unit i ; r_i^u and r_i^d – up- and down-spinning reserves scheduled in the pre-contingency state for the generating unit i ; f_l – power flow passing through line l in the pre-contingency schedule; θ_b – phase angle of bus b in the pre-contingency state. The complete first-level problem is formulated as follows.

$$\begin{aligned} \min_{\substack{\Delta D_{K,\Sigma}, \theta_b, \bar{F}_l^C, i \in I \\ f_l, p_i, r_i^d, r_i^u, v_l, y_l}} \quad & \sum_{i \in I} C_i^P p_i + \sum_{i \in I} C_i^d r_i^d + \sum_{i \in I} C_i^u r_i^u + \sum_{l \in \mathcal{L}^C} (C_l v_l + C_l^{Cap} \bar{F}_l^C) \\ & + \sum_{b \in N^{RE}} C_b^{RE} y_b + \sum_{K \in \mathcal{K}} C_K^I \Delta D_{K,\Sigma}(\mathbf{x}, \mathbf{y}, \mathbf{q}) \quad (\text{A.1}) \end{aligned}$$

subject to:

$$\sum_{i \in I_b} p_i + \sum_{l \in \mathcal{L} | to(l)=b} f_l - \sum_{l \in \mathcal{L} | fr(l)=b} f_l = \hat{D}_b - \hat{W}_b; \forall b \in N^E \quad (\text{A.2})$$

$$\sum_{i \in I_b} p_i + \sum_{l \in \mathcal{L} | to(l)=b} f_l - \sum_{l \in \mathcal{L} | fr(l)=b} f_l = -y_b \hat{W}_b; \forall b \in N^{RE} \quad (\text{A.3})$$

$$\sum_{b \in N^{RE}} y_b \hat{W}_b + \sum_{b \in N^E} \hat{W}_b \geq Target \sum_{b \in N^E} \hat{D}_b \quad (\text{A.4})$$

$$f_l = \frac{1}{x_l} (\theta_{fr(l)} - \theta_{to(l)}); \forall l \in \mathcal{L}^E \quad (\text{A.5})$$

$$-M_l(1 - v_l) \leq f_l - \frac{1}{x_l} (\theta_{fr(l)} - \theta_{to(l)}) \leq M_l(1 - v_l); \forall l \in \mathcal{L}^C \quad (\text{A.6})$$

$$-\bar{F}_l \leq f_l \leq \bar{F}_l; \forall l \in \mathcal{L}^E \quad (\text{A.7})$$

$$-\bar{F}_l^C \leq f_l \leq \bar{F}_l^C; \forall l \in \mathcal{L}^C \quad (\text{A.8})$$

$$v_l \bar{F}_l^{Min} \leq \bar{F}_l^C \leq v_l \bar{F}_l^{Max}; \forall l \in \mathcal{L}^C \quad (\text{A.9})$$

$$\sum_{l \in \mathcal{L}^C | to(l)=b} v_l + \sum_{l \in \mathcal{L}^C | fr(l)=b} v_l \leq y_b M_b^0; \forall b \in N^{RE} \quad (\text{A.10})$$

$$0 \leq p_i \leq \bar{P}_i; \forall i \in I \quad (\text{A.11})$$

$$p_i + r_i^u \leq \bar{P}_i; \forall i \in I \quad (\text{A.12})$$

$$p_i - r_i^d \geq 0; \forall i \in I \quad (\text{A.13})$$

$$0 \leq r_i^u \leq R_i^U; \forall i \in I \quad (\text{A.14})$$

$$0 \leq r_i^d \leq R_i^D; \forall i \in I \quad (\text{A.15})$$

$$v_l \in \{0, 1\}; \forall l \in \mathcal{L}^C \quad (\text{A.16})$$

$$y_b \in \{0, 1\}; \forall b \in N^{RE} \quad (\text{A.17})$$

$$\Delta D_{K,\Sigma}(\mathbf{x}, \mathbf{y}, \mathbf{q}) \leq \overline{\Delta D}_{K,\Sigma}, \forall K \in \mathcal{K} \quad (\text{A.18})$$

$$\Delta D_{K,\Sigma}(\mathbf{x}, \mathbf{y}, \mathbf{q}) = \text{solution of (A.20)-(A.34)} \quad (\text{A.19})$$

The objective function (A.1) minimizes the following cost-related terms: generation (p_i), up- and down-reserves (r_i^{up}, r_i^{dw}), line investment (v_l, \bar{F}_l^C), RES-related expansion (y_b), and system power imbalance costs. Generation costs are calculated via linear cost functions. Up and down reserves costs are associated with reserves scheduled in order to ensure that the system will be able to meet demand under the outage of any combination of up to K elements, any demand scenario, and any RES generation realization within a pre-defined uncertainty set. Investment in transmission lines has two terms. The first one is related to the fixed cost of building the line (C^l) and the second one refers to the line capacity (C^{Cap}). RES-related costs are associated with the incentives that are diminished from society as subsidies for RES investments. The last term is the worst-case system power imbalance (RES spillage, power surplus, and loss of load) cost associated with the security criterion adopted by the transmission planner.

Constraints (A.2) and (A.3) represent the nodal power balance of existing buses and new candidate RES nodes, respectively. Note that demand and RES generation are fixed to their nominal values for this pre-contingency problem. Constraint (A.4) imposes a minimum amount of RES participation in the demand supply defined by the parameter *Target*, which can be set to a value between 0 and 1. Constraints (A.5) and (A.6) model the DC power flow approach to describe the line flows in terms of nodal voltage angles for existing and candidates lines, respectively. For each candidate line l , the binary decision variable v_l assumes value equal to 1 if the line is built or equal to 0 otherwise. The parameter M_l is a large-enough constant. Constraints (A.7) and (A.8) establish power flow capacity limits for existing and candidate lines, respectively. Constraints (A.9) enforce the line capacity of a candidate line to be 0 if the line is not constructed or to be between predefined minimum and maximum line capacity bounds, otherwise. To avoid network loops where new RES nodes are built without RES investment, we have included the logic constraints (A.10). Thus, it is not possible to invest in lines that connect a new RES node to the existing system if there is no RES investment in such node. In addition, the power generation of each unit is limited in (A.11). The scheduled up-spinning reserves are constrained by the power capacity left in each generating unit in (A.12). Down-spinning reserves cannot exceed the scheduled power generation in (A.13). Moreover, maximum up and down spinning reserves are limited for each generating unit based on their technological constraints in (A.14) and (A.15). The binary nature of line and RES investment variables is ensured in (A.16) and (A.17). In (A.18), the system power imbalance for the worst-case scenario is limited to be less than or equal to a certain user-defined threshold. Finally, the worst-case imbalance is an outcome of the middle-level problem solution as represented in (A.19).

A.2 Middle-level: worst-case demand, RES supply and contingency scenario

The middle-level problem (2.9) identifies the contingency vector \mathbf{a} and demand and renewable generation realization \mathbf{d} and \mathbf{w} , respectively, that lead to the highest level of system power imbalance. The binary availability vector \mathbf{a} is written as $\mathbf{a} = [\mathbf{a}^G, \mathbf{a}^L]^T$, where each component a_i^G of vector \mathbf{a}^G corresponds to the status (1 for on service and 0 for out of service) of a generating unit i . Analogously, each component a_l^L of \mathbf{a}^L is associated with the availability of a transmission line l . Vector \mathbf{d} is composed of elements D_b that represent the demand of each bus b . Similarly, elements W_b of vector \mathbf{w} are related to the renewable generation provided by each bus b . Auxiliary variables $e_b^{D(+)}$ and $e_b^{D(-)}$, respectively, represent positive and negative errors comprised in vector \mathbf{e}^d used in (2.6). Likewise, vector \mathbf{e}^w is composed of variables $e_b^{W(+)}$ and $e_b^{W(-)}$. Within this context, for a given security parameter K and pair of covariance matrices $\Sigma = (\Sigma^d, \Sigma^w)$, the second-level problem (2.9) is formulated as follows:

$$\Delta D_{K,\Sigma}(\mathbf{x}, \mathbf{y}, \mathbf{q}) = \max_{\delta, a_i^G, a_l^L, D_b, e_b^{D(+)}, e_b^{D(-)}, e_b^{W(+)}, e_b^{W(-)}, W_b} \delta(\mathbf{x}, \mathbf{y}, \mathbf{q}, \mathbf{a}, \mathbf{d}, \mathbf{w}) \quad (\text{A.20})$$

subject to:

$$\sum_{i \in I} a_i^G + \sum_{l \in \mathcal{L}} a_l^L \geq n - K \quad (\text{A.21})$$

$$a_i^G \in \{0, 1\}; \forall i \in I \quad (\text{A.22})$$

$$a_l^L \in \{0, 1\}; \forall l \in \mathcal{L} \quad (\text{A.23})$$

$$D_b = \hat{D}_b + s^d \sum_{b' \in N^E | b' \leq b} L_{b,b'}^D (e_{b'}^{D(+)} - e_{b'}^{D(-)}); \forall b \in N^E \quad (\text{A.24})$$

$$W_b = \hat{W}_b + s^w \sum_{b' \in N | b' \leq b} L_{b,b'}^W (e_{b'}^{W(+)} - e_{b'}^{W(-)}); \forall b \in N \quad (\text{A.25})$$

$$0 \leq e_b^{D(+)} \leq 1; \forall b \in N^E \quad (\text{A.26})$$

$$0 \leq e_b^{D(-)} \leq 1; \forall b \in N^E \quad (\text{A.27})$$

$$0 \leq e_b^{W(+)} \leq 1; \forall b \in N \quad (\text{A.28})$$

$$0 \leq e_b^{W(-)} \leq 1; \forall b \in N \quad (\text{A.29})$$

$$\sum_{b \in N^E} \left(e_b^{D(+)} + e_b^{D(-)} \right) \leq \Gamma^D \quad (\text{A.30})$$

$$\sum_{b \in N} \left(e_b^{W(+)} + e_b^{W(-)} \right) \leq \Gamma^W \quad (\text{A.31})$$

$$\underline{D}_b \leq D_b \leq \overline{D}_b; \forall b \in N^E \quad (\text{A.32})$$

$$\underline{W}_b \leq W_b \leq \overline{W}_b; \forall b \in N \quad (\text{A.33})$$

$$\delta(\mathbf{x}, \mathbf{y}, \mathbf{q}, \mathbf{a}, \mathbf{d}, \mathbf{w}) = \text{solution of (A.35)–(A.44)} \quad (\text{A.34})$$

The objective function (A.20) determines the maximum system power imbalance, which is also minimized in the lower-level problem as a reaction of the system operator against the worst-case scenario identified by the middle-level problem (A.34). Constraint (A.21) imposes the joint generation and transmission security criteria. According to (A.21), the feasible region of the middle-level considers up to K failures of elements of the system. The binary nature of the variables associated with outages of generators and lines is enforced by constraints (A.22) and (A.23), respectively.

Uncertainties in demand and RES supply are represented by constraints (A.24)–(A.33). Cholesky decompositions [101] of the nodal-demand covariance matrix and of the RES-nodal supply covariance matrix are used to capture the correlations among nodes in (A.24) and (A.25). The parameters s^d and s^w are used to control the amplitude of the deviations of demand and RES supply, respectively. Nominal demand and RES supply are represented by \hat{D}_b and \hat{W}_b in each node, respectively. Perturbation parameters $(e_{b'}^{D(+)}, e_{b'}^{D(-)}, e_{b'}^{W(+)}, e_{b'}^{W(-)})$ are constrained within the interval between 0 and 1 in constraints (A.26)–(A.29). Constraints (A.30) and

(A.31), respectively, limit the number of demand and RES generation deviations among buses to given user-defined uncertainty budgets Γ^D and Γ^W . These uncertainty budgets control the conservativeness of the solution. Minimum and maximum nodal deviations for demand and RES generation are constrained in (A.32) and (A.33), respectively.

A.3 Lower-level: system corrective actions

The lower-level problem comprises the reaction of the system operator against the worst-case combination of post-contingency state and realization (scenario) of demands and renewable generation identified by the second-level problem. In (2.9), the third-level decision vector \mathbf{z} is composed of variables related to a new operating point: p_i^{wc} – energy scheduled in the worst-case post-contingency state for the generating unit i ; f_l^{wc} – power flow transferred through line l in the worst-case post-contingency schedule; θ_b^{wc} – phase angle of bus b in the worst-case post-contingency state. Given the investment decisions and pre-contingency schedule defined by \mathbf{x} , \mathbf{y} , and \mathbf{q} , the linear program that models the system operator redispatch under the worst-case state, represented by $(\mathbf{a}, \mathbf{d}, \mathbf{w})$, is the following:

$$\delta(\mathbf{x}, \mathbf{y}, \mathbf{q}, \mathbf{a}, \mathbf{d}, \mathbf{w}) = \min_{\substack{\Delta D_b^{+wc}, \Delta D_b^{-wc} \\ \theta_b^{wc}, f_l^{wc}, p_i^{wc}}} \sum_{b \in N} \Delta D_b^{-wc} + \sum_{b \in N/N^W} \Delta D_b^{+wc} + \gamma^{Spil} \sum_{b \in N^W} \Delta D_b^{+wc} \quad (\text{A.35})$$

subject to:

$$\sum_{i \in I_b} p_i^{wc} + \sum_{l \in \mathcal{L} | to(l)=b} f_l^{wc} - \sum_{l \in \mathcal{L} | fr(l)=b} f_l^{wc} - \Delta D_b^{+wc} + \Delta D_b^{-wc} = D_b - W_b : (\beta_b); \forall b \in N^E \quad (\text{A.36})$$

$$\sum_{i \in I_b} p_i^{wc} + \sum_{l \in \mathcal{L} | to(l)=b} f_l^{wc} - \sum_{l \in \mathcal{L} | fr(l)=b} f_l^{wc} - \Delta D_b^{+wc}$$

$$+ \Delta D_b^{-wc} = -y_b W_b : (\beta_b); \forall b \in N^{RE} \quad (\text{A.37})$$

$$\begin{aligned} -M_l(1 - a_l^L) &\leq f_l^{wc} - \frac{1}{x_l} (\theta_{fr(l)}^{wc} - \theta_{to(l)}^{wc}) \\ &\leq M_l(1 - a_l^L) : (\omega_l, \psi_l); \forall l \in \mathcal{L}^E \end{aligned} \quad (\text{A.38})$$

$$\begin{aligned} -M_l(1 - v_l a_l^L) &\leq f_l^{wc} - \frac{1}{x_l} (\theta_{fr(l)}^{wc} - \theta_{to(l)}^{wc}) \\ &\leq M_l(1 - v_l a_l^L) : (\pi_l, \sigma_l); \forall l \in \mathcal{L}^C \end{aligned} \quad (\text{A.39})$$

$$-a_l^L \bar{F}_l \leq f_l^{wc} \leq a_l^L \bar{F}_l : (\xi_l, \phi_l); \forall l \in \mathcal{L}^E \quad (\text{A.40})$$

$$-a_l^L \bar{F}_l^C \leq f_l^{wc} \leq a_l^L \bar{F}_l^C : (\gamma_l, \chi_l); \forall l \in \mathcal{L}^C \quad (\text{A.41})$$

$$a_i^G (p_i - r_i^d) \leq p_i^{wc} \leq a_i^G (p_i + r_i^u) : (\zeta_i, \lambda_i); \forall i \in I \quad (\text{A.42})$$

$$0 \leq p_i^{wc} \leq \bar{P}_i : (\mu_i); \forall i \in I \quad (\text{A.43})$$

$$\Delta D_b^{+wc}, \Delta D_b^{-wc} \geq 0; \forall b \in N. \quad (\text{A.44})$$

The objective function (A.35) minimizes the total system power imbalance, which is defined here as the weighted sum of load shedding, power surplus, and wind spillage. RES spillage is weighted by a factor γ^{Spil} in order to make spillage costs comparable with load shedding costs. Note that N^W is the set of buses containing wind generation, which can be composed of both existing and candidate buses. It is worth mentioning that minimizing total imbalance cost at the lower level is an equivalent problem (objective function is multiplied by a factor C_K^I). Constraints (A.36) and (A.37) are associated with nodal power balance considering positive and negative imbalance for existing nodes and new RES candidate nodes, respectively. Power flows are described via constraints (A.38) for the existing lines and (A.39) for the candidate lines. Power flow limits for the contingency states are imposed in (A.40) and (A.41) for existing and candidates lines, respectively. Constraints (A.42) set power generation limits based on pre-contingency scheduled energy and reserve. Generation limits are set in (A.43). Finally, non-negativity is enforced in (A.44) for nodal power imbalance variables.

APPENDIX B

Detailed solution methodology for the problem of Chapter 2

The proposed reliable RG-TEP problem formulation (A.1)–(A.44) belongs to the class of trilevel optimization models with multiple recourse functions [45], which can be solved by a column-and-constraint generation algorithm. Here, we describe our column-and-constraint generation approach that comprises the iterative solution of a master problem and a group of subproblems (as many as the number of simultaneously considered security criteria).

B.1 Master Problem

The master problem is an approximation of the original trilevel problem where, in each iteration, primal polyhedral constraints are added to locally characterize $\Delta D_{K,\Sigma}$ for each security criterion. The formulation of the master problem is written as follows.

$$\begin{aligned} \text{Minimize}_{\alpha, \theta_b, \bar{F}_l^C, f_l, p_i, r_i^d, r_i^u, v_l, y_l} & \sum_{i \in I} C_i^P(p_i) + \sum_{i \in I} C_i^d(r_i^d) + \sum_{i \in I} C_i^u(r_i^u) + \sum_{l \in \mathcal{L}^C} (C_l v_l + C_l^{Cap} \bar{F}_l^C) \\ & + \sum_{b \in N^{RE}} C_b^{RE} y_b + \sum_{k \in \{1, \dots, K\}} C_k^I \alpha_k \quad (\text{B.1}) \end{aligned}$$

subject to:

$$\text{Pre-contingency constraints (A.2)–(A.17)} \quad (\text{B.2})$$

$$\begin{aligned} \sum_{i \in I_b} p_{k,i}^m + \sum_{l \in (\mathcal{L} \cup \mathcal{L}^C) | to(l)=b} f_{k,l}^m - \sum_{l \in (\mathcal{L} \cup \mathcal{L}^C) | fr(l)=b} f_{k,l}^m - \Delta D_{k,b}^{+m} + \Delta D_{k,b}^{-m} = D_{k,b}^{(m)} \\ - W_{k,b}^{(m)}; \forall b \in N^E, \forall k = 0, \dots, K, \forall m = 1, \dots, j-1 \quad (\text{B.3}) \end{aligned}$$

$$\begin{aligned} \sum_{i \in I_b} p_{k,i}^m + \sum_{l \in (\mathcal{L} \cup \mathcal{L}^C) | to(l)=b} f_{k,l}^m - \sum_{l \in (\mathcal{L} \cup \mathcal{L}^C) | fr(l)=b} f_{k,l}^m - \Delta D_{k,b}^{+m} + \Delta D_{k,b}^{-m} = \\ - y_b W_{k,b}^{(m)}; \forall b \in N^{RE}, \forall k = 0, \dots, K, \forall m = 1, \dots, j-1 \quad (\text{B.4}) \end{aligned}$$

$$\begin{aligned} f_{k,l}^m - \frac{1}{x_l} (\theta_{k,fr(l)}^m - \theta_{k,to(l)}^m) \geq -M_l (1 - a_{k,l}^{L(m)}); \\ \forall l \in \mathcal{L}^E, m = 1, \forall k = 0, \dots, K, \forall m = 1, \dots, j-1 \quad (\text{B.5}) \end{aligned}$$

$$\begin{aligned} f_{k,l}^m - \frac{1}{x_l} (\theta_{k,fr(l)}^m - \theta_{k,to(l)}^m) \leq M_l (1 - a_{k,l}^{L(m)}); \\ \forall l \in \mathcal{L}^E, m = 1, \forall k = 0, \dots, K, \forall m = 1, \dots, j-1 \quad (\text{B.6}) \end{aligned}$$

$$\begin{aligned} f_{k,l}^m - \frac{1}{x_l} (\theta_{k,fr(l)}^m - \theta_{k,to(l)}^m) \geq -M_l (1 - (a_{k,l}^{L(m)} v_l)); \\ \forall l \in \mathcal{L}^C, m = 1, \forall k = 0, \dots, K, \forall m = 1, \dots, j-1 \quad (\text{B.7}) \end{aligned}$$

$$\begin{aligned} f_{k,l}^m - \frac{1}{x_l} (\theta_{k,fr(l)}^m - \theta_{k,to(l)}^m) \leq M_l (1 - (a_{k,l}^{L(m)} v_l)); \\ \forall l \in \mathcal{L}^C, m = 1, \forall k = 0, \dots, K, \forall m = 1, \dots, j-1 \quad (\text{B.8}) \end{aligned}$$

$$-a_{k,l}^{L(m)}\bar{F}_l \leq f_{k,l}^m \leq \bar{F}_l a_{k,l}^{L(m)}; \forall l \in \mathcal{L}^E, \forall k = 0, \dots, K, \forall m = 1, \dots, j-1 \quad (\text{B.9})$$

$$-a_{k,l}^{L(m)}\bar{F}_l^C \leq f_{k,l}^m \leq \bar{F}_l^C a_{k,l}^{L(m)}; \forall l \in \mathcal{L}^C, \forall k = 0, \dots, K, \forall m = 1, \dots, j-1 \quad (\text{B.10})$$

$$a_{k,i}^{G(m)}(p_i - r_i^D) \leq p_{k,i}^m \leq (p_i + r_i^U)a_{k,i}^{G(m)}; \forall i \in I, \forall k = 0, \dots, K, \\ \forall m = 1, \dots, j-1 \quad (\text{B.11})$$

$$0 \leq p_{k,i}^m \leq \bar{P}_i; \forall i \in I, \forall k = 0, \dots, K, \forall m = 1, \dots, j-1 \quad (\text{B.12})$$

$$\Delta D_{k,b}^{+m}, \Delta D_{k,b}^{-m} \geq 0; \forall b \in N, \forall k = 0, \dots, K, \forall m = 1, \dots, j-1 \quad (\text{B.13})$$

$$\alpha_k \geq \sum_{b \in N} (\Delta D_{k,b}^{+m} + \Delta D_{k,b}^{-m}); \forall k = 0, \dots, K, \forall m = 1, \dots, j-1 \quad (\text{B.14})$$

$$\alpha_k \leq \bar{\Delta D}_k; \forall k = 0, \dots, K \quad (\text{B.15})$$

B.2 Subproblem

At each iteration and for each security criteria, the subproblem determines the worst-case contingency for the pre-contingency scheduling of power and reserves identified by the master problem. Mathematically, the subproblem is a mixed-integer linear max-min problem that comprises the two lowermost optimization levels. This particular instance of bilevel programming (A.35)–(A.44) can be conveniently recast as an equivalent single-level program. To carry out this transformation, we take the following steps: 1) the original second-level objective function (A.20) is rewritten to maximize the third-level dual-objective function; 2) the new objective function is subjected to constraints of the original second level problem and to dual feasibility constraints associated with the third-level problem; 3) bilinear terms associated with products between binary variables of the second-level problem (line and generation contingency variables, a_i^G and a_l^L) and dual variables of the third-level problem are linearized by means of disjunctive constraints; and 4) bilinear terms associated with products between third-level dual variables and second-level continuous variables

(related to renewable injection and load scenarios) are linearized by means of the binary expansion approach.¹

In light of the aforementioned steps, the MILP subproblem is defined in (B.16)-(B.56).

$$\begin{aligned}
\Delta D_{K,\Sigma} = & \text{Maximize} \sum_{b \in N^E} (\Phi_b - \Psi_b) - \sum_{b \in N^{RE}} y_b \Psi_b - \sum_{l \in \mathcal{L}^E} M_l (\omega_l - q_l) \\
& \Phi_b, \Psi_b, \beta_b, \gamma_l, \zeta_i, \\
& \vartheta_{jb}, \lambda_i, \mu_i, \xi_l, \\
& \pi_l, \omega_{jb}, \varrho_{jb}, \sigma_l, \\
& \varsigma_{jb}, \phi_l, \chi_l, \psi_l, \omega_l \\
& a_i^G, a_l^L, c_l, D_b, \\
& d_l, e_b^{D(+)}, e_b^{D(-)}, \\
& e_b^{W(+)}, e_b^{W(-)}, g_i, h_l, \\
& m_l, q_l, o_l, s_l, u_i, W_b, z_l \\
& - \sum_{l \in \mathcal{L}^E} M_l (\psi_l - c_l) - \sum_{l \in \mathcal{L}^C} M_l (\pi_l - v_l z_l) - \sum_{l \in \mathcal{L}^C} M_l (\sigma_l - v_l h_l) - \sum_{l \in \mathcal{L}^E} \bar{F}_l s_l \\
& - \sum_{l \in \mathcal{L}^E} \bar{F}_l m_l - \sum_{l \in \mathcal{L}^C} \bar{F}_l^C d_l - \sum_{l \in \mathcal{L}^C} \bar{F}_l^C o_l + \sum_{i \in I} (p_i - r_i^d) u_i - \sum_{i \in I} (p_i + r_i^u) g_i \\
& - \sum_{i \in I} \bar{P}_i \mu_i \quad (\text{B.16})
\end{aligned}$$

subject to:

$$\text{Constraints (A.21)–(A.23)} \quad (\text{B.17})$$

$$\beta_b + \zeta_i - \lambda_i - \mu_i \leq 0 : (p_i^{wc}); \forall b \in N, \forall i \in I_b \quad (\text{B.18})$$

$$\beta_{to(l)} - \beta_{fr(l)} + \omega_l - \psi_l + \xi_l - \phi_l = 0 : (f_l^{wc}); \forall l \in \mathcal{L}^E \quad (\text{B.19})$$

$$\beta_{to(l)} - \beta_{fr(l)} + \pi_l - \sigma_l + \gamma_l - \chi_l = 0 : (f_l^{wc}); \forall l \in \mathcal{L}^C \quad (\text{B.20})$$

$$\begin{aligned}
& \sum_{l \in \mathcal{L}^E | to(l)=b} \frac{1}{x_l} (\omega_l - \psi_l) + \sum_{l \in \mathcal{L}^E | fr(l)=b} \frac{1}{x_l} (\psi_l - \omega_l) + \sum_{l \in \mathcal{L}^C | to(l)=b} \frac{1}{x_l} (\pi_l - \sigma_l) \\
& + \sum_{l \in \mathcal{L}^C | fr(l)=b} \frac{1}{x_l} (\sigma_l - \pi_l) = 0 : (\theta_b^{wc}); \forall b \in N \quad (\text{B.21})
\end{aligned}$$

$$-1 \leq \beta_b \leq 1 : (\Delta D_b^{+wc}, \Delta D_b^{-wc}); \forall b \in N/N^W \quad (\text{B.22})$$

$$-\gamma^{Spil} \leq \beta_b \leq 1 : (\Delta D_b^{+wc}, \Delta D_b^{-wc}); \forall b \in N^W \quad (\text{B.23})$$

¹It is relevant to say that the uncorrelated case, extensively explored in the literature ([41, 43, 102], just to mention a few), fits in the proposed model by considering Σ^d and Σ^w as identity matrices.

$$\omega_l, \psi_l, \xi_l, \phi_l \geq 0; \forall l \in \mathcal{L}^E \quad (\text{B.24})$$

$$\pi_l, \sigma_l, \gamma_l, \chi_l \geq 0; \forall l \in \mathcal{L}^C \quad (\text{B.25})$$

$$\zeta_i, \lambda_i, \mu_i \geq 0; \forall i \in I \quad (\text{B.26})$$

$$D_b = \underline{D}_b + \kappa \sum_{j=1}^{J_b} 2^{j-1} \zeta_{jb}; \forall b \in N^E \quad (\text{B.27})$$

$$W_b = \underline{W}_b + \kappa \sum_{j=1}^{J_b} 2^{j-1} \vartheta_{jb}; \forall b \in N \quad (\text{B.28})$$

$$\Phi_b = \underline{D}_b \beta_b + \kappa \sum_{j=1}^{J_b} 2^{j-1} \omega_{jb}; \forall b \in N^E \quad (\text{B.29})$$

$$\Psi_b = \underline{W}_b \beta_b + \kappa \sum_{j=1}^{J_b} 2^{j-1} \varrho_{jb}; \forall b \in N \quad (\text{B.30})$$

$$-M^\beta(1 - \zeta_{jb}) \leq \omega_{jb} - \beta_b \leq M^\beta(1 - \zeta_{jb}); \forall b \in N^E, \forall j = 1, \dots, J_b \quad (\text{B.31})$$

$$-M^\beta \zeta_{jb} \leq \omega_{jb} \leq M^\beta \zeta_{jb}; \forall b \in N^E, \forall j = 1, \dots, J_b \quad (\text{B.32})$$

$$-M^\beta(1 - \vartheta_{jb}) \leq \varrho_{jb} - \beta_b \leq M^\beta(1 - \vartheta_{jb}); \forall b \in N, \forall j = 1, \dots, J_b \quad (\text{B.33})$$

$$-M^\beta \vartheta_{jb} \leq \varrho_{jb} \leq M^\beta \vartheta_{jb}; \forall b \in N, \forall j = 1, \dots, J_b \quad (\text{B.34})$$

$$-M^\omega(1 - a_l^L) \leq q_l - \omega_l \leq M^\omega(1 - a_l^L); \forall l \in \mathcal{L}^E \quad (\text{B.35})$$

$$0 \leq q_l \leq M^\omega a_l^L; \forall l \in \mathcal{L}^E \quad (\text{B.36})$$

$$-M^\psi(1 - a_l^L) \leq c_l - \psi_l \leq M^\psi(1 - a_l^L); \forall l \in \mathcal{L}^E \quad (\text{B.37})$$

$$0 \leq c_l \leq M^\psi a_l^L; \forall l \in \mathcal{L}^E \quad (\text{B.38})$$

$$-M^\pi(1 - a_l^L) \leq z_l - \pi_l \leq M^\pi(1 - a_l^L); \forall l \in \mathcal{L}^C \quad (\text{B.39})$$

$$0 \leq z_l \leq M^\pi a_l^L; \forall l \in \mathcal{L}^C \quad (\text{B.40})$$

$$-M^\sigma(1 - a_l^L) \leq h_l - \sigma_l \leq M^\sigma(1 - a_l^L); \forall l \in \mathcal{L}^C \quad (\text{B.41})$$

$$0 \leq h_l \leq M^\sigma a_l^L; \forall l \in \mathcal{L}^C \quad (\text{B.42})$$

$$-M^\xi(1 - a_l^L) \leq s_l - \xi_l \leq M^\xi(1 - a_l^L); \forall l \in \mathcal{L}^E \quad (\text{B.43})$$

$$0 \leq s_l \leq M^\xi a_l^L; \forall l \in \mathcal{L}^E \quad (\text{B.44})$$

$$-M^\phi(1 - a_l^L) \leq m_l - \phi_l \leq M^\phi(1 - a_l^L); \forall l \in \mathcal{L}^E \quad (\text{B.45})$$

$$0 \leq m_l \leq M^\phi a_l^L; \forall l \in \mathcal{L}^E \quad (\text{B.46})$$

$$-M^\gamma(1 - a_l^L) \leq d_l - \gamma_l \leq M^\gamma(1 - a_l^L); \forall l \in \mathcal{L}^C \quad (\text{B.47})$$

$$0 \leq d_l \leq M^\gamma a_l^L; \forall l \in \mathcal{L}^C \quad (\text{B.48})$$

$$-M^\chi(1 - a_l^L) \leq o_l - \chi_l \leq M^\chi(1 - a_l^L); \forall l \in \mathcal{L}^C \quad (\text{B.49})$$

$$0 \leq o_l \leq M^\chi a_l^L; \forall l \in \mathcal{L}^C \quad (\text{B.50})$$

$$-M^\zeta(1 - a_i^G) \leq u_i - \zeta_i \leq M^\zeta(1 - a_i^G); \forall i \in I \quad (\text{B.51})$$

$$0 \leq u_i \leq M^\zeta a_i^G; \forall i \in I \quad (\text{B.52})$$

$$-M^\lambda(1 - a_i^G) \leq g_i - \lambda_i \leq M^\lambda(1 - a_i^G); \forall i \in I \quad (\text{B.53})$$

$$0 \leq g_i \leq M^\lambda a_i^G; \forall i \in I \quad (\text{B.54})$$

$$\varsigma_{jb} \in \{0, 1\}; \forall b \in N^E, \forall j = 1, \dots, J_b \quad (\text{B.55})$$

$$\vartheta_{jb} \in \{0, 1\}; \forall b \in N, \forall j = 1, \dots, J_b. \quad (\text{B.56})$$

B.3 Solution Algorithm

The iterative algorithm proposed to solve the problem under consideration is based on column and constraint generation algorithm. At each iteration, the solution of the master problem provides a lower bound for the original trilevel problem as well as an expansion plan and a pre-contingency scheduling of power and reserves. For each considered security criterion, the subproblem identifies the worst case system power imbalance and provides an upper bound for the original trilevel problem. Relevant information from the subproblem is sent to the master problem, which is updated with new columns and constraints to accommodate such information. The master problem is then solved again to generate a new lower bound that will be compared to the new upper bound provided by the subproblem. This procedure is repeated until lower and upper bounds are sufficiently close.

The solution algorithm is described in detail as follows.

Iterative Algorithm

(i) *Initialization.*

- Initialize the iteration counter: $j \leftarrow 1$;
- Solve the master problem (B.1)-(B.2) without cuts. This step provides $\alpha^{(1)}$, $\bar{F}_l^{C(1)}$, $p_i^{(1)}$, $r_i^{d(1)}$, $r_i^{u(1)}$, $v_l^{(1)}$, $y_b^{(1)}$, and the same lower bound for the optimal cost of all the multiple security criteria accounted for, which is described by the expression $LB_k = \sum_{i \in I} C_i^P(p_i^{(1)}) + \sum_{i \in I} C_i^d(r_i^{d(1)}) + \sum_{i \in I} C_i^u(r_i^{u(1)}) + \sum_{l \in \mathcal{L}^C} (C_l v_l^{(1)} + C_l^{Cap} \bar{F}_l^{C(1)}) + \sum_{b \in N^{RE}} C_b^{RE} y_b^{(1)}$.

(ii) *Subproblem solution.* Solve a subproblem (B.16)-(B.56) for each imposed security criteria, given $\bar{F}_l^{C(j)}$, $p_i^{(j)}$, $r_i^{d(j)}$, $r_i^{u(j)}$, $v_l^{(j)}$, and $y_b^{(j)}$. This step provides $a_{k,i}^{G(j)}$, $a_{k,l}^{L(j)}$, $D_{k,b}^{(j)}$, $W_{k,b}^{(j)}$, and $\Delta D_k^{(j)}$, and an upper bound for the optimal cost of each single security criterion considered in the model as $UB_k = C_i^P(p_i^{(j)}) + \sum_{i \in I} C_i^d(r_i^{d(j)}) + \sum_{i \in I} C_i^u(r_i^{u(j)}) + \sum_{l \in \mathcal{L}^C} (C_l v_l^{(j)} + C_l^{Cap} \bar{F}_l^{C(j)}) + \sum_{b \in N^{RE}} C_b^{RE} y_b^{(j)} + C_k^I \Delta D_k^{(j)}$.

(iii) *Stopping criterion.* If $\frac{UB_k - LB_k}{UB_k} \leq \epsilon_k; \forall k = 0, \dots, K$, then stop the algorithm; otherwise go to step 4.

(iv) *Iteration counter updating.* Increase the iteration counter: $j \leftarrow j + 1$.

(v) *Master problem solution.* Solve the full master problem (B.1)-(B.15). This step provides $\alpha^{(k)}$, $\bar{F}_l^{C(j)}$, $p_i^{(j)}$, $r_i^{d(j)}$, $r_i^{u(j)}$, $v_l^{(j)}$, $y_b^{(j)}$, and an lower bound for the optimal cost of each single security criterion considered in the model as $LB_k = C_i^P(p_i^{(j)}) + \sum_{i \in I} C_i^d(r_i^{d(j)}) + \sum_{i \in I} C_i^u(r_i^{u(j)}) + \sum_{l \in \mathcal{L}^C} (C_l v_l^{(j)} + C_l^{Cap} \bar{F}_l^{C(j)}) + \sum_{b \in N^{RE}} C_b^{RE} y_b^{(j)} + C_k^I \alpha_k^{(j)}$. Go to step 2.

APPENDIX C

Oracle formulation for methodology presented in Chapter 3

The oracle mentioned in Section 3.4.1 is formulated as follows:

$$\begin{aligned}
 \Delta D_t^{wc} = & \text{Maximize} \quad \sum_{b \in N} D_{bt} \beta_{bt} - \sum_{l \in \mathcal{L}^C} (1 - a_{lt}^l v_l) M_l \sigma_{lt}^+ \\
 & \beta_{bt}, \gamma_{it}^+, \gamma_{it}^-, \\
 & \eta_{it}^+, \eta_{it}^-, \pi_{it}^+, \pi_{it}^-, \\
 & \sigma_{it}^+, \sigma_{it}^-, \chi_{it}^+, \chi_{it}^-, \omega_{it} \\
 & - \sum_{l \in \mathcal{L}^C} (1 - a_{lt}^l v_l) M_l \sigma_{lt}^- - \sum_{l \in (\mathcal{L}^F \cup \mathcal{L}^{PS})} \bar{F}_l \pi_{lt}^+ - \sum_{l \in (\mathcal{L}^F \cup \mathcal{L}^{PS})} \bar{F}_l \pi_{lt}^- - \sum_{l \in \mathcal{L}^C} a_{lt}^l f_l^C \chi_{lt}^+ \\
 & - \sum_{l \in \mathcal{L}^C} a_{lt}^l f_l^C \chi_{lt}^- + \sum_{l \in I} a_{it}^G (p_{it} - r_{it}^d) \gamma_{it}^+ - \sum_{l \in I} a_{it}^G (p_{it} + r_{it}^u) \gamma_{it}^- - \sum_{l \in \mathcal{L}^{PS}} v_l \bar{\psi} \eta_{lt}^+ \\
 & - \sum_{l \in \mathcal{L}^{PS}} v_l \bar{\psi} \eta_{lt}^- \quad (C.1)
 \end{aligned}$$

subject to:

$$\text{Constraints (3.21)-(3.23)} \quad (\text{C.2})$$

$$\beta_{bt} + \gamma_{it}^+ - \gamma_{it}^- \leq 0 : (p_{it}^{wc}); \forall b \in N, i \in I_b \quad (\text{C.3})$$

$$\beta_{to(l),t} - \beta_{fr(l),t} + \omega_{lt} + \pi_{lt}^+ - \pi_{lt}^- = 0 : (f_{lt}^{wc}); \forall l \in (\mathcal{L}^F \cup \mathcal{L}^{PS}) \quad (\text{C.4})$$

$$\beta_{to(l),t} - \beta_{fr(l),t} + \sigma_{lt}^+ - \sigma_{lt}^- + \chi_{lt}^+ - \chi_{lt}^- = 0 : (f_{lt}^{wc}); \forall l \in \mathcal{L}^C \quad (\text{C.5})$$

$$-1 \leq \beta_{fr(l),t} \leq 1 : (\Delta D_{bt}^+, \Delta D_{bt}^-); \forall b \in N \quad (\text{C.6})$$

$$\begin{aligned} & \sum_{l \in (\mathcal{L}^F \cup \mathcal{L}^{PS}) | to(l)=b} \frac{a_{lt}^L}{x_l} \omega_{lt} - \sum_{l \in (\mathcal{L}^F \cup \mathcal{L}^{PS}) | fr(l)=b} \frac{a_{lt}^L}{x_l} \omega_{lt} + \sum_{l \in \mathcal{L}^C | to(l)=b} \frac{\sigma_{lt}^+}{x_l} \\ & - \sum_{l \in \mathcal{L}^C | fr(l)=b} \frac{\sigma_{lt}^+}{x_l} + \sum_{l \in \mathcal{L}^C | fr(l)=b} \frac{\sigma_{lt}^-}{x_l} - \sum_{l \in \mathcal{L}^C | to(l)=b} \frac{\sigma_{lt}^-}{x_l} = 0 : (\theta_{lt}^{wc}); \forall b \in N \end{aligned} \quad (\text{C.7})$$

$$- \frac{a_{lt}^L}{x_l} \omega_{lt} + \eta_{lt}^+ - \eta_{lt}^- = 0 : (\psi_{lt}^{wc}); \forall l \in \mathcal{L}^{PS} \quad (\text{C.8})$$

$$\sigma_{lt}^+, \sigma_{lt}^-, \chi_{lt}^+, \chi_{lt}^- \geq 0; \forall l \in \mathcal{L}^C \quad (\text{C.9})$$

$$\pi_{lt}^+, \pi_{lt}^- \geq 0; \forall l \in (\mathcal{L}^F \cup \mathcal{L}^{PS}) \quad (\text{C.10})$$

$$\gamma_{it}^+, \gamma_{it}^- \geq 0; \forall i \in I \quad (\text{C.11})$$

$$\eta_{lt}^+, \eta_{lt}^- \geq 0; \forall l \in \mathcal{L}^{PS}. \quad (\text{C.12})$$

Formulation (C.1)-(C.12) is a mixed-integer nonlinear programming problem. Following well-known algebra results [103], the bilinear product $a_{lt}^L \sigma_{lt}^+$ for instance can be linearized in two steps. Firstly the auxiliary variable e_{lt}^+ is created to replace $a_{lt}^L \sigma_{lt}^+$ in (C.1). Secondly, the following constraints are included in the oracle to represent the linearization of the aforementioned bilinear product.

$$0 \leq \sigma_{lt}^+ - e_{lt}^+ \leq (1 - a_{lt}^L) M_l \quad (\text{C.13})$$

$$0 \leq e_{lt}^+ \leq a_{lt}^L M_l \quad (\text{C.14})$$

The same rationale is used to linearize the other bilinear products, namely $a_{lt}^L \sigma_{lt}^-$, $a_{lt}^L \chi_{lt}^+$, $a_{lt}^L \chi_{lt}^-$, $a_{lt}^L \omega_{lt}$, $a_{it}^G \gamma_{it}^+$, and $a_{it}^G \gamma_{it}^-$. Once such linearizations are performed, the oracle is recast into a MILP problem.

Regarding the big-M values used in the aforementioned linearizations, it is worth mentioning that, as discussed in [17], if any of constraints (3.26)–(3.28) and (3.30) is modified in the right hand side by an infinitesimal value, the largest change in the objective function of the fifth-level (3.24) will be limited to the aforementioned infinitesimal value multiplied by 2. This effect is because every variable f_{lt}^{wc} is present in two nodal power balance constraints since each f_{lt}^{wc} has a sending and a receiving bus. Therefore, big-M values associated with the linearizations of products $a_{lt}^L \sigma_{lt}^+$, $a_{lt}^L \sigma_{lt}^-$, $a_{lt}^L \chi_{lt}^+$, $a_{lt}^L \chi_{lt}^-$, and $a_{lt}^L \omega_{lt}$ can be set equal to 2. Likewise, any perturbation in the right hand side of (3.31) would lead to a change in the value of the objective function (3.24) limited to the magnitude of such perturbation. Consequently, the big-M values related to the linearizations of $a_{it}^G \gamma_{it}^+$, and $a_{it}^G \gamma_{it}^-$ can be set equal to 1.